NASA TECHNICAL NOTE

NASA TN D-6754

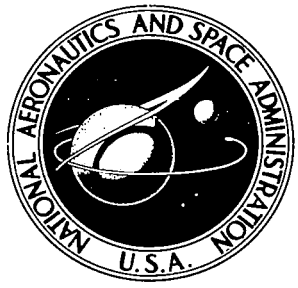

A FLIGHT EVALUATION OF A VTOL JET TRANSPORT UNDER VISUAL AND SIMULATED INSTRUMENT CONDITIONS

by Curt A. Holzhauser, Samuel A. Morello, Robert C. Innis, and James M. Patton, Jr.

Ames Research Center
Moffett Field, Calif. 94035

and

Langley Research Center
Hampton, Va. 23365

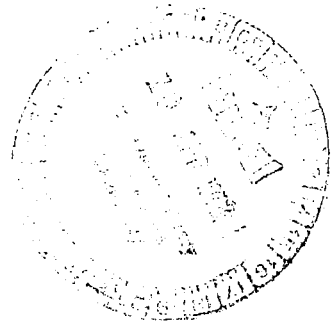

NATIONAL AERONAUTICS AND SPACE ADMINISTRATION • WASHINGTON, D. C. • MARCH 1972

1. Report No.	2. Government Accession No.	3. Recipient's Catalog No.
NASA TN D-6754		

4. Title and Subtitle	5. Report Date
A FLIGHT EVALUATION OF A VTOL JET TRANSPORT UNDER VISUAL AND SIMULATED INSTRUMENT CONDITIONS	March 1972
	6. Performing Organization Code

7. Author(s)	8. Performing Organization Report No.
Curt A. Holzhauser, Samuel A. Morello, Robert C. Innis and James M. Patton, Jr.	A-4023
	10. Work Unit No.
9. Performing Organization Name and Address	721-54-10-01-00-21
NASA Ames Research Center Moffett Field, Calif., 94035 and Langley Research Center Hampton, Virginia 23365	11. Contract or Grant No.
	13. Type of Report and Period Covered
12. Sponsoring Agency Name and Address	Technical Note
National Aeronautics and Space Administration Washington, D. C. 20546	14. Sponsoring Agency Code

15. Supplementary Notes

16. Abstract

A flight investigation was performed with the Dornier DO–31 VTOL to evaluate the performance, handling qualities, and operating characteristics that are considered to be important in the operation of a commercial VTOL transport in the terminal area. The DO-31, a 20,000 kilogram transport, has a mixed jet propulsion system; main engines with nozzles deflect from a cruise to a hover position, and vertical lift engines operate below 170 knots. This VTOL mode incorporates pitch and roll attitude and yaw rate stabilization.

The tests concentrated on the transition, approach, and vertical landing. The mixed jet-propulsion system provided a large usable performance envelope that enabled simulated IFR approaches to be made on 7° and 12° glide slopes. In these approaches management of thrust magnitude and direction was a primary problem, and some form of integrating the controls will be necessary. The handling qualities evaluation pointed out the need for additional research to define flight-path criteria.

The aircraft had satisfactory control and stability in hover out of ground effect. The recirculation effects in a vertical landing were large below 15 meters.

17. Key Words (Suggested by Author(s))	18. Distribution Statement
VTOL jet transport Flight tests of handling qualities and terminal area operation	Unclassified – Unlimited

19. Security Classif. (of this report)	20. Security Classif. (of this page)	21. No. of Pages	22. Price*
Unclassified	Unclassified	66	$3.00

*For sale by the National Technical Information Service, Springfield, Virginia 22151

TABLE OF CONTENTS

NOTATION

A_X	longitudinal acceleration of center of gravity as measured by an accelerometer, $\sin\theta + \frac{1}{g}\frac{dv_x}{dt}$, g
A_Y	lateral acceleration of center of gravity as measured by an accelerometer, $\sin\phi + \frac{1}{g}\frac{dv_y}{dt}$, g
A_Z	normal acceleration of center of gravity as measured by an accelerometer, $\cos\theta + \frac{1}{g}\frac{dv_z}{dt}$, g
a_X	longitudinal acceleration of aircraft, $\frac{dv_x}{dt}$, m/sec^2
a_Y	lateral acceleration of aircraft, $\frac{dv_y}{dt}$, m/sec^2
a_Z	normal acceleration of aircraft, $\frac{dv_z}{dt}$, m/sec^2
C_D	drag coefficient, including propulsive thrust
$C_{L_1 g}$	lift coefficient in steady-state flight, including propulsive thrust
C_{L_α}	power-off lift-curve slope, per deg
FCU_L	position of fuel control unit for left lift engines, deg
FCU_R	position of fuel control unit for right lift engines, deg
g	acceleration of gravity, 9.81 m/sec^2
h	height above the runway, m
I_{XX}, I_{YY}, I_{ZZ}	moments of inertia, kg-m^2
L	rolling moment, newton-m
m	mass, kg
N_1	speed of lift engine farthest forward in left pod, rpm
N_5	speed of lift engine farthest forward in right pod, rpm

N_F	main engine fan speed, measured for left engine in percent of maximum speed, percent
q_∞	free-stream dynamic pressure, N/m^2
$\frac{R}{C}$	rate of climb, m/sec
$\frac{R}{S}$	rate of sink, m/sec
S	wing area, m^2
s	horizontal distance, m or km
T	thrust, newtons
T_A	ambient temperature, °C
T_1	average temperature at main engine inlet, °C
t	time, sec
V	true airspeed, knots or m/sec
V_C	calibrated airspeed, $V\sqrt{\sigma}$, knots
v_x, v_y, v_z	velocities in body axes, m/sec
W	weight, newtons
X	longitudinal displacement, m
Y	lateral displacement, m
α	uncorrected angle of attack measured at nose boom, deg
β	uncorrected angle of sideslip measured at nose boom, deg
γ	flight-path angle (climb, positive), deg
γ_G	glide-slope angle at centerline of ILS (descent, positive), deg
δ_A	left aileron deflection (trailing edge down, positive), deg
δ_E	elevator deflection (trailing edge down, positive), deg

δ_F	flap deflection (trailing edge down, positive), deg
δ_{LP}	lateral stick deflection (right, positive), deg
δ_{MP}	longitudinal stick deflection (aft, positive), deg
δ_{NP}	rudder pedal deflection (right pedal forward, positive), mn
δ_{PN}	pitch nozzle deflection (nose-up pitching moment, positive), deg
δ_R	rudder deflection (trailing edge left, positive), deg
ϵ_G	glide-slope error (above, positive), dots or deg
ϵ_L	localizer error (to right, positive), dots or deg
θ	pitch attitude (nose up, positive), deg
$\dot{\theta}$	pitch rate (nose up, positive), deg/sec
θ_{TRIM}	pitch trim position (nose up, positive), deg
ξ_L	roll stabilization actuator position (right rolling moment, positive), deg
ξ_M	pitch stabilization actuator position (nose-up pitching moment, positive), deg
ξ_N	yaw stabilization actuator position (right yawing moment, positive), deg
ξ_{VTOL}	VTOL roll rate damper actuator position (right roll rate, positive), deg
σ	density ratio
σ_{FCU}	lift engine thrust lever position, deg
σ_M	main engine nozzle lever position, deg
σ_{NL}	nozzle deflection for left lift engines (aft, positive), deg
σ_{NR}	nozzle deflection for right lift engines (forward, positive), deg
σ_T	main engine thrust lever, measured for left engine, deg
ϕ	bank angle (right wing down, positive), deg
$\dot{\phi}$	roll rate (right wing down, positive), deg/sec
$\ddot{\phi}$	angular acceleration in roll (right wing down, positive), rad/sec^2

ψ	heading angle, measured clockwise from true north, deg
$\dot{\psi}$	yaw rate (nose right, positive), deg/sec

A FLIGHT EVALUATION OF A VTOL JET TRANSPORT UNDER VISUAL AND SIMULATED INSTRUMENT CONDITIONS

Curt A. Holzhauser, Samuel A. Morello, Robert C. Innis,
and James M. Patton, Jr.

Ames Research Center
and
Langley Research Center

SUMMARY

A flight investigation was performed with the Dornier DO–31 VTOL to evaluate the performance, handling qualities, and operating characteristics that are considered to be important in the operation of a commercial VTOL transport in the terminal area. The DO–31, a 20,000 kilogram jet transport, has a mixed propulsion system; main engines with nozzles deflect from a cruise to a hover position, and vertical lift engines operate below 170 knots. This VTOL mode incorporates pitch and roll attitude and yaw rate stabilization.

The tests concentrated on the transition, approach, and vertical landing. The mixed jet-propulsion system provided a large usable performance envelope that enabled simulated IFR approaches to be made on 7° and 12° glide slopes. In these approaches management of thrust magnitude and direction was a primary problem, and some form of integrating the controls will be necessary. The handling qualities evaluation pointed out the need for additional research to define flight-path criteria.

The aircraft had satisfactory control and stability in hover out of ground effect. The recirculation effects in a vertical landing were large below 15 meters.

INTRODUCTION

Commercial V/STOL aircraft offer the possibility of overcoming many of the shortcomings of present short-haul air travel. Their low-speed characteristics allow them to operate from small airfields conveniently located near the centers of population. Additionally, these characteristics should reduce air and ground maneuver time and improve reliability under adverse weather conditions (refs. 1 to 5). Although considerable research and development have been done over the past decade in the United States and abroad on the performance, handling qualities, and operating characteristics of different types of V/STOL aircraft (refs. 6 to 14), it has been difficult to assess the potential of commercial V/STOL transport aircraft realistically and to define the desired characteristics, particularly for IFR conditions. Each aircraft tested had limitations either due to size, stability and control, inherent characteristics, or inability to represent IFR flight.

Consequently, a flight evaluation was made with the Dornier DO–31 jet VTOL transport because this aircraft has several features that make it superior to other research aircraft for assessing the terminal-area operation. First, it is sufficiently large (20,000 kg) to represent a first generation transport. Second, it has a mixed propulsion system (main fan-jets with vectoring nozzles plus lift-jet engines) that provides a very broad performance envelope. Third, it has an advanced control and stabilization system that can reduce pilot workload. Fourth, the controls and displays are duplicated so that IFR operation can be simulated. The NASA flight tests concentrated primarily on the transition, approach, and vertical landing phases of operation since these are generally considered to be the most demanding in terms of aircraft performance and handling qualities. The tests were conducted on 7° and 12° glide slopes with some simulated IFR operation.

The tests were conducted by NASA personnel from Ames and Langley Research Centers in cooperation with the Dornier Company, Bundesministerium für Wissenshaft und Forschung (BWF), Bundesministerium für Verteidigung (BMVg), and the Deutsche Forschungs und Versuchsanstalt für Luft und Raumfahrt (DFVLR).

DESCRIPTION OF AIRPLANE AND EQUIPMENT

The DO–31 is a high-wing, mixed-propulsion, jet V/STOL transport with two main engines (vectored lift-cruise) and eight lift engines. The aircraft was designed and constructed by the Dornier Company for a V/STOL research program initiated in 1962 and sponsored by the German Federal Ministry of Defense. Figure 1(a) is a photograph of the airplane in the VTOL mode and figure 1(b) is a three-view drawing. Additional details are given in table 1. The first flight of the aircraft in 1967 was followed by 24 hours of flight tests primarily to define the operational envelope and document the performance. The subsequent NASA program for 11 flight hours primarily evaluated and documented handling qualities in the V/STOL mode and simulated IFR operation. The normal operating mass of the aircraft was about 19,500 kg (43,000 lb).

Propulsion

The DO–31 aircraft is equipped with two Rolls Royce Pegasus 5–2 turbofan engines and eight Rolls Royce RB–162–4D lift jet engines. The two Pegasus 5–2 engines are mounted under the wing and have nozzles to vector the thrust. Each engine has four nozzles that vector the total thrust force from a 10° thrusting to a 120° braking position. The engine and nozzle arrangement is essentially the same as used on the Hawker-Siddeley Harrier VTOL aircraft. Each Pegasus 5–2 engine is rated at 67,200 N (15,100 lbf) of uninstalled sea-level static thrust. At each wing tip four RB–162–4D lift engines are housed in pods. Each RB–162–4D engine is rated at 18,700 N (4,200 lbf) of uninstalled thrust at sea level.

Flight Controls

Figure 2 shows schematically the separate control functions, and figure 3 shows the cockpit layout. The flight attitude controls are a stick and rudder pedals. In cruise the controls are linked to the ailerons, elevator, and rudder. In hover, rolling moments are produced by differential thrust

between left and right sets of lift engines. The thrust is commanded by the fuel control units (FCU) which are linked in each pod to the stabilization system and the stick. The pitching moments are produced by reaction controls located at the aft end of the fuselage; high pressure air is supplied from each main engine through separate ducts and nozzles. Yawing moments are created by fore and aft movements of nozzles on the tail pipes of the lift engines. As with roll control, the pitching and yawing motions can be controlled by either the pilot or the stabilization system. In the transition the moments are produced by a combination of the hover and conventional controls because the latter move at all speeds. In addition to the stick and rudder pedals, one set of main engine throttles, two main engine nozzle control levers (one for each pilot), and one lift engine thrust lever are used for flight control and are located in the center console.

The DO–31 flight control system is powered by dual hydraulic actuators with control rods, summing bars, etc. The relation between the control forces and deflections is given in figure 4. The stick deflection in millimeters is given on the secondary scale of the deflection in degrees. It should be noted that this transport has a stick rather than a wheel, and also that the lateral control motion is obtained by movement about a pivot near the center of the stick (fig. 3(a)). The pilots found the use of a stick preferable to a wheel for a transport VTOL because it did not obstruct their view, and it was more natural to use with the one-hand method of control required during transition and hover. The forces and deflections were quite satisfactory.

Figure 5 relates the throttle and engine characteristics. The lift engines are started together with the lever at 17° FCU; after about 10 sec, a stable subidle is achieved and the individual warning lights are extinguished. The lever is then advanced to 30°, and 10 sec later a stable flight idle is attained and another set of lights are extinguished. The forces and deflections of the engine levers were satisfactory except for the fact that it was undesirable to have the height control in the VTOL mode split between the main and lift engines; one control combining the two functions would be preferable. The main engine nozzle control was satisfactory, but the deflection had to be monitored with the indicator on the panel, and a better display was warranted.

Stabilization System

The aircraft is equipped with a full-authority, single-channel, attitude command control system for the pitch and roll axes and rate command control for the yaw axis. Figure 6 presents the block diagrams of the stabilization and control system of each axis in the VTOL mode. Figure 7 is a schematic of the stabilization system for each axis. The pitch and roll attitude stabilization system compares the commanded attitude from the control stick signal to the actual aircraft attitude derived from the attitude gyro signal. In the yaw axis, rate is compared rather than attitude. These error signals are then used through the servo-motors to drive the aircraft to the commanded steady-state conditions shown in figure 8. The maximum pitch and bank angles available with full stick deflection were sufficient for all maneuvering; the yaw rate available was too low. The control signals are introduced additively through a mechanical linkage; thus, in the event of a stabilization system failure, the control immediately reverts to a direct mechanical and unaugmented control. If the control is deflected beyond the position of the limit switch (fig. 8), the stabilization system is disengaged for safety since this would infer a "hard over" failure. Consequently, the pilots were reluctant to use large control deflections for fear of disengaging the stabilization system. They considered this method of disengaging the system unsatisfactory because the control reverted to an acceleration command system. The aircraft has a roll damper to improve the lateral controllability

throughout all flight modes. In the VTOL mode, trim is provided in pitch only, and there was a desire to have lateral trim. The pilot can control the pitch trim in two manners: (1) by a trim switch on his stick, and (2) by a preselect switch on the instrument panel (fig. 3(a)). For the latter case, he can dial in the desired pitch attitude at any time, and by pressing a button on the stick the attitude changes to the preselected value at the rate of 3° per second. This rate was satisfactory; a lower rate would not be satisfactory. The preselect trim system was a desirable feature, but the panel-mounted switch was somewhat awkward to use. In the conventional mode, trim is provided for each control.

Cockpit Instrumentation and Displays

Figure 3(b) illustrates the arrangement of the cockpit instruments and displays for the evaluation pilot. For the NASA tests only glide slope and localizer error information was used; this was displayed on the attitude director indicator (ADI). True airspeed was obtained from the "Fluglog" (a free-turning, self-alining propeller utilizing the anemometer principle with optical pickups to sense rpm), developed by Dornier and mounted on the end of the nose boom. The face of the standard production airspeed indicator was changed to display 5-knot increments of true airspeed. Angle of attack and sideslip were taken from the deflection of the fluglog and displayed to the pilot.

Data Acquisition

The airborne equipment was capable of registering 208 different data channels simultaneously. One portion of the data was stored in analog form on magnetic tape onboard the aircraft, and at the same time transmitted to a ground station onto magnetic tape. The remaining data were sampled and then stored in digital form on a tape recorder in the aircraft. Safety of flight information was telemetered to a ground station to be recorded and monitored during the flights. Computers were used to reduce the data to engineering units on plots and tabulated printouts for data analysis.

A ground-based radar operated by DFVLR was used to obtain the position of the aircraft during the approach and landing phase of the flights. The measurements were printed out at 1 sec intervals and were time correlated with airborne data.

Guidance

Guidance for the instrument approaches was provided by ILS equipment based at the airfield and operated by DFVLR. This system was capable of providing a wide range of glide-path angles and sensitivities. Figure 9 illustrates the profiles and sensitivities used during this investigation. The half beam width provided a full-scale deflection of 3 dots on the ADI. No other approach or navigational aids were available. The glide-slope transmitter was located adjacent to the VTOL landing area (see fig. 9).

TEST PROCEDURES AND CONDITIONS

Test Location

All tests were made at the Dornier Flugplatz in the outskirts of Munich, Germany. The field elevation was 600 m and the temperature ranged between 0 and 12° C. The flights were made under Visual Flight Rules (VFR) over a range of wind conditions. The wind speeds from 0 to 10 m/sec measured near the ground with an anemometer included headwind, crosswind, and tailwind. For all flights the Dornier pilot was in command in the left seat.

Hover-Rig Tests

A hover-rig simulating the DO–31 in the VTOL mode was used for pilot checkout and training. This rig, shown on the pedestal in figure 10, was also flown in free flight over a range of speeds up to 40 knots (forward and sideward) and a range of altitudes up to 100 m above the runway. The tests were limited to 5 minutes by the fuel available and the continuous lift engine running time. The rig was similar to the DO–31 in terms of the VTOL propulsion, control, and stabilization systems, and had similar responses. Three rather than four lift engines were installed in each pod, and the mass and inertia of the rig were lower than the DO–31. When mounted on the pedestal in its raised operating position, the hover rig had restricted angular movement and no vertical movement. The rig was very useful because the pilots could evaluate the angular response in hover with and without stabilization and also the angular response to shutting down a lift engine or main engine. After a few pedestal runs each pilot made several free-flight tests. These included tests with the stabilization system turned off, but did not include engine failures.

DO–31 Tests

All flight tests were within the operational envelope established by the Dornier Company. Engine failures were not simulated or performed. All tests were made with the stabilization system engaged, except for limited tests with the yaw rate stabilization disengaged during the approach.

Most flights began with a conventional takeoff at a mass of about 21,500 kg (47,000 lb), and consisted of three to five approaches, terminating at about 70 m altitude either in a waveoff at 50 knots or a hover and a vertical landing at a mass of about 18,500 kg (41,000 lb). These procedures were used primarily to maximize research time with the limited lift engine time and fuel. Several vertical takeoffs and some hover evaluation was also made. The lift engine time was limited to 5 min per start by the simple oil system, and each flight lasted about 20 min. One flight was devoted to a climb to 3,000 m to document and evaluate the use of the main engine thrust deflection for rapid descent and deceleration from cruise altitude and speed. The total of 11 flight hours was equally divided between the Ames and Langley pilots. This flight time permitted 90 approaches to be made, of which 40 simulated IFR operation.

The glide-slope angles and sensitivities were varied during the program. Tests were made primarily with a 7° glide slope with a beam width of ±2°. Limited tests were made with 7° ±1° and with 12° ±2°. The variations in flight profile tested are tabulated below:

Glide slope, deg	Intercept altitude, m (ft)	Lift engine starting condition
7	600 (2000)	Level flight
7	450 (1500)	Level flight
7	300 (1000)	Level flight
7	600 (2000)	On glide slope
7	450 (1500)	On base leg in turning flight
12	600 (2000)	Level flight
12	450 (1500)	Level flight
12	900 (3000)	On glide slope

During most of these tests, the location of the aircraft was recorded and correlated with on-board measurements.

STOL tests were not performed by NASA because of limited time available and because of potential damage to the runway and aircraft. Concern about damage was due to the runway's being surfaced by asphalt (except in the VTOL landing area, fig. 9) which could not withstand the hot gases from the lift engines for any extended time.

RESULTS AND DISCUSSION

To fully realize the commercial potential of VTOL transports, they will be required to operate routinely to low visibility minimum under Instrument Flight Rules (IFR) and to minimize ground and air maneuver time, fuel, airspace and noise. These requirements clearly indicate the landing approach to be the most critical flight condition for these aircraft. Further, previous NASA research has shown the approach phase to be the most demanding in terms of pilot workload and has indicated that a number of unresolved questions exist. Therefore, the NASA flight tests of the DO–31 concentrated on evaluating the performance, handling and operating characteristics of this mixed jet-propulsion concept with an advanced stabilization system in simulated IFR approaches.

It must be recognized that the flight test time of the program was limited, and included the time required to familiarize the two NASA pilots. Consequently, the operating procedures and patterns used were primarily those developed by Dornier personnel, and the documentation and evaluation of handling qualities were limited. For these reasons the pilot comments are given in an adjective and commentary form rather than in a quantitative form.

The section entitled "Performance and Test Procedures" contains static climb and descent characteristics supplied by Dornier to describe the operating envelope. Time histories are included that illustrate a typical vertical takeoff and transition to conventional flight, and a transition to VTOL configuration, approach, and vertical landing. The "Handling Qualities" section contains the measured characteristics to support the NASA pilots' evaluation of workload in approach and landing. The last section "Terminal Area" presents primarily the results of complete approaches.

There are also some results of translating near hover, and a simplified comparison of different approach and landing techniques in terms of airspace and time used.

Performance and Basic Operating Procedures

Low-speed operational envelope– The operational envelope for the DO–31 is illustrated in figure 11 as climb and descent for unaccelerated flight versus airspeed. Included in these figures are lines of 10° and 20° climbing and descending flight paths in unaccelerated flight. Since most tests were made in accelerating or decelerating flight, it should be recognized that these lines also approximate 0.17 and 0.35g acceleration and deceleration in level flight; that is,

$$\gamma_{rad} + \frac{1}{g}\frac{dV}{dt} = -\frac{C_D}{C_{L_1} g}$$

First, in the conventional mode where the lift engines are inoperative (fig. 11(a)), it can be seen that with the two main engines operating at a high power setting, an extremely large range of flight paths can be obtained by deflecting the nozzles of the main engines from 10° (thrusting) to 120° (braking). Buffet occurs with nozzle deflections greater than 85° at the higher airspeed; however, more than sufficient descent performance is provided for a rapid letdown. Although 20 to 30 knot reductions in stalling speeds were achieved over the power off value, the operational speed could not be reduced because of the minimum control speed requirement, V_{MC}. The V_{MC} was defined with the nozzles at 10°, and it was limited by the directional control of the conventional rudder. For this condition with an engine inoperative the rate of climb was 5 m/sec (1000 ft/min).

In the VTOL mode with all of the lift engines operating, the range of operation is very large (fig. 11(b)). The curves shown are illustrative of the configurations used during the NASA tests. The range of lift engine throttle settings shown for the approach configuration leave a margin above flight idle and below emergency thrust to provide sufficient modulation for lateral control. The curve with $\sigma_{FCU} = 40°$, $N_F = 80$ percent, $\sigma_M = 120°$ is about the maximum descent capability of the DO–31. The main engine speed, N_F, was not reduced below 80 percent so that sufficient bleed air could be provided for pitch control. Steady descent rates below a 50 knot airspeed were not defined, but it can be presumed that instantaneous values greater than 10 m/sec are attainable. In hover, the maximum descent rate is dictated by the landing gear touchdown design speed of 4 m/sec. The waveoff is with a typical approach power setting and the nozzle deflection reduced from 120° to 70°. The takeoff case is with reducing nozzle deflection as speed increases (artificially presented at 0 acceleration for comparative purposes). Obviously, different performance curves can be established for different power settings, nozzle deflections, and angles of attack, depending on the desired feature to be optimized. The maximum airspeed at which the lift engines have been operated is 170 knots; normally, the maximum airspeed was 160 knots to have a margin and to avoid instability of the fixed-gain stabilization system. Although it is not shown in the figure, a positive climb can be achieved over the entire speed range with one lift engine inoperative, and over a large part of the range with a main engine inoperative.

The thrust-weight ratios available in hover, out of ground effect are given in figure 12 for an aircraft mass of 18,500 kg and a field elevation of 600 m. Three curves are shown: the upper curve is for all lift engines operating at maximum continuous thrust and both main engines at a 2-1/2 min

rating, the middle and lower curves show the effect of a lift-engine failure and a main engine failure, respectively; for both cases lateral symmetry is maintained. It should be noted that the vertical force can be further increased by utilizing a main engine emergency rating. These curves illustrate the magnitude of thrust-weight ratio that is installed to compensate for an engine failure and that might be available to develop normal acceleration for maneuvering near hover out of ground effect. It is seen that the effect of a lift engine failure is small compared to a main engine failure; however, even in the latter case the aircraft can be balanced and a thrust-weight ratio in excess of 1 can be developed.

The proximity of the ground ($h < 15$ m) was estimated to reduce the vertical force by about 10 percent; this reduction was caused by recirculation and reingestion of gases into the main engines.

Vertical takeoff and transition– The takeoff performance and procedures are illustrated in figure 13. Once the lift engines have been started it is necessary to proceed rapidly with the takeoff for two reasons: (1) the idle thrust is so high that the aircraft is very light on the gear, and (2) it is desirable to move away from the large hot gas cloud developing. A nozzle deflection of 75° is used for takeoff to minimize the recirculation effects. Even though the main engine nozzles and the lift engines are now both deflected 15° aft of the vertical, there is practically no ground roll in the takeoff because of the large thrust-to-weight ratio applied at takeoff. The result is a steep, high acceleration takeoff and transition with an average acceleration of more than 0.2 g. In just over 20 sec sufficient airspeed is attained to shut off the lift engines. A steep climbout can be continued because of the high thrust-weight ratio of the main engines (T/W = 0.6).

Approach and vertical landing– The procedures and flight paths used for two different approaches to a vertical landing are illustrated in figure 14. The three primary phases of the approach for this VTOL are:

1. The conversion from conventional mode to the VTOL mode;
2. The initial transition where the aircraft is decelerated from about 150 knots to 50 knots during which time a precision approach is made;
3. The final transition to hover from 50 knots at 60 m followed by a vertical landing.

For the pilot to complete these three phases with repeatable precision and low workload, specific changes in engine thrust, nozzle deflection and attitude were prescribed that he performed at selected locations on the path. In order to hover with no charge in main engine throttle and with only a small adjustment to the lift engine thrust, the approaches were made near zero aerodynamic lift (at small negative angles of attack).

The first phase of the approach began with the pilot establishing the preconversion configuration before the localizer was acquired; that is, lowering the gear and flaps, reducing the airspeed to about 140 knots, opening the lift engine pod doors, engaging the attitude stabilization system, and setting the desired pitch attitude on the preselect switch. The 140 knot airspeed was necessary to avoid instability caused by the fixed gain stabilization, and to preclude high lift engine rotational speeds before they are started. The pilots noted that little time was needed to engage and verify that the stabilization system was operative. Next, the conversion was initiated by starting the lift engines and advancing them to an idle speed ($\sigma_{FCU} = 30°$); all eight engines are started automatically, and it required about 20 sec to obtain a stable idle. During this period, the pilot

changed the pitch attitude to reduce the wing lift to compensate for the vertical force of the idle lift engines, and he deflected the nozzles to maintain constant airspeed. The lift engines were started before or after the glide slope was intercepted.

The second phase was the precision approach where the pilot made corrections primarily by modulating the lift engines with the aircraft stabilized at the selected pitch attitude. The main engine nozzle deflection for this phase usually was at 120° (maximum braking) to provide the desired deceleration schedule; in some cases deflections were smaller to adjust for headwinds. At about 60 m altitude, the pilot began the third and final phase of the approach by rotating the aircraft to +5° attitude (through the preselect trim system), changing the nozzle to 95°, and making small lift-engine corrections to attain a stable hover. He then adjusted the lift engine throttles to establish the desired sink rate for the vertical touchdown.

Handling Qualities

The NASA handling qualities tests concentrated on selected stability and control characteristics of the aircraft and stabilization system that would be of general interest for future commercial V/STOL transports. Figure 15 gives a detailed range and time history of one of the simulated IFR approaches where the lift engines were started in level flight, a 7° glide slope was tracked to 75 m altitude, after which the aircraft was flared to commence the vertical landing under visual conditions. These data are presented as a basis for the following discussion of handling.

A major element in the success of the DO–31 to perform a precision approach and to make a safe vertical landing is the pitch and roll attitude stabilization system. This system has 100-percent authority and dominates the basic aerodynamic stability and control characteristics. It is designed so that the pilot can command pitch and roll attitude and yaw rate in proportion to control deflection over the major range of pilot inputs (see fig. 8) and over the speed range for the VTOL configuration (from about 160 knots to hover). An automatic trim feature permits the pilot to preselect the desired pitch attitude which is then commanded with a button on the stick. The system has been optimized for the hover task, and it minimizes aircraft disturbance due to turbulence, configuration change, or asymmetry such as caused by an engine failure.

Because of the limited test time, extensive documentation was not performed and the information should be considered as an overview rather than a detailed analysis. It should also be noted that prevailing atmospheric conditions of winds and gusts were accepted and may have affected some of the initial and transient conditions.

Conversion– When the lift engines are started in level flight according to the procedures described earlier, the conversion can be performed with little altitude change and only a small attitude change (fig. 15(b)). In several cases the lift engines were started after the glide slope was intercepted rather than in level flight, for example, on the 12° hooded approach shown in figure 16. The conversion procedures were similar to those for starting the lift engines in level flight, and incurred no major piloting problems, provided the intercept altitude was raised to allow sufficient time for tracking after the lift engines were brought to approach thrust.

No significant handling qualities problems existed in maneuvering the aircraft to intercept the localizer in the conventional flight regime. The aircraft handles as a large docile fighter with light

control forces. The conventional surface deflection per unit control deflection is reduced with a gear changer as airspeed is increased to give good response, force, and force per unit acceleration characteristics at the higher speeds (appendix B).

ILS acquisition and tracking; longitudinal flight-path control– At the higher speeds, say above 100 knots, changes in angle of attack produced by pitch attitude changes were very effective (1) in maintaining flight path while the lift engines were advanced to the approach setting, and (2) in changing the flight path to acquire the ILS. For example, a stick deflection that rapidly changed angle of attack only 1° or 2° caused an acceleration of 0.1 g normal to the flight path. When the preselect feature of the stabilization system was used to change flight-path angle, moderate pitch rates occurred (3°/sec). Making large attitude changes (to acquire the glide slope, for example) caused a horizontal acceleration at a time when the pilot desired either to maintain constant airspeed or to reduce airspeed. The main engine nozzles were very effective and easy to use in controlling the airspeed at these times (see figs. 15(a-c)).

As the airspeed was decreased below 100 knots the longitudinal control became less effective in changing flight path. In the decelerating approach not only does the angular response to control input change, but the flight-path response to angle of attack also changes; consequently, the pilot must continually readjust his gains as the airspeed decreases. At speeds of about 50 knots large changes in angle of attack must be made to develop the desired normal acceleration, and these introduce undesirable airspeed changes because of the rotation of the thrust vector with respect to the flight path. Therefore other methods of flight path and airspeed control were evaluated and documented in the 60 to 90 knot speed range. These were the use of (1) lift-engine thrust, (2) main-engine thrust, (3) main-engine nozzle deflection, and (4) pitch attitude. The peak measured incremental normal and longitudinal accelerations produced by these controls are compared in figure 17 with values calculated from the thrust components. Figure 18 presents time histories of the aircraft response to these controls; the incremental changes in velocity, altitude, and flight path were calculated from the accelerometer readings and represent the change due only to the control (see appendix A).

At speeds below 90 knots the pilots preferred to modulate lift engines for tracking, but noted that control was insufficient for large upward corrections. Modulation of the lift engine produced a maximum of ±0.1 g normal acceleration (fig. 17(a)). A small acceleration parallel to the flight path was produced because the lift engine axes are inclined 15° from the fuselage reference line (fig. 2), and the aircraft was flow near 0° angle of attack. The peak normal acceleration was rapidly achieved because the engine time constant was small (about 1/4 sec), and the measured accelerations agreed well with the values computed from the thrust components. The normal acceleration decreases rapidly after the throttle input (fig. 18(a)) because of the damping in heave (change in lift with angle of attack) at constant pitch attitude. The result is a fairly constant increment in vertical velocity 3 sec after the input. In figure 18(a), the altitude change in response to a control input of about 60 percent of the maximum is small; after 10 sec the altitude increased only 6 m which is equivalent to only 1/10 of the glide-slope beam width at an altitude of 200 m (assuming $\gamma_G = 7° \pm 1°$, fig. 9).

For a main engine throttle step (fig. 17(b)) the magnitude of normal acceleration was similar to that produced by the lift engine. However, a large longitudinal deceleration accompanied an increase in propulsive force because the nozzles were deflected 120° for the desired flight path and deceleration schedule. There is little damping to reduce the longitudinal acceleration; therefore, a

large unwanted decrease in airspeed occurs. The magnitude of the speed change indicated in figure 18(b) was sufficient that the pilot had to compensate with a change in nozzle deflection, thereby increasing his workload. He considered the use of main engine thrust modulation with the nozzles at 120° to be an unsatisfactory flight-path control. He felt that the time constant of either the main or lift engines (about 1/2 sec and 1/4 sec, respectively) did not detract from the tracking task during this portion of the approach.

Modulating only the nozzles of the main engines (figs. 17(c) and 18(c)) was unsatisfactory for making flight-path corrections while tracking the ILS because little normal acceleration was developed compared to the longitudinal acceleration. Since a large longitudinal acceleration was rapidly produced, this nozzle control was useful in correcting airspeed and in making long period adjustments for large flight path changes (such as required for intercepting the glide slope and adjusting for headwinds). The nozzle deflection could be rapidly changed, and 0.1 g longitudinal acceleration was obtained with about 15° nozzle movement.

Figure 18(d) shows the response of the aircraft to an attitude change. A normal acceleration of 0.15 g was produced by pitching the aircraft 6°. This change in attitude caused a deceleration of 0.1 g along the flight path, causing an unwanted airspeed error of 8 knots after 6 sec. The combination of normal acceleration and longitudinal deceleration was similar to that for a main-engine step, and when combined with the large attitude increment required to develop the desired normal acceleration produced an unsatisfactory flight-path control. Figure 17(d) shows that the normal acceleration and longitudinal deceleration changes can be approximated by the lift change with angle of attack and the rotation of the resultant force ($\Delta\theta/57.3$), respectively.

As illustrated in figures 15 and 16 good tracking of the glide slope could be achieved by using the lift engines provided the pilot is initially on the glide slope. In the process of evaluating flight-path control, glide slope offsets were purposely introduced to simulate situations that might occur in normal operations, such as those caused by wind shear and turbulence. With the glide slope set at 7° ±2°, offsets of 1/2 dot (1/3°) or less below the glide slope and any offsets above the glide slope posed no major problems. Offsets of 1 dot (2/3°) or more below the glide slope brought about expected power management problems because the lift engines produced insufficient normal acceleration. This problem is illustrated in figure 19. At t = 14 sec the pilot advanced lift engines to the maximum normal thrust level, but there was little change in glide-slope error. At t = 30 sec the nozzle deflection was reduced, but this did not correct the glide-slope error because the primary effect of reducing nozzle deflection was to increase airspeed. Finally, at t = 39, the aircraft attitude was increased; then the glide-slope error decreased, and the airspeed also decreased. If the aircraft had first been pitched, the glide-slope error could have been corrected earlier, but the airspeed would have dropped to a much lower value than desired. Figure 20 shows a tracking run made with main engine rather than lift engine modulation. While tracking was equally as good as that in figure 15, the pilot workload was greater when he tracked with the main engines because of the undesirable airspeed perturbations. This effect on the open loop deceleration is evident in figure 20 at t = 39 sec where the main engine thrust was increased to avoid going lower on the flight path; shortly thereafter the airplane decelerated to below 60 knots which was below the desired speed scheduled. The pilot then decreased the nozzle deflection to increase airspeed, but the increase to 80 knots was too large, and the nozzles were rotated back to the full braking position to arrest this overspeed. Thus, one large tracking error can possibly force the pilot to modulate two, three, or four control levers at a time when he prefers as many parameters as possible to remain constant.

Reference 7 presented a criterion for satisfactory STOL flight-path control during ILS tracking as ±0.1 g normal acceleration to be achieved in less than 1.5 sec. This criterion was satisfied by the DO–31 operating in the 60 to 90 knot range with lift or main engine thrust modulation, but the pilots considered either control unsatisfactory for tracking an ILS. It is concluded that the criterion was inadequate becaue it only specified a maximum acceleration normal to the flight path to be achieved within a given time. It appears that flight-path control criteria should include changes in altitude or flight path or both after several seconds, and should also limit airspeed and attitude changes. Such a criterion would be analogous to lateral control criteria where time to bank 30° is specified with the maximum permitted cross coupling. There are insufficient data at present to revise the criteria for tracking an ILS with V/STOL aircraft; however, the following recommendations are made:

1. The control of acceleration normal to the flight path should be achieved with little acceleration along the flight path (i.e., direct lift control is desired). When normal acceleration is increased (upwards), an acceleration along the flight path is preferred over a deceleration; a deceleration along the flight path greater than 50 percent of the normal acceleration is unsatisfactory. The flight path should be changed at least 2° within 2 sec after the control input; thereafter the flight path should not return toward the initial conditions.

2. Independent control to produce an acceleration along the flight path should cause no appreciable downward acceleration, and a small upward acceleration is desired.

Additional simulation and flight tests are required to define the criteria and provide limits to cross coupling (such as unwanted airspeed changes).

Final transition and vertical landing; longitudinal and height control– The final transition to a vertical landing was shown in time history form in figure 15(e). To reduce the pilot workload the normal precision approach procedure was to fly the aircraft near zero lift so that the main and lift engine settings were near hover values and to use a main nozzle deflection of about 120° to decelerate the aircraft to an airspeed of 50 to 60 knots by the time the altitude was down to 50 to 70 m. At this point (t = 110 sec in fig. 15(e)) the aircraft is flared by pitching to +5° attitude with the preselect trim system; then the lift engine thrust, main engine nozzle deflection, and aircraft heading are adjusted to maintain the aircraft over the touchdown area. The lift engine thrust is readjusted to produce a small sink rate (less than 2 m/sec). As the aircraft descends below 15 m altitude, recirculation and reingestion increase the sink rate. In the descent from 60 to 15 m, the pilot can increase the lift engine thrust to reduce the sink rate; however, there was concern that the resulting increase in gas cloud could increase reingestion into the main engine and increase rather than decrease sink rate. Figure 21 illustrates the suckdown magnitude during a vertical landing in the DO–31. This time history of altitude, sink rate, and vertical acceleration is typical for a low sink rate descent when there is no increase in lift engine thrust just prior to landing to compensate for (1) suckdown forces on the under surfaces of the airplane, and (2) main engine thrust loss due to exhaust gas reingestion. The result is a downward acceleration of approximately 0.10 g 1 sec before landing with a touchdown impact of about 2.5 m/sec induced by the combined suckdown and reingestion factors. For the example given in figure 15(e), the lift engine thrust was increased to the maximum normal thrust setting just before touchdown, yet the touchdown descent rate was more than 1 m/sec. Thus it can be seen that below 10 m altitude the landing commitment is definite. Even though the main engine thrust could have been increased, the effect on the

reingestion was of concern; thus there was no "go around" capability in these tests. At any point down to 30 m, waveoffs were easily accomplished by pitching the aircraft to ±5° and repositioning the nozzles to 65°.

The NASA pilots considered the available control from lift engine modulation insufficient for descent control in hover. Since the normal acceleration was less than 0.1 g, the vertical velocity damping near zero, and the lift engine time constants small, these results agree with those of references 12 and 14. When this limited control was coupled with the recirculation effects, the NASA pilots rated the vertical descent and landing unacceptable for a commercial VTOL transport.

ILS tracking; lateral-directional flight-path control– At speeds above 50 knots large lateral corrections were difficult to make. The aircraft response to a lateral step with the stabilization engaged on all axes and with rudder pedals fixed is given in figure 22(a). For this test the stabilization system maintains zero yaw rate, there is no change in heading; and the sideslip is related to the bank angle. The pilots noted that large bank angles were needed to develop the desired lateral velocity, high sideslip angles developed, and it took longer to make the correction than was desired. It was concluded that large lateral corrections could not be made satisfactorily by only translating the aircraft. When the pilots used the directional control (which commanded yaw rate) to coordinate the maneuver, it was impossible to find the correct input to maintain small sideslip angles; the aircraft responded as if it had no directional stability. Tests were also made with the yaw rate stabilization off. For this condition and no pedal input (fig. 22(b)), the sideslip excursion was proportional to the bank angle ($\Delta\beta/\Delta\phi = 1$), and the aircraft had a fairly long directional period (7-8 sec) with low directional damping. It was concluded that additional augmentation for turn coordination was needed. In reference 7 it was pointed out that for satisfactory handling, $\Delta\beta/\Delta\phi$ should be less than 0.3, and methods to achieve these levels were discussed.

The requirement for large bank angles to develop suitable lateral velocities was not expected based on small-scale tests of the DO–31 (ref. 8) nor on predictions made by Dornier personnel. The static lateral-directional characteristics measured in flight are given in figure 23. These data show that 10° of bank angle are needed to achieve a lateral velocity of 10 knots at 60 knots forward speed. The bank angle per unit sideslip was 2 to 3 times that calculated from the tests of reference 8 where the lift engine flow was simulated but the main engine flow exhausted at 0° rather than 120° used in the flight tests.

The easiest procedure for making small corrections while tracking the localizer beam was to use the directional control (with yaw stabilization engaged) and let the aircraft translate laterally with the wings held level by the attitude stabilization system. The desired heading could be maintained by the stabilization system and this avoided the wandering exhibited by other V/STOL aircraft at comparable approach speeds (ref. 7).

Lateral control, sensitivity, and response were satisfactory at the transition speeds; however, the attitude command feature required the pilot to maintain a lateral force in turning flight, and even though the force was low the pilot found it unnatural and uncomfortable.

Final transition and vertical landing; lateral control– Considerable research has been performed by NASA and others on the magnitude of lateral control power needed for satisfactory performance of the hover task (refs. 9 and 10); however, considerable postulation remains on the

effects of aircraft size and degree of stabilization (refs. 11 and 12). Since the DO–31 is the largest VTOL tested by NASA (45,000 lb), has an attitude command stabilization system, and has a relatively low lateral control power installed (0.8 rad/sec^2), it offered a unique opportunity to examine the lateral controllability in flight in a realistic environment and to compare the results with simulator prognostications. The following evaluation and discussion of the lateral control power characteristics of the DO–31 during very low speed flight (at or near hover) is in the form of reference 12 where the maneuver, trim (balance) and upset requirements were discussed. It is assumed that the aircraft is being operated as a commercial V/STOL transport; that is, only modest VTOL maneuvering is required, an engine failure must be controlled, and the aircraft must be operated in adverse weather conditions.

Maneuvering characteristics: The effect of stick deflection on the static rolling moment available and on the angular acceleration is shown in figure 24. It is seen that the maximum rolling moment is essentially independent of the lift-engine throttle setting (σ_{FCU}). Figure 24(b) contains several measured peak roll acceleration values. These values are larger than the calculated values of L/I_X because the rolling moment is based on a static value and the stabilization system initially commands higher acceleration to give more rapid angular response to a pilot's normal input. The more rapid response is evident in the time histories of a stick step (fig. 25). With stabilization (left hand figure) the lift engine fuel control units (FCU) are commanded to very large deflections shortly after a pilot's input of 1/4 stick deflection, and the initial response ($t < 2$ sec) is greater than without stabilization (right hand figure). With the same input and stabilization a 5° bank angle was attained in 1 sec, and the bank angle reached 90 percent of the steady-state commanded value, 10°, in about 2-1/2 sec. As the pilot input is increased in magnitude, the differences in aircraft response with and without stabilization becomes less because there is less excess moment available to increase the acceleration. The pilot input for the bank step with stabilization is a stick step and is easy to perform. The lag of peak RPM behind the stick input reflects the lift engine time constant of 0.2 to 0.3 sec. The aircraft response closely matched a calculated time history based on a natural frequency of 2.5 rad/sec, a damping ratio of 1.1, and an initial lag of 0.2 sec; these characteristics were within the optimum areas defined by the simulator study reported in reference 10. Since the pilots rated the lateral control sensitivity and maximum control power (a value of 0.8 rad/sec^2) as satisfactory good agreement was obtained with the study of reference 10. The pilots also considered the response, displacement and damping to be satisfactory. It should be noted that care was taken to keep the friction and force gradient of the control system low (fig. 4(b)). The values correspond to those recommended in reference 12.

The control inputs of figure 25 were made to document the aircraft response, and do not provide a measure of the lateral control needed for maneuvering. To make this evaluation the pilot was given two tasks: one was to perform what he believed to be the most extensive lateral maneuvering that would be required around the hover area, and the other was to determine the maximum lateral velocities that he would expect to use normally with commercial VTOL operation. Figure 26 illustrates the pilot input and control needed to maneuver the aircraft extensively near hover. Figure 27 shows the time history where the pilot slowly increased the bank angle in order to establish and measure lateral velocities. From these tests it was found that the maximum control power needed for control and stabilization during lateral maneuvering was ±0.4 rad/sec^2, and the maximum lateral velocity over the ground that would normally be expected in maneuvering V/STOL transports was 10 m/sec (20 knots). Higher lateral airspeeds may be encountered when it is necessary to position the aircraft precisely in crosswinds.

Trim or balance aspects: Some VTOL aircraft have required large amounts of lateral control to trim lateral moments developed in sideward flight. It can be inferred from the lack of change in differential RPM as lateral velocity increased (fig. 27) that the DO–31 required little or no control moment in sideward flight, at least for velocities of 10 m/sec. Another control requirement is to balance an engine failure. Figure 28 shows that the static moment resulting from a lift-engine failure can be easily balanced. Sufficient moment is also available to balance a main engine failure; however, little moment is available if the remaining main engine is advanced to a high setting to compensate for the lift loss. The dynamic response to a lift engine failure is shown in a time history of the shutdown of the number 1 lift engine performed with the hover rig on the pedestal (fig. 29). It is seen that with the stick fixed the aircraft rolls only 2° and within 1 sec of engine shutdown, the aircraft starts to return to the wings level position. During this compensation the remaining lift engines are initially commanded to a near emergency FCU level in the left pod and a near idle in the right pod to limit the rolling; shortly thereafter the difference in FCU levels reduced to a level required to maintain static symmetry. A larger bank angle was produced by a main engine failure and it took longer to return to wings level. From a piloting viewpoint the response to an engine failure was satisfactory; however, since the asymmetric moment was automatically trimmed out without changing stick position or force, the pilot had no direct way of knowing that he was near a control limit except by referring to actuator position gages on the instrument panel. From these data it can be ascertained that an engine failure on the DO–31 requires the greatest lateral trim. No flight tests were performed with an engine failed, but since three-fourths of the lateral control would be used for static balance, it would be expected that control for a vertical landing would be marginal. A lift engine failure would require less control moment; and the remaining lateral control power should be satisfactory for some maneuvering during the landing.

Compensation for gusts: The control power needed to compensate for gusts could not be determined, but the stabilization system was very effective in controlling upsets due to atmospheric conditions. In fact, the pilots remarked that the aircraft was very stable in a large variety of conditions, such as headwinds, crosswinds, and gusty air. The effectiveness of the stabilization system is illustrated by the compensation for an engine failure (fig. 29) which would be comparable to a gust producing an angular acceleration of about 0.4 rad/sec^2.

In conclusion, the lateral control power of the DO–31 (0.8 rad/sec^2) was sufficient to provide a satisfactory hover control provided that attitude stabilization was utilized. It should be noted that engine failures were not adequately evaluated in these tests. Although a research pilot could fly the aircraft with the stabilization system off, in commercial operation the workload required to hover and land such a craft would be unacceptable even for an emergency operation. Based on these tests significant reduction in control power cannot be recommended for this class and configuration of aircraft.

Trim considerations in transition and hover– Throughout the flight regime with lift engines operating, the attitude command stabilization system very effectively performed the trimming function so that the pilot was generally not aware of out-of-trim moments. Although the system greatly simplified the pilot's task, some warning must be given to the pilot if control limits are approached. For example, the previous section pointed out that a large amount of control was needed to compensate for an engine failure, and yet the pilot was not aware of the remaining control because the stick remained centered. This situation also occurred during a vertical takeoff

and transition (fig. 13). The pitch nozzle position indicates that 80 percent of the longitudinal control is required to compensate for the nose-up pitching moment at 40 knots and yet the stick is centered.

Another aspect of stabilization systems that must be considered is the pilot's complaint that a force must be maintained in turning flight at transition speeds. In this respect a rate command with attitude hold may be preferable to an attitude command system.

The ability to preselect the desired pitch attitude and to command it with the button on the control stick was a very desirable feature of the pitch attitude command system, because it reduced pilot workload during the approach when discrete pitch changes were required.

Terminal Area Operation

It was noted earlier that a wide range of ILS approaches could be made with this aircraft because of its large operational envelope and good control and stabilization system. This section will review the approach in terms of constraints that may be imposed on a commercial V/STOL transport operating in the terminal area.

Cruise letdown to preapproach configuration– Figure 30 presents a time history of a letdown from cruise altitude where the deflection of the nozzles of the main engines is used for controlling descent rate. The descent started at an altitude of about 2500 m and an airspeed of 260 knots and ended at an altitude of 450 m and 140 knots with localizer capture; the engines were set at a moderate thrust level, N_F = 72 percent. The maximum nozzle deflection permitted from structural considerations was 90° between 250 and 200 knots, and 120° below 200 knots. A heavy buffet accompanied the 120° setting during the descent and would be unacceptable from an operational standpoint. It was determined that an 85° nozzle setting was about maximum to avoid buffet, and this setting resulted in descent rates in excess of 20 m/sec, a sufficiently high descent rate for rapid letdowns. The use of the nozzles is considered an excellent method of establishing a varying rate of descent during the letdown.

Conversion– Before converting to the VTOL configuration, the pilot maneuvers to intercept the localizer; he then tracks it for about 30 sec while the aircraft stabilizes from the preconversion changes of gear and flap deflection. Then he starts the lift engines. Little change in altitude or airspeed occurs during this operation (fig. 15(b)) when pitch attitude, nozzle deflection, and main engine thrust are properly combined. It took about 20 sec to start all engines and attain a stable flight idle; the pilots considered this loo long because it distracted them from other flying tasks. This monitoring task was thus assigned to the copilot. Since there was no ground based guidance information, such as distance measuring equipment or beacons, level flight conversions were difficult to initiate at the proper location except when position was determined from visible landmarks.

The lift engines were also started on the glide slope (fig. 16), and in this case a better reference for starting the lift engines was provided by reference to the altitude. Because of the length of time required to start the lift engines, the intercept altitude had to be raised when they were started on the glide slope so that sufficient time remained to track after the aircraft stabilized.

ILS acquisition– With reference to figure 15, before the glide slope is intercepted, the desired pitch attitude for the approach is selected (-10° for 7° glide slope). When the aircraft nears the glide-slope centerline, the acquisition is initiated by releasing the preselect trim, by advancing the lift engine throttle to a hover setting, by deflecting the nozzles from 65° to 120° (braking), and by increasing the main engine thrust. The pilot performs all these changes in less than 4 sec. It is seen that if these procedures are followed, the flight path is changed with little overshoot, and about 15 sec later the pilot is confident that the glide slope has been acquired. At this point (t = 70 sec) the aircraft has decelerated to about 100 knots and is at an altitude of 250 m; the pilot can then proceed to track the ILS. By properly combining main and lift engine throttles, main engine nozzle deflection and longitudinal pitch control, the pilot could intercept 7° and 12° glide slopes and track these slopes with acceptable accuracy while decelerating from 140 to 50 knots and descending to a breakout altitude of 70 m. However, the NASA pilots considered the workload imposed by the numerous discrete control steps to be unacceptable for commercial VTOL transport operation.

In order to examine the feasibility of reducing the time in the V/STOL configuration, approaches on the 7° glide slope were made with intercept altitudes of 300, 450, and 600 m. The 450 m intercept altitude was preferred when the lift engines were started in level flight since it permitted a reasonable glide-slope acquisition and tracking time (~1 min). The 300 m intercept did not allow enough tracking time with the given deceleration schedule. The 600 m altitude was used when more time was needed, for example, when the lift engines were started on the 7° glide slope. Because of the higher descent rates that occur during 12° approaches, the intercept was raised to 600 m when the lift engines were started in level flight. To obtain adequate tracking time when the lift engines were started on the 12° glide slope instead of in level flight, the intercept altitude had to be raised to 900 m.

Although these intercept altitudes may be peculiar to the DO–31 configuration and will vary for other concepts, this study and similar studies (ref. 15) show that with only simple, situations information displays, the pilot needs 20 to 30 sec for acquisition (time from intercepting the glide slope to acquiring it confidently) and 20 to 30 sec for tracking to assess the approach so that he can confidently proceed to a landing.

ILS tracking– Once the glide slope is acquired, tracking is accomplished by modulating lift engine thrust. If the glide slope is accurately acquired and no large errors are introduced, the tracking performance is good (see figs. 15 and 16), and the pilot's workload is relatively low. The simulated IFR portion of the approach is ended at a breakout altitude of about 70 m at which point the airspeed has stabilized at 50–60 knots. The use of attitude stabilization contributed significantly to the success of these approaches. The pilots commented on the usefulness of the main engine nozzles to match the approach schedule with the desired ground speed. By giving the copilot the task of controlling airspeed with the nozzle, the pilot workload was significantly reduced during the simulated IFR approaches. For some tests the glide-slope beam width for the 7° approach was decreased from ±2° to ±1° with no apparent increase in pilot workload or degradation in tracking performance.

The capabilities and deficiencies of the different controls for glide-slope tracking were presented in the section "Handling Qualities." Even though any individual control was insufficient for controlling flight path during the approach and landing, it was evident that combining various controls provided sufficient control capability; however, further research is required to

mechanically or automatically integrate these controls into a more manageable form. It should be possible to integrate throttles and nozzle deflection, or it might be desired to add a servo-system to provide a speed or deceleration command system. Consideration should also be given to displays that give the pilot a better visualization of the thrust vector.

Most ILS approaches were made at low lift to reduce the pilot workload. These approaches were made at an angle of attack of about -3°; the relationship, $\theta = \gamma + \alpha$ dictates a pitch attitude of -10° for a -7° approach and -15° for a -12° approach, respectively. Since these approaches were made with a large nose down attitude and with the aircraft decelerating, the resulting force on the pilot (and potential passengers) is impractical for commercial operation. Therefore, several approaches were attempted with the fuselage more nearly level. These were notably unsuccessful. Insufficient time was available to explore the problem; however, it can be partially attributed to the decelerating approach where the lift at a positive angle of attack is significantly reduced as the approach progresses. From static considerations, the lift deficit, at constant thrust, would be about 0.15 times the aircraft weight when decelerating from 100 knots to 60 knots, nearly the total range of lift engine thrust modulation. In addition to properly increase the thrust to compensate for this lift deficit, the pilot must also modulate thrust to track the ILS. This problem requires further examination since future V/STOL concepts envision the use of wing lift to reduce both nose-down approach attitudes for passenger acceptance and power requirements for noise acceptance.

Final transition and vertical landing– At an altitude of 70 m and an airspeed of 50 knots, the IFR portion of the approach is terminated and a flare is initiated. The steps and procedures required to accomplish a safe vertical landing were discussed in the "Handling Qualities" section. Note in figure 15(a) that shortly after breakout the pilot went below the flight path; this was done to assure himself that he would not overshoot the touchdown area. During the vertical descent it was difficult to see the touchdown area, and he had to rely on radar altitude and rate of descent indicators. Another factor that complicated the landing was the magnitude of the suckdown and reingestion, which precluded low altitude hovering. This is illustrated in figure 21 where the sink rate is shown to increase just prior to touchdown even though the throttle is advanced. This condition is unacceptable for a commercial VTOL transport. For complete IFR hover and landing operation, displays must be developed that provide additional situation information.

Low-speed translation– Forward translation in hover can be accomplished by either modulating main engines nozzle deflection (fig. 31(a)) or by changing pitch attitude (fig. 31(b)). Modulating nozzle deflection was attractive because little lift engine thrust change was necessary to maintain altitude. Stopping on a desired spot was difficult, however, because it was hard to predict the deceleration from a given nozzle setting. Accurately and quickly selecting a nozzle position during the demanding task of maintaining altitude while maneuvering was made difficult by the small size of the nozzle position instrument. When pitch attitude was used for translating, large attitude changes were required which impaired visibility, particularly when stopping. Even though the lift engine thrust had to be coordinated with attitude change to maintain altitude, the use of pitch attitude change as the primary means of translating for short distances was preferred over the nozzle modulation, since it did not require looking in the cockpit to monitor nozzle deflection. The pilots felt that if (1) the nozzle position were more clearly displayed, and (2) the stabilization system had a height control feature, nozzle deflection modulation might be the preferred control for translating, particularly for longer distances.

Lateral maneuvering in hover is accomplished by changing roll attitude which tilts the thrust vector. Figure 27 presented a time history of a lateral translation. The maximum speed obtained during this test was 10 m/sec, which the NASA pilot considered to be the maximum lateral velocity normally required for a commercial VTOL transport of this size. The stabilization system reduces aircraft disturbances from the unusual wind conditions near the ground and allows the translation to be executed with low pilot workload.

Environmental effects at transition speeds– In the course of the test program a large range of environmental conditions was encountered. The wind speed ranged from 12 m/sec (24 knots) to calm, and from headwind to crosswind to tailwind. Light to moderate turbulence was encountered on several flights. In the preconversion mode (airspeeds greater than 140 knots) the aircraft was quite disturbed in the lateral-directional mode; however, when the stabilization system was engaged and lift engines started, the aircraft was no longer affected by the turbulence and "it felt steady as a rock." It was gratifying to note that the aircraft was relatively unaffected by gusts, adverse winds, or crosswinds. This result was somewhat surprising in view of the large side force due to sideslip (fig. 23). Tests could not be conducted to isolate the factor that produced the favorable response in gusty air; it can only be surmised that the ability to maintain constant attitude through the stabilization system was the primary contributor to the favorable ride. This is borne out by recent tests with an attitude command stabilization system in a light plane (ref. 16).

In the approach it was found that a sideslipping approach could not comfortably compensate for crosswinds because large bank angles were required. At 60 knots a 10 knot crosswind necessitated a 10° bank which not only was unconfortable in terms of side force, but also because a lateral force had to be held by the pilot; consequently, the preferred method of compensating for crosswinds was to crab the aircraft. In decelerating approaches the heading was slowly changed to keep sideslip near zero as the aircraft slows to a hover. With proper displays, the workload should not be too high. Thus, the crosswind problem does not appear to be as serious as with some STOL aircraft where it is necessary to decrab the aircraft abruptly before touchdown (ref. 7).

Environmental effects at very low speeds– Figure 32 illustrates the effect of wind and sink rate on the main engine intake temperature rise during vertical landing. The landings with increased headwind and greater sink rate generally resulted in less hot-gas reingestion. For comparison purposes, one short landing data point has been added to the vertical landing data. Along with sink rate and wind, the immediate shut down of lift engines and reduction of thrust on main engines after touchdown is very important. Greater peak temperatures occur when the power plants continue to exhaust their hot gases after the landing impact is made. This landing procedure added to the pilot workload during the final phase of the landing.

The techniques and procedures minimizing recirculation effects for a vertical takeoff have been discussed, and the effect of wind on recirculation and hot gas ingestion is presented in figure 33. Figures 33(a) and (c) show that a 60° – 90° crosswind at takeoff considerably increases the main engine inlet temperature on the upwind side (20° – 25° C). The crosswind might be pushing the gas cloud from the lift engines on that side into the inlet of the main engine. The same effect can be seen with a lesser crosswind (fig. 33(d)), the difference being a somewhat smaller increase in main engine inlet temperature. The vertical takeoff with a 6 knot headwind (fig. 33(b)) yields the smallest rise in inlet temperature.

Each main engine inlet on the airplane had only four temperature probes; they were located at the 12, 3, 6, and 9 o'clock positions, and the plots show the average value. The limited number of probes could not show temperature distortion across the engine inlets that can cause compressor stalls; it should be noted that no compressor stalls were encountered during the NASA evaluation.

Comparison of approaches– The selection of an approach and approach technique for a V/STOL aircraft must consider the exposure of the landing and approach area to noise. (Some measurements of the noise level for the DO–31 have been made by Dornier and can be found in ref. 17.) A comparison of different approaches with different lift engine starting procedures is shown in figure 34. This figure shows that for glide slopes of 12° or 7°, starting the lift engines on the glide slope can reduce the noise exposure on the ground. First, this procedure results in less time spent with the lift engines operating. Second, less area is subjected to the high noise level since the lift engines are started 2000 to 3000 m closer to the landing site and at a higher altitude. These approaches and landings required 2 to 3 min, and are shorter than predicted in reference 10. However, approaches considerably shorter than 2 to 3 min are theoretically achievable based on the aircraft's performance.

Previous studies (refs. 7 and 9) reported that the descent rates in an ILS approach should be less than 5 m/sec (1000 ft/min) at altitudes below 100 m (300 ft). The descent rates used during these tests were greater. Figure 35 is a graphical representation of the relationship between glide-slope angle, airspeed, and rate of descent. In the DO–31 approach airspeed range from 120 knots at glide-slope intercept to 50 knots at flare on a 7° approach, the rate of descent varies from approximately 7 m/sec at the start of the approach to 3 m/sec at breakout. For the 12° approach, the rate of descent varies from 13 to 5 m/sec. The pilots considered the high rate of descent at the beginning of the approach to be no problem because (1) it was decreasing as the aircraft was decelerating on schedule, (2) the attitude command control system allowed more attention to be devoted to approach performance parameters, and (3) altitude was sufficient (70 m) that the aircraft could be flared to arrest the sink rate. The NASA pilots felt that approaches steeper than 12° were not practical with the DO–31 primarily because of the nose-down attitude. In figure 15(a) it can be seen that the time to flare the aircraft and to land was as long as the time to acquire and track the glide slope. It would be expected that attempts to reduce the landing time (e.g., by not flaring to zero vertical velocity at 70 m) would make the rate of descent in the approach more critical and the high rates of descent might not be tolerated.

The close-in pattern presented in figure 36 represents the type of approach that might be required in a restricted area. The lift engines are started during the turn made to acquire the localizer. The altitude during the turn is held at the intercept altitude (450 m), and the distance of the turn from the landing point was dictated by length of time required to bracket the localizer prior to glide-slope intercept. After the localizer is captured, the rest of the approach is the same as when the lift engines are started in level flight on the localizer. The pilots considered this pattern to be feasible if appropriate terminal-area navigation aids were available.

CONCLUDING REMARKS

A flight investigation was performed with the Dornier DO–31 VTOL transport to evaluate the performance, handling, and operating characteristics that are considered to be important when

operating a commercial VTOL transport in the terminal area. The DO–31, a 20,000 kg transport, has a mixed jet propulsion system; that is, there are main engines with nozzles that deflect from a cruise to a hover position, and vertical lift engines that operate below 170 knots. In this VTOL mode pitch and roll attitude and yaw rate stabilization are incorporated, and the main and lift engines are used to augment the forces and moments. The tests concentrated on the transition, approach and vertical landing.

The flight tests showed that this mixed jet-propulsion system provided a large usable performance envelope that enabled a broad range of simulated IFR approaches to be made. Glide slopes of 7° and 12° were intercepted at 140 knots and tracked while the aircraft decelerated to 50 knots and a breakout altitude of about 70 m; the transition to hover and a vertical landing had to be made visually because displays were lacking. The aircraft could be easily converted to the VTOL mode either before or after the glide slope was intercepted. Once acquired, the glide slope was easy to track because corrections could be made normal and parallel to the flight path (via lift engine thrust and main engine nozzle deflection, respectively), while the stabilization system maintained attitude. However, if large corrections were needed, the pilots reported that the normal acceleration available from the lift engines (±0.1 g) was insufficient for flight-path control. Controlling the flight path by pitching the aircraft was unsatisfactory because of the changing control power and lift in the decelerating approach, and also because of the large unwanted airspeed changes at the lower airspeeds.

During the transition and approach the aircraft was stabilized in pitch, roll, and yaw; and then the pilot's prime job was power management (control of thrust magnitude and direction). This entailed numerous discrete changes to lift and main engine throttle, main engine nozzle deflection, and pitch attitude. To simplify this task most of the approaches were made with the fuselage nearly parallel to the flight path. However, there were still too many changes when considering a commercial transport operation. When the ILS was tracked with a more level fuselage attitude, the workload increased and the performance deteriorated. Further research is needed to integrate the different longitudinal controls and simplify power management, and to define appropriate flight-path control criteria that considers the aircraft response after a period of time and limits the cross coupling.

Several other observations were made pertaining to the transition and approach mode. First, when the aircraft was maneuvered laterally, the roll-attitude stabilization required the pilot to use a lateral force for an uncomfortably long time, and the yaw rate command made it difficult to coordinate the turn. When the aircraft was not maneuvered, the heading hold feature of the yaw rate stabilization greatly assisted in maintaining the aircraft track. Second, with the stabilization system engaged and lift engines operating, the aircraft was relatively unaffected by turbulence. Finally, in the approach "crabbing" the aircraft easily compensated for crosswinds; a "sideslipped" approach was unsatisfactory.

In hover, the lateral control power (0.8 rad/sec^2), sensitivity, attitude stability, and damping were satisfactory. The results agree with previously reported NASA simulation studies. The pilots felt that attitude stabilization was mandatory for satisfactory VTOL operation. A sudden failure to an acceleration system in the VTOL mode would be unacceptable. The vertical landing was unacceptable because of the recirculation effects below 15 m and because of insufficient height control.

When the complete terminal area operation was considered, the time in the VTOL mode was shorter than observed in other IFR flight studies. An ILS approach, starting with intercepting the localizer beam at 140 knots and ending with a vertical landing, could be completed in less than 3 min. The pilot needed 20 to 30 sec to track the localizer; 60 to 90 sec to acquire the glide slope, start the lift engines, and track and decelerate to 50 knots at the breakout altitude (70 m); and 45 to 60 sec to hover and make the vertical landing. In a vertical takeoff the aircraft has a high acceleration and a steep climbout; in just over 20 sec the aircraft attained 120 knots, a sufficient airspeed to shut off the lift engines.

Ames Research Center
National Aeronautics and Space Administration
Moffett Field, California, 94035, Dec. 17, 1971

APPENDIX A

COMPUTATION OF DATA PERTAINING TO FLIGHT–PATH DEVIATIONS

In order to relate the pilot comments on flight-path control with the aircraft characteristics and motion, it is necessary to realize the significant difference between the change in aircraft flight-path angle, $\Delta\gamma$, and the glide-slope error displayed to the pilot, ϵ_G. This is schematically illustrated in figure 37, and additional comments follow to describe the computations that were made for the figures illustrating flight-path control in the body of the report. During ILS tracking the pilot's reference is the ILS beam which is ground based, set at the desired flight path, γ_G, and his position information is in the form of deviation from the centerline of the ILS glide-slope beam, ϵ_G, displayed on the ADI. When the pilot makes a correction with a control input, a normal acceleration is integrated into a flight-path change, $\Delta\gamma$, which is *not* directly related to ϵ_G. The $\Delta\epsilon_G$ is a function of the change in altitude which is an integration of $\Delta\gamma$ (hence, a second integration of normal acceleration). Further, the corrective control input produces a change in velocity that may or may not be desired by the pilot. In a constant speed approach, the pilot can observe the response to the control as a change in rate of climb and a change in airspeed. For the decelerating approaches of the present tests, the responses shown by the indicators can be misleading, and insufficient situation information is displayed to the pilot by the ADI. These changes are also more difficult to measure by normal flight-test techniques. It was found that the radar data of the aircraft's position was not accurate enough to determine the changes in flight path produced by control inputs. Better information was obtained by integrating the measured aircraft accelerations; the rational for these computations is given in the following paragraphs.

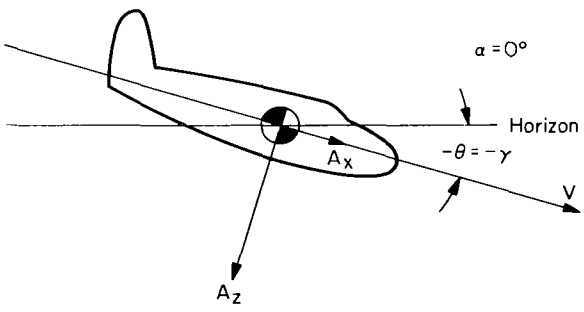

First, an analysis will be made for the simple case where the aircraft is stabilized in pitch, the angle of attack is near zero, the initial flight path is -7°, and the aircraft is decelerating. For this case $\cos\theta = \cos\gamma \approx 1$.

The perturbation of the aircraft to a control input is obtained by using the measured normal and longitudinal accelerometer readings (A_Z and A_X) over the 10 sec period of interest minus the initial measured acceleration to obtain the incremental values, $\Delta a_Z/g$ and $\Delta a_X/g$. Consequently, it has been assumed that the initial accelerations would exist for the 10 sec period of the integration if there had been no control input. In figures 17 and 18 the ordinate of normal acceleration is inverted to have the direction of the curve in the sense of the aircraft motion. The change in vertical velocity is now obtained by

$$\Delta v_Z = \int \Delta a_Z \, dt$$

Then $\Delta\alpha = -(\Delta v_Z/V) \times 57.3$, and since the attitude is fixed, the change in flight path, $\Delta\gamma$, is equal to $\Delta\alpha$. This is also presented on the figures for comparison with the observed angle of attack changes; in view of the poor quality of angle of attack information at the low speeds the agreement is reasonable. Conversely, it can be seen why it would be difficult to use the angle of attack information to compute flight-path changes. Next the change in altitude is obtained by a second integration of normal acceleration

$$\Delta h = \int \int - \Delta a_Z \, dt^2$$

For comparison, the change in altitude that corresponds to a 1 dot glide-slope change (ϵ_G) at 200 m altitude is shown for a glide slope of -7° with a beam width of ±1°. The change in velocity, Δv_X, is obtained as

$$\Delta v_X = \int \Delta a_X \, dt$$

it should be noted that this does not correspond to the change in velocity that would be observed on the airspeed meter because the initial condition of the aircraft is decelerating flight, and Δv_X represents the perturbation due to control input only.

The computations are similar for evaluating the flight-path change due to pitching the aircraft; however, the accelerations are transformed to earth-fixed axes before computations are performed. Since the $\cos\theta \approx 1$, the normal change in acceleration is retained in the form of $\Delta a_Z/g$ to be more easily compared with the data at constant attitude. The change in longitudinal acceleration (along the flight path) is given as $(\Delta dV/dt)/g$. Because of the changing attitude and angle of attack, $\Delta\gamma$ is presented in lieu of Δv_Z.

It should be noted that the previous derivations are only approximate, but are sufficiently accurate to assess the initial motions of the aircraft to relate aircraft characteristics and pilot comments.

APPENDIX B

MISCELLANEOUS ENGINE AND CONTROL RELATIONS

THRUST AND FUEL FLOW

The thrust and fuel flow characteristics of one main and one lift engine are given in figure 38. The relations between throttle position and engine speed were presented in figure 5.

CONTROL DEFLECTIONS

The variations of the VTOL control deflection and of the conventional surface deflection with the pilot control are given in figures 39 to 41. Also included are the maximum hover control power about each axis for a nominal hover configuration. Since the conventional surfaces are simultaneously deflected with the VTOL control, the control power increases with forward speed. In the conventional flight regime above 155 knots, a gear changer reduces the surface deflection per unit of pilot control to maintain a better stick force per unit acceleration. The reduction in control surface deflection is illustrated in part (b) of these figures by the reduction in the maximum surface deflection with increased dynamic pressure. For each axis the maximum deflection of the stabilization system actuator is 40°.

REFERENCES

1. Fry, Bernard L.; and Zabinsky, Joseph M.: Feasibility of V/STOL Concepts for Short-Haul Transport Aircraft. NASA CR–743, 1967.

2. Marsh, K. R.: Study on the Feasibility of V/STOL Concepts for Short-Haul Transport Aircraft. NASA CR–670, 1967.

3. Anon.: Study on the Feasibility of V/STOL Concepts for Short-Haul Transport Aircraft. NASA CR–902, 1967.

4. Anon.: STOL–V/STOL City Center Transport Aircraft Study. FAA–ADS–26, McDonnell Aircraft Corporation, Oct. 1964.

5. Waldo, Richard K.; and Filton, Peter D.: An Economic Analysis of Commercial VTOL and STOL Transport Aircraft. FAA–ADS–25, Stanford Research Institute, Feb. 1965.

6. Kelley, Henry L.; and Champine, Robert A.: Flight Investigation of a Tilt Wing VTOL Aircraft in the Terminal Area Under Simulated Instrument Conditions. AIAA Paper No. 71–7, Jan. 1971.

7. Innis, Robert C.; Holzhauser, Curt A.; and Quigley, Hervey C.: Airworthiness Considerations for STOL Aircraft. NASA TN D–5594, 1970.

8. Smith, Charles C., Jr.; and Parlett, Lysle P.: Flight Tests of a 0.13-Scale Model of a Vectored – Thrust Jet VTOL Transport Airplane. NASA TN D–2285, 1964.

9. Garren, John F.; Kelley, James R.; and Reeder, John P.: A Visual Flight Investigation of Hovering and Low-Speed VTOL Control Requirements. NASA TN D–2788, 1965.

10. Greif, Richard K.; Fry, Emmett B.; Gossett, Terrence D.; and Gerdes, Ronald M.: Simulator Investigations of Various Control Systems for VTOL Aircraft. NASA SP–116, 1966.

11. Anderson, Seth B.: Considerations for Revision of V/STOL Handling Qualities Criteria. NASA SP–116, 1966.

12. Anon.: V/STOL Handling, I–Criteria and Discussion. AGARD Rep. 577, 1970.

13. Rolls, L. Stewart; and Gerdes, Ronald M.: Flight Evaluation of Tip Turbine-Driven Fans for Lateral Control and a Hovering VTOL Aircraft. NASA TN D–5491, 1969.

14. Kelley, James R.; Garren, John F.; and Deal, Perry L.: Flight Investigation of V/STOL Height-Control Requirements for Hovering and Low-Speed Flight Under Visual Conditions. NASA TN D–3977, 1967.

15. Reeder, John P.: The Impact of V/STOL Aircraft on Instrument Weather Operations. NASA TN D–2702, 1965.

16. Loscke, Paul C.; Barber, Marvin G.; Jarvis, Calvin R.; and Enevoldsen, Einar K.: Handling Qualities of Lift Aircraft With Advanced Control Systems and Displays: NASA Aircraft Safety and Operating Problems. NASA SP–270, 1971.

17. Flemming, M.; and Schotten, R. (Dornier GmbH): Noise Problems of VTOL With Particular Reference to the Dornier DO–31. Roy. Aeron. J., Aug. 1969.

TABLE 1.– AIRCRAFT DIMENSION AND DESIGN DATA

General:		
Length, m (ft)	20.60	(67.6)
Height to top of vertical fin, m (ft)	8.53	(28.0)
Wing:		
Area, m^2 (ft^2)	57.0	(613)
Span, m (ft)	17.0	(55.8)
Mean aerodynamic chord, m (ft)	3.415	(11.2)
Aspect ratio	5.05	
Sweep, deg	8.5	
Airfoil section, root	NACA 64(A412)–412.5	
Airfoil section, tip	NACA 64(A412)–410	
Incidence angle, deg	2	
Dihedral angle, deg	1.5	
Taper ratio, deg	0.615	
Flap deflection (max), deg	45	
Flap area, m^2 (ft^2)	6.64	(71.4)
Flap chord, m (ft)	0.85	(2.8)
Aileron deflection, deg	±25	
Horizontal tail:		
Area, m^2 (ft^2)	16.4	(176)
Span, m (ft)	8.0	(26.2)
Mean aerodynamic chord, m (ft)	2.13	(7.0)
Airfoil section	NACA–63A–010	
Aspect ratio	3.9	
Elevator deflection, deg	±25	
Vertical tail:		
Total area, m^2 (ft^2)	15.4	(166)
Span, m (ft)	4.4	(14.4)
Mean aerodynamic chord, m (ft)	3.61	(11.8)
Airfoil section	NACA–63A–010	
Rudder area, m^2 (ft^2)	5.59	(60)
Rudder deflection, deg	±30	
Mass:		
Maximum conventional takeoff, kg (lb mass)	24,500	(53,900)
Maximum vertical takeoff, kg (lb mass)	21,800	(48,000)
Standard empty, kg (lb mass)	16,594	(34,300)
Weight:		
Maximum vertical takeoff, N (lb force)	213,000	(48,000)
Moment of inertia for 20,500 kg mass (45,000 lb mass) and gear down:		
I_{XX}, kg m^2 (slug-ft^2)	385,000	(284,000)
I_{YY}, kg m^2 (slug ft^2)	277,000	(205,000)
I_{ZZ}, kg m^2 (slug-ft^2)	606,000	(447,000)
Center of gravity:		
Percent of mean aerodynamic chord	23.0	

TABLE 1.– AIRCRAFT DIMENSION AND DESIGN DATA – Concluded.

Propulsion system:		
Main engine, 2 installed		
Rolls Royce Pegasus 5–2 turbofan		
Maximum thrust per engine at S.L.S. for 2-1/2 min, N (lb force)	67,200	(15,100)
Emergency thrust per engine at S.L.S. for 40 sec, N (lb force)	76,000	(17,200)
Weight, per engine, with nozzles, N (lb force)	16,000	(3,500)
Lift engine, 8 installed		
Rolls Royce RB–162–4D lift jet		
Maximum thrust per engine at S.L.S., N (lb force)	18,700	(4,200)
Emergency thrust per engine at S.L.S. for 40 sec, N (lb force)	19,600	(4,400)
Weight, per engine, with yaw nozzle, N (lb force)	1,570	(350)
Total maximum thrust at S.L.S., N (lb force)	285,000	(64,000)

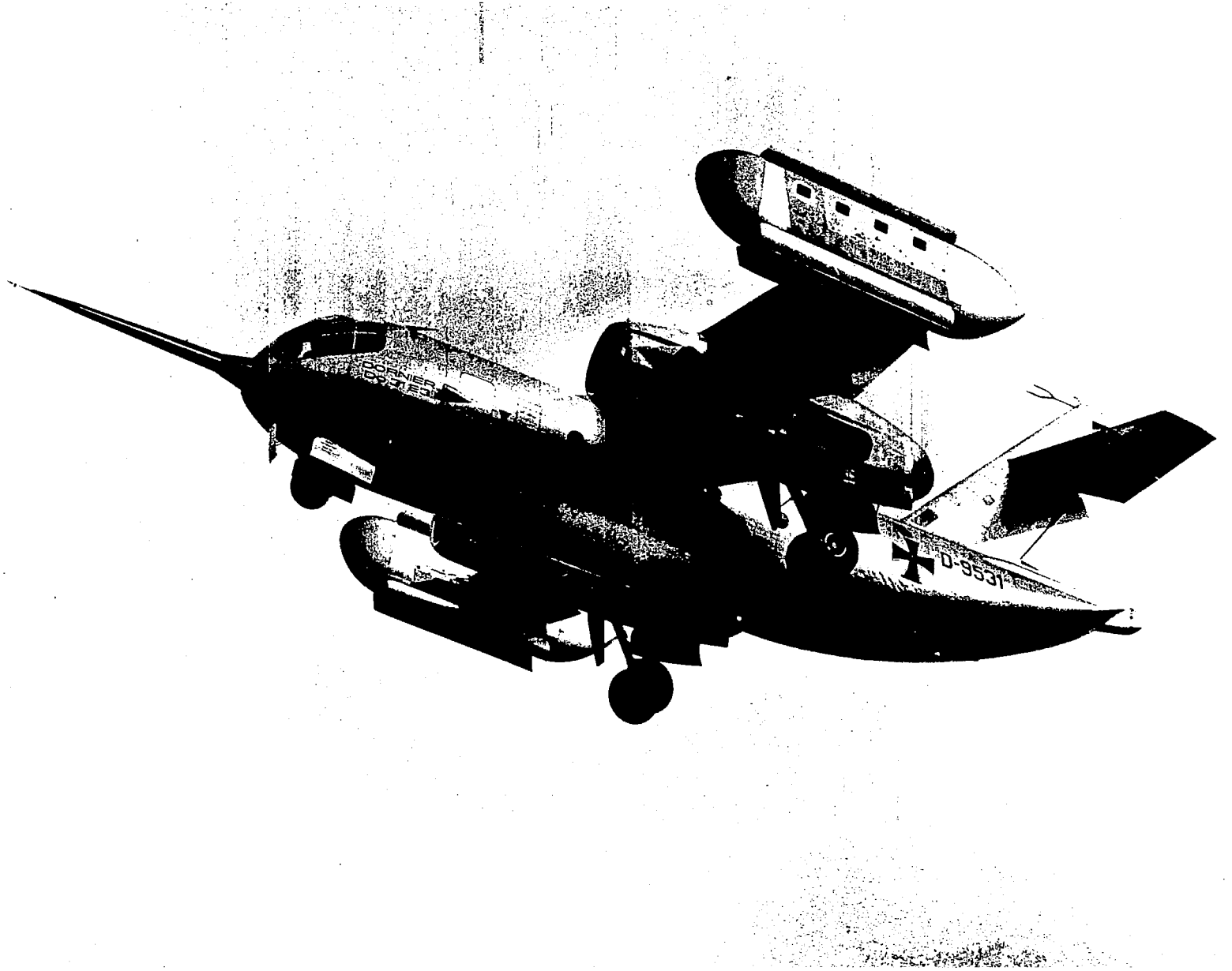

(a) In VTOL flight.

Figure 1.– Test aircraft – the Dornier DO–31.

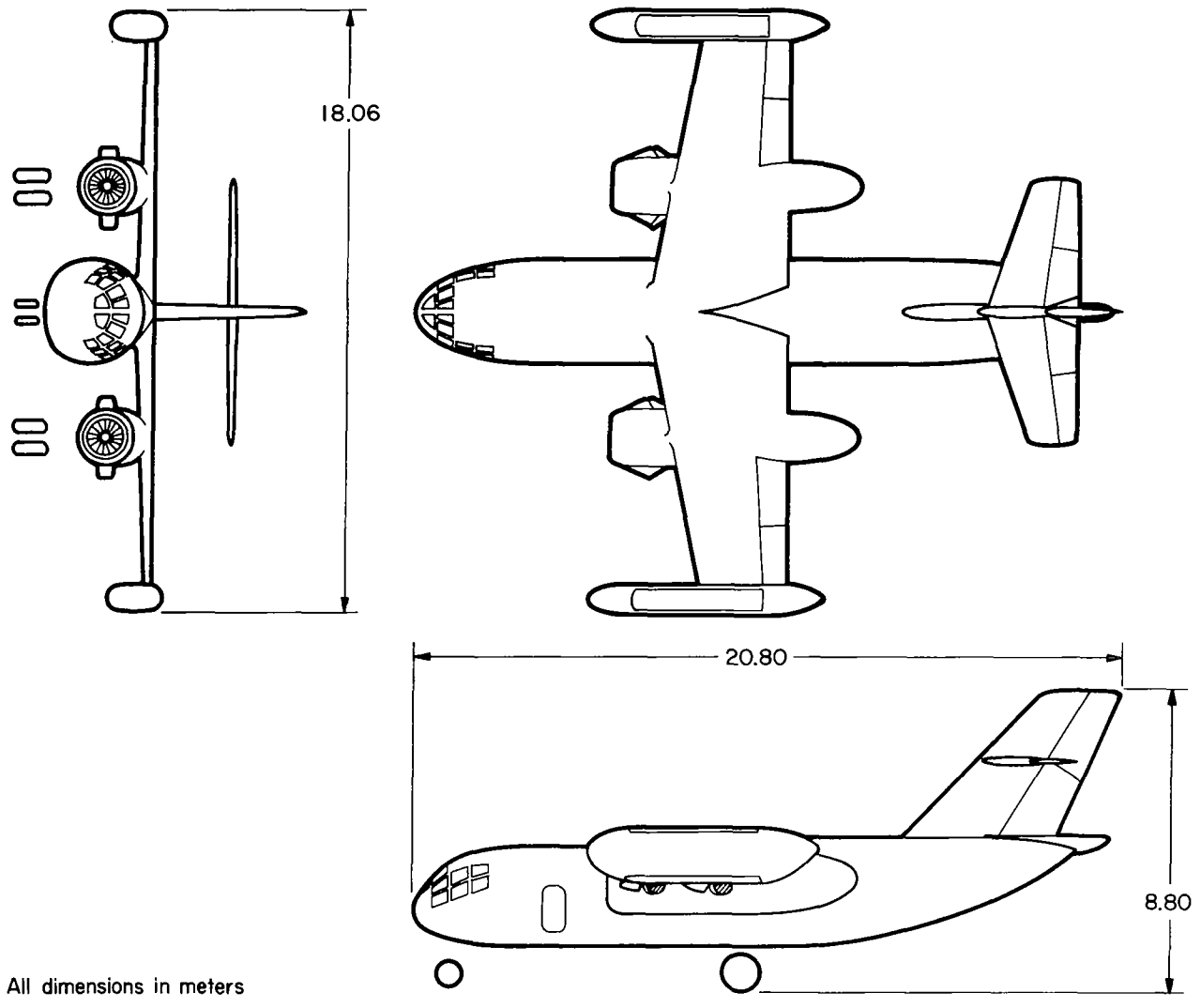

(b) Three-view sketch in conventional mode

Figure 1.– Concluded.

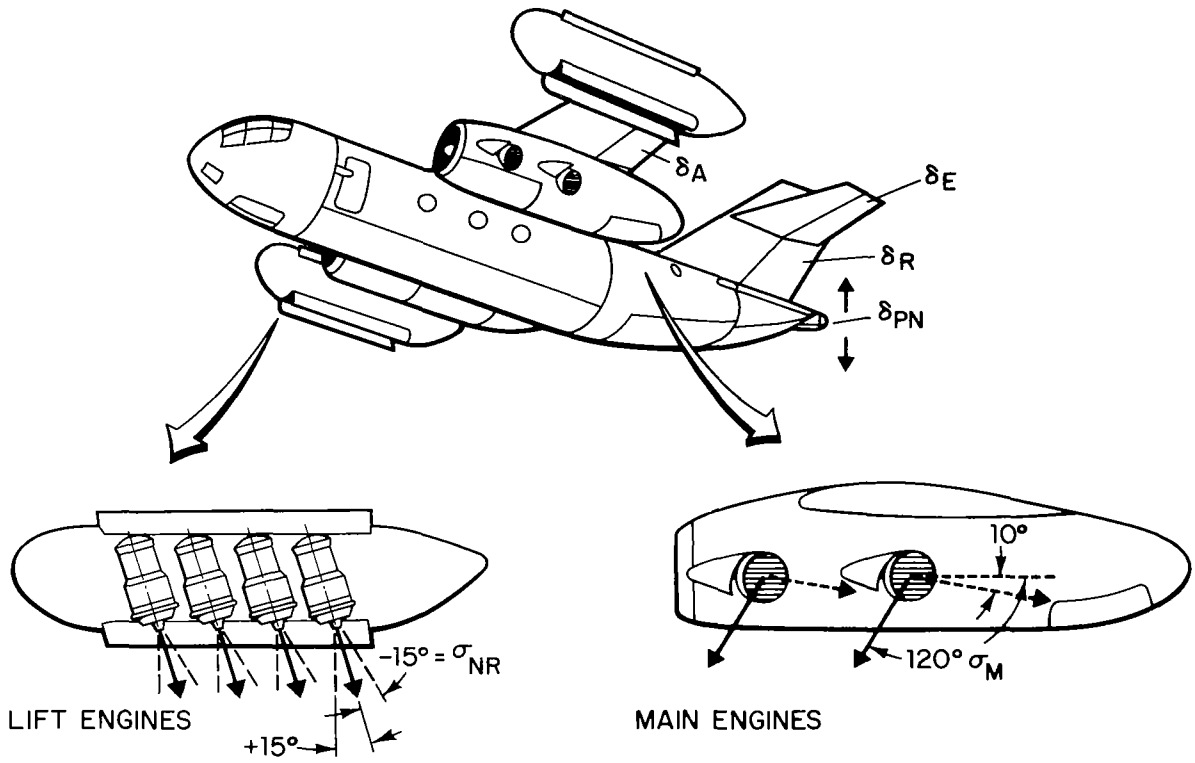

Rotation :

(1) Longitudinal stick, δ_{MP}, controls elevator (δ_E) and pitch nozzle (δ_{PN})

(2) Lateral stick, δ_{LP}, controls ailerons (δ_A) and differential thrust of lift engines ($FCU_L - FCU_R$)

(3) Rudder pedal, δ_{NP}, controls rudder (δ_R) and differential lift engine nozzle deflection ($\sigma_{NL} + \sigma_{NR}$)

Translation :

(1) One lift engine throttle, σ_{FCU}, controls thrust of lift engines collectively

(2) Two main engine throttles, σ_{TL} and σ_{TR}, control thrust of each main engine

(3) One main engine nozzle lever, σ_M, controls deflection of all main engine nozzles collectively

Figure 2.– Schematic of control functions.

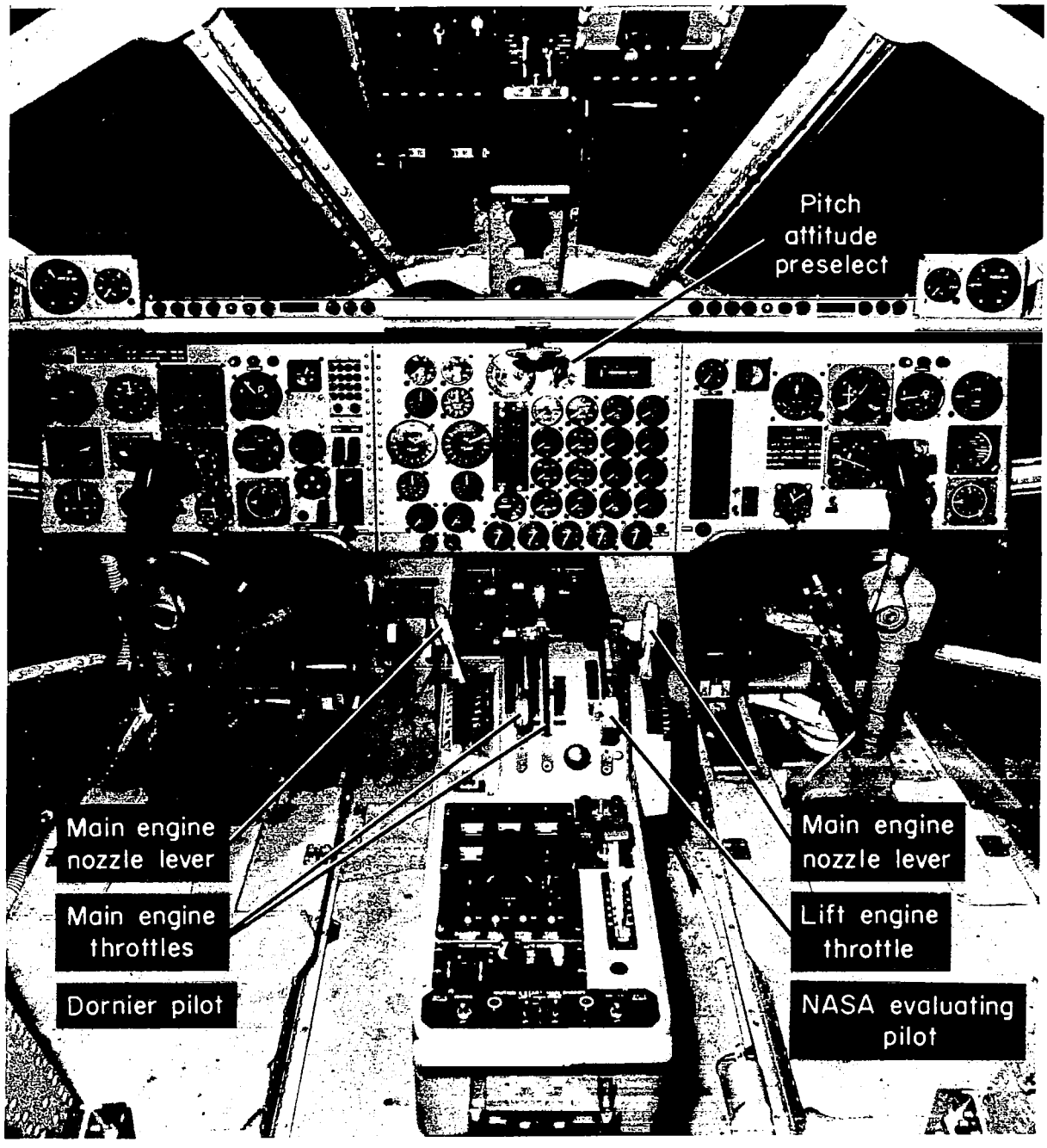

(a) Overall view of cockpit.

Figure 3.– Cockpit control and display layout.

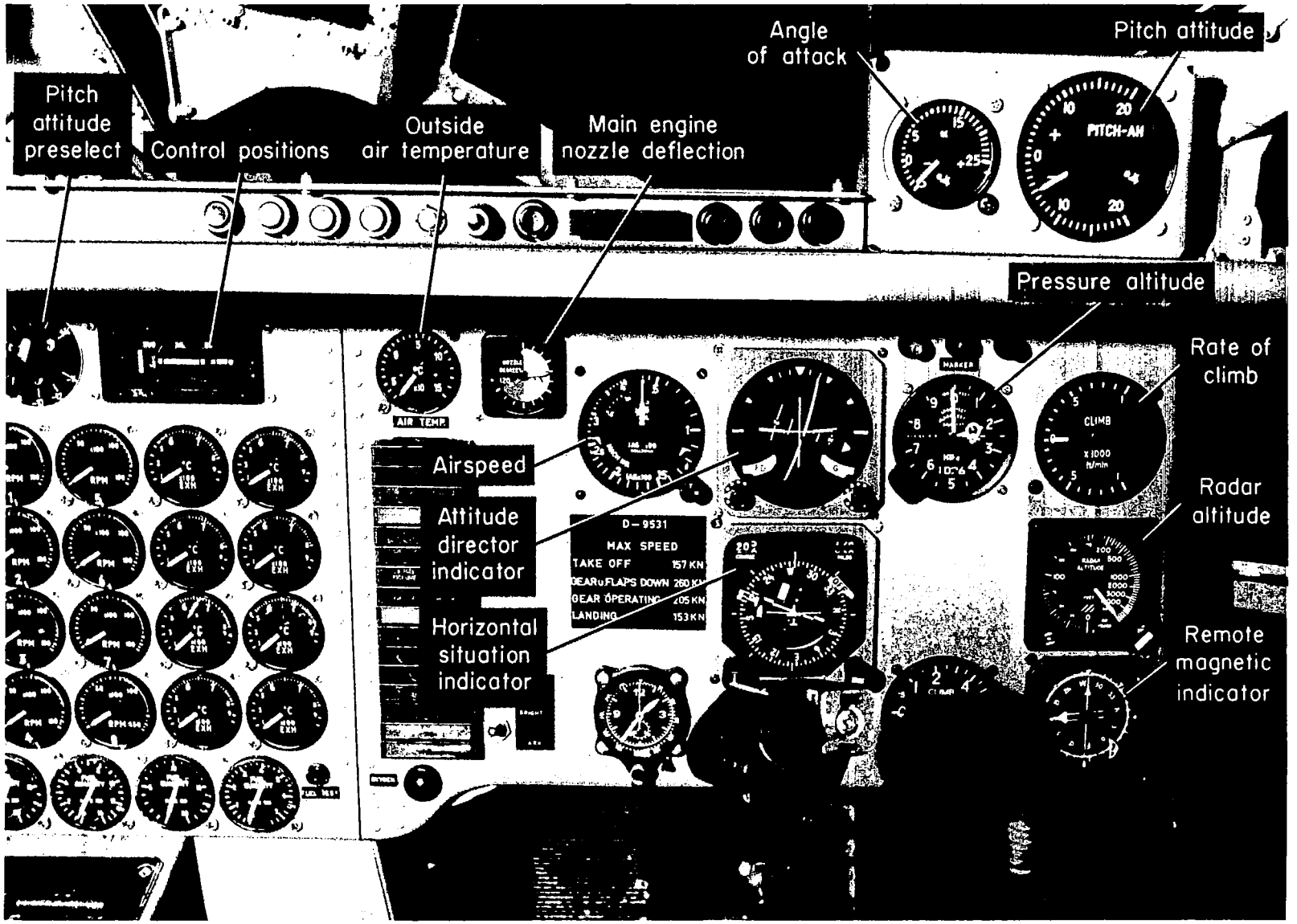

Display for evaluating pilot.

Figure 3.– Concluded.

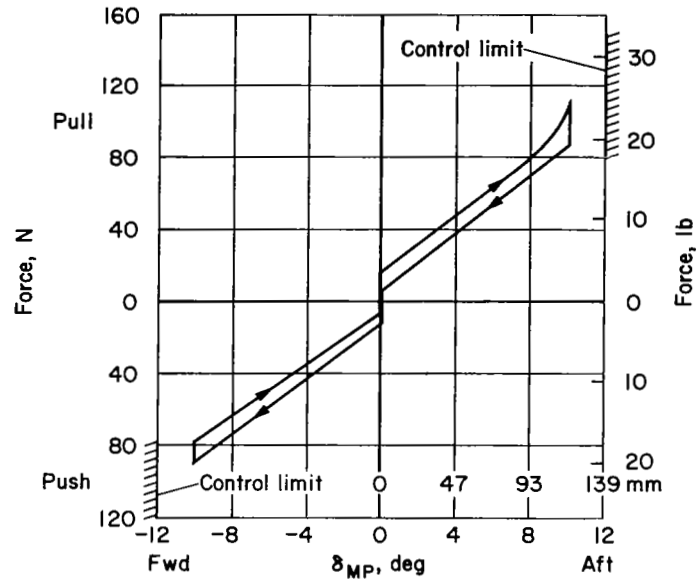

(a) Longitudinal control

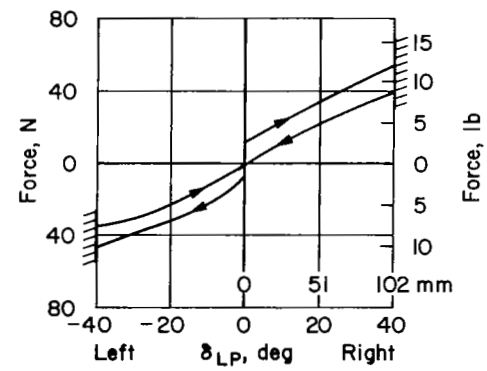

(b) Lateral control

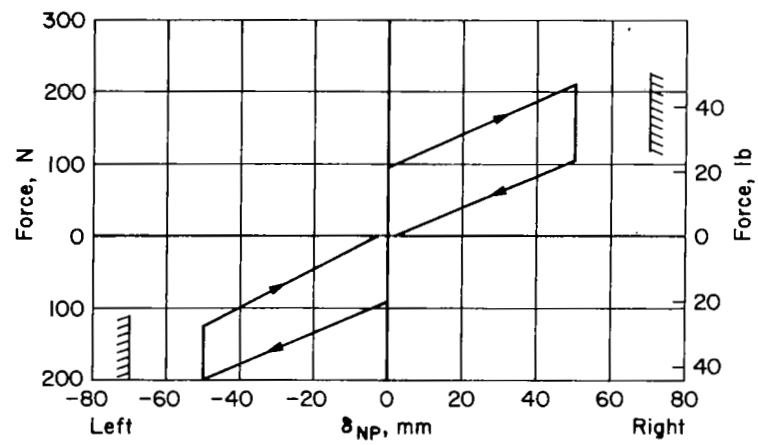

(c) Directional control

Figure 4.– Pilot control force-deflection relations.

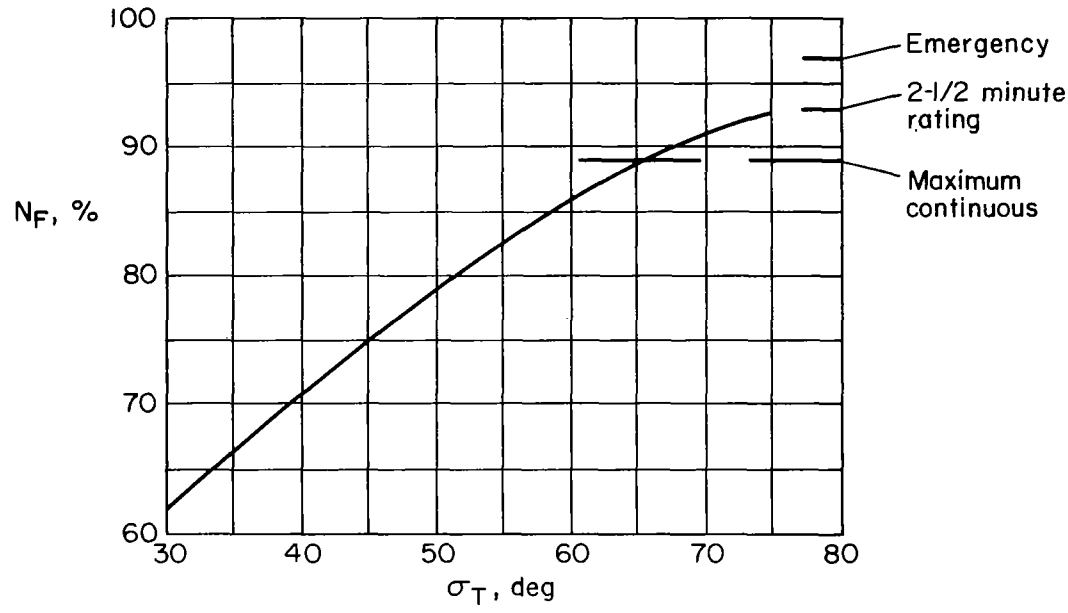

(a) Main engine throttle, length of lever = 220 mm

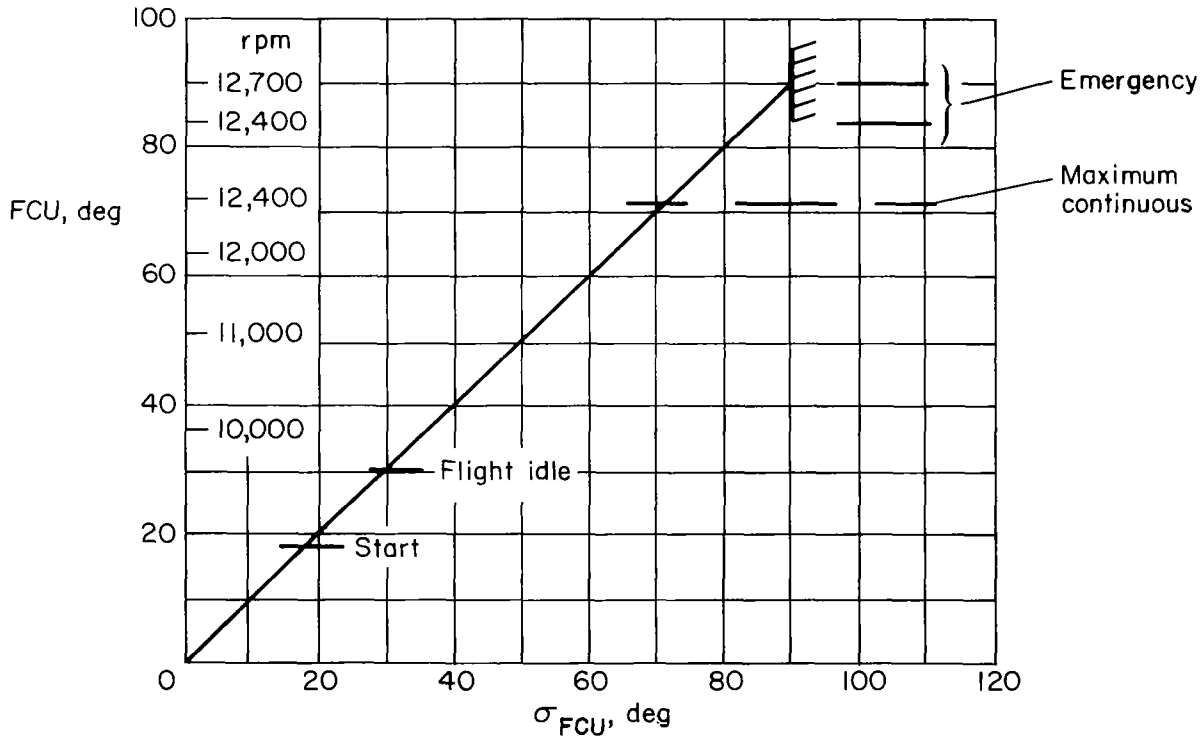

(b) Lift engine throttle, length of lever = 240 mm

Figure 5.– Throttle relations.

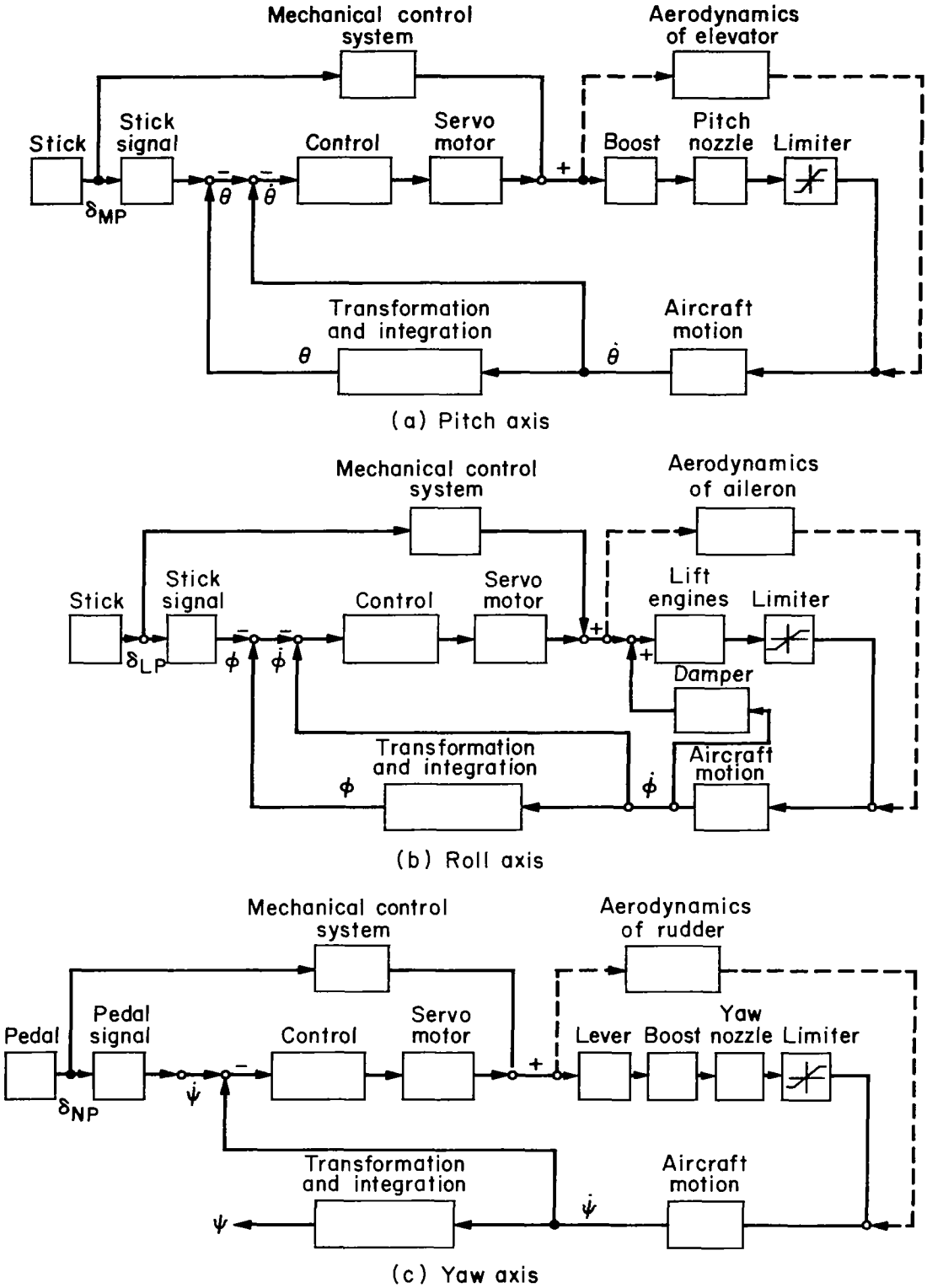

Figure 6.– Block diagram of stabilization and control system; VTOL mode.

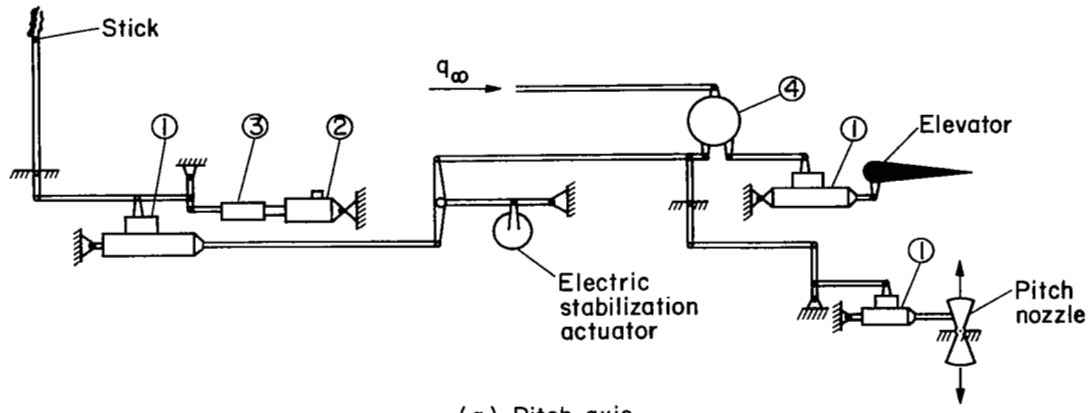

(a) Pitch axis

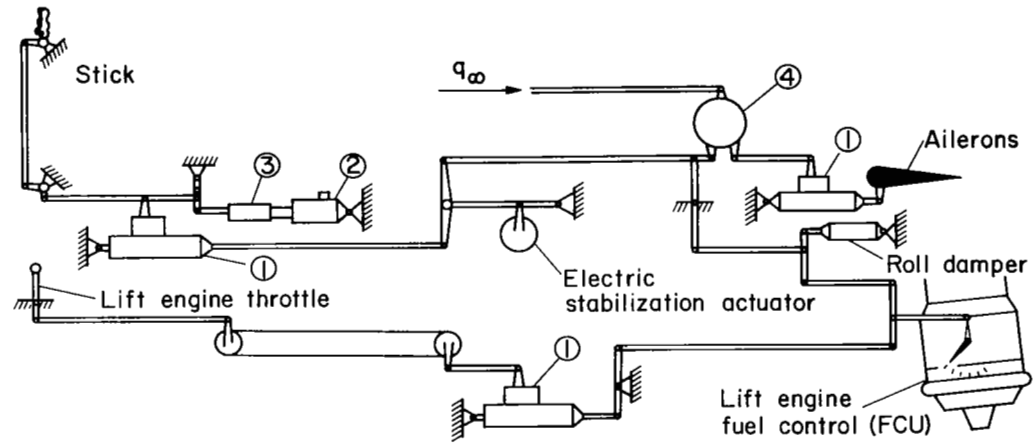

(b) Roll axis

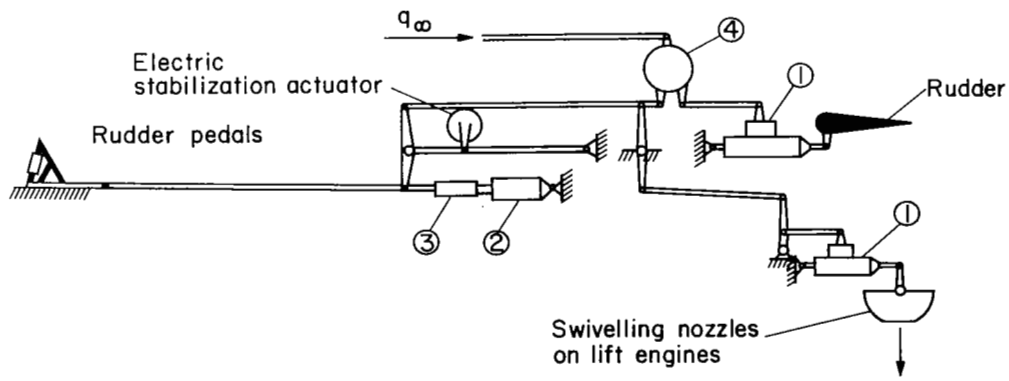

① Hydraulic actuator
② Trim motor in cruise configuration
③ Centering spring
④ Gear changer, a function of dynamic pressure

(c) Yaw axis

Figure 7.– Schematic of control system.

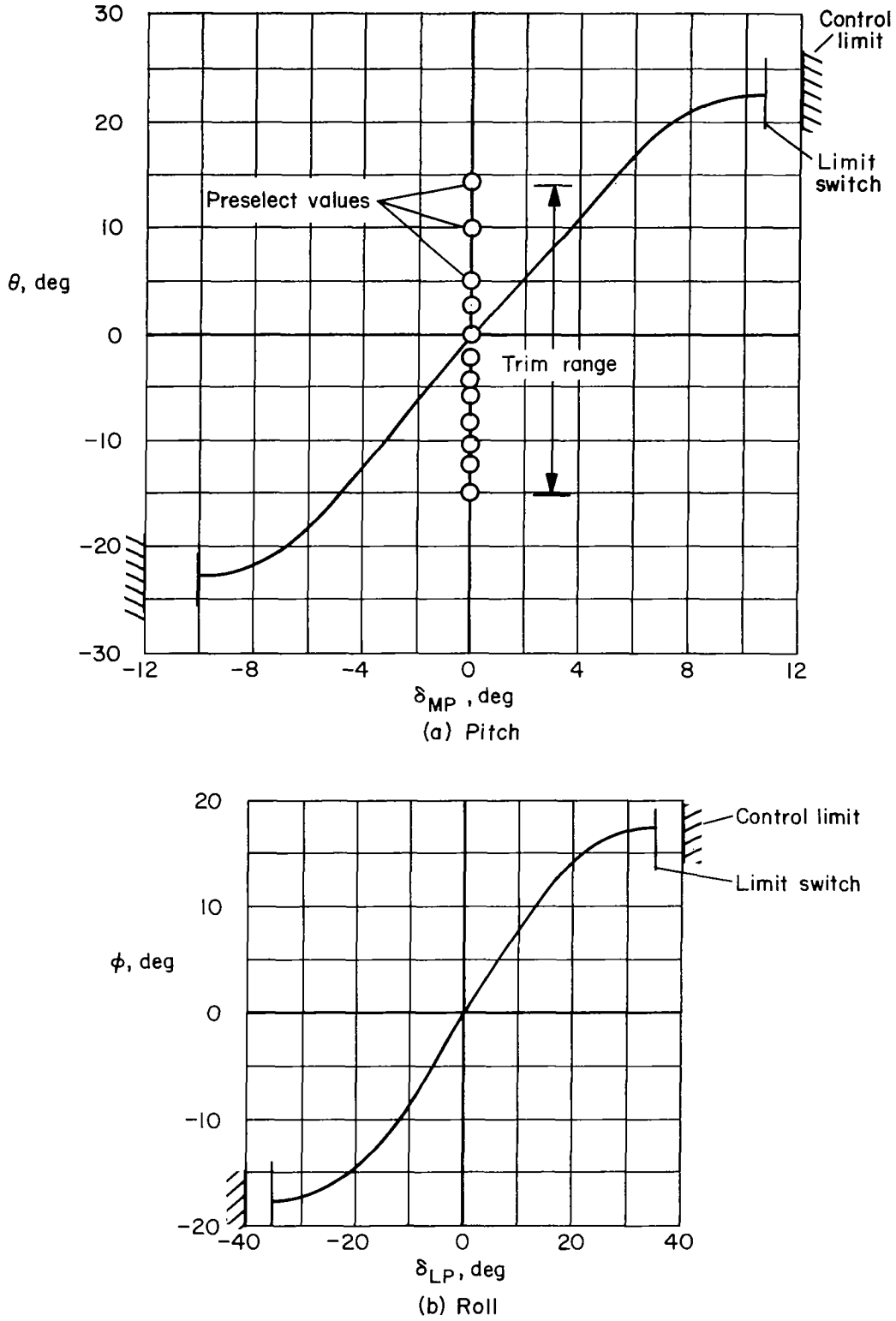

Figure 8.– Steady-state conditions commanded by pilot control position; VTOL mode.

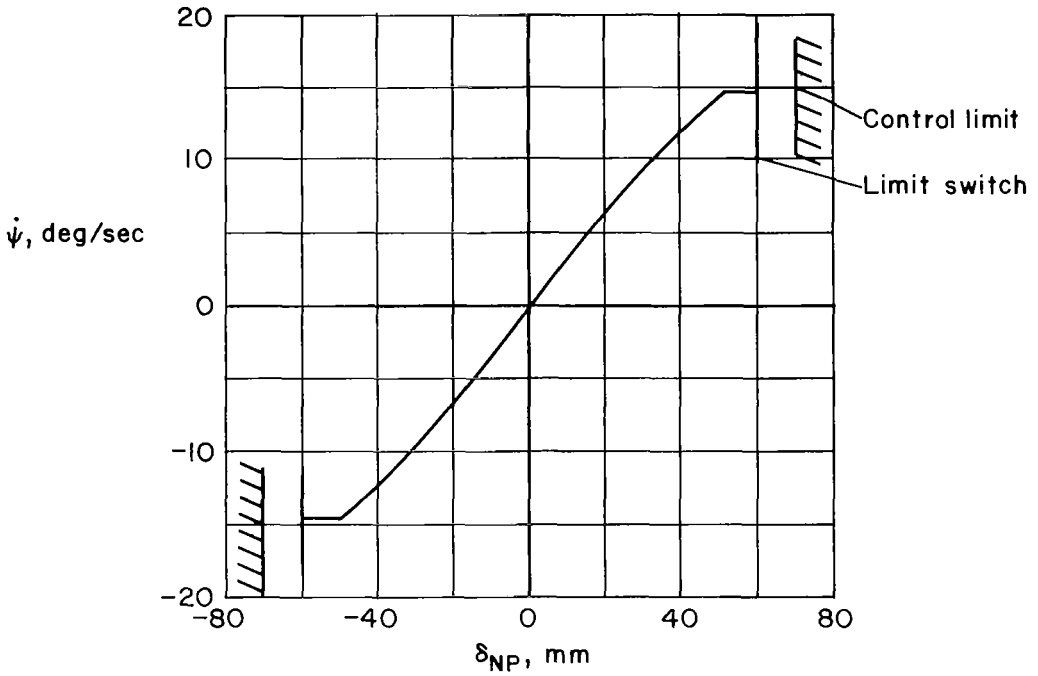

(c) Yaw

Figure 8.– Concluded.

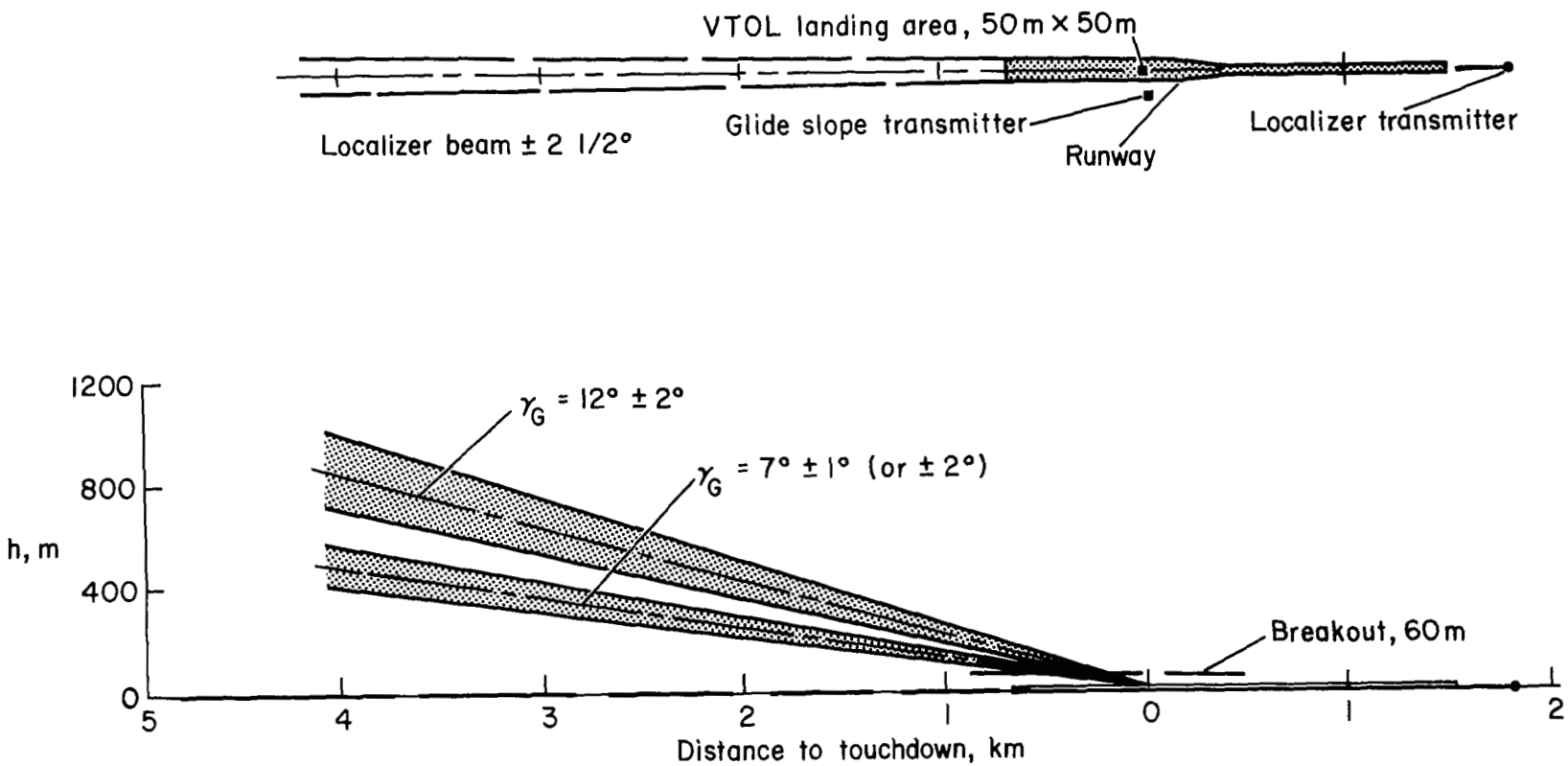

Figure 9.– Runway and guidance characteristics.

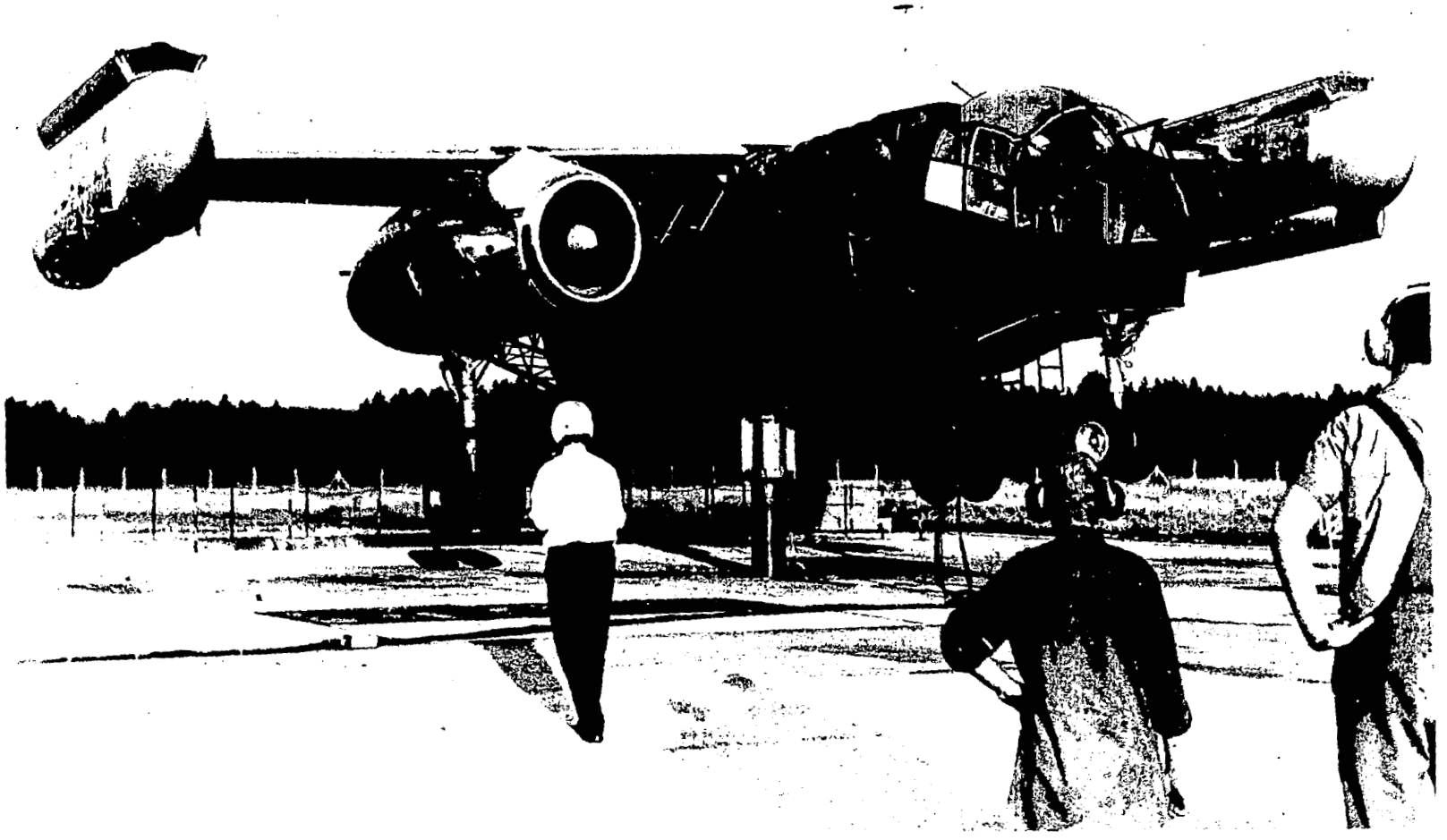

Figure 10.– Hover rig on pedestal.

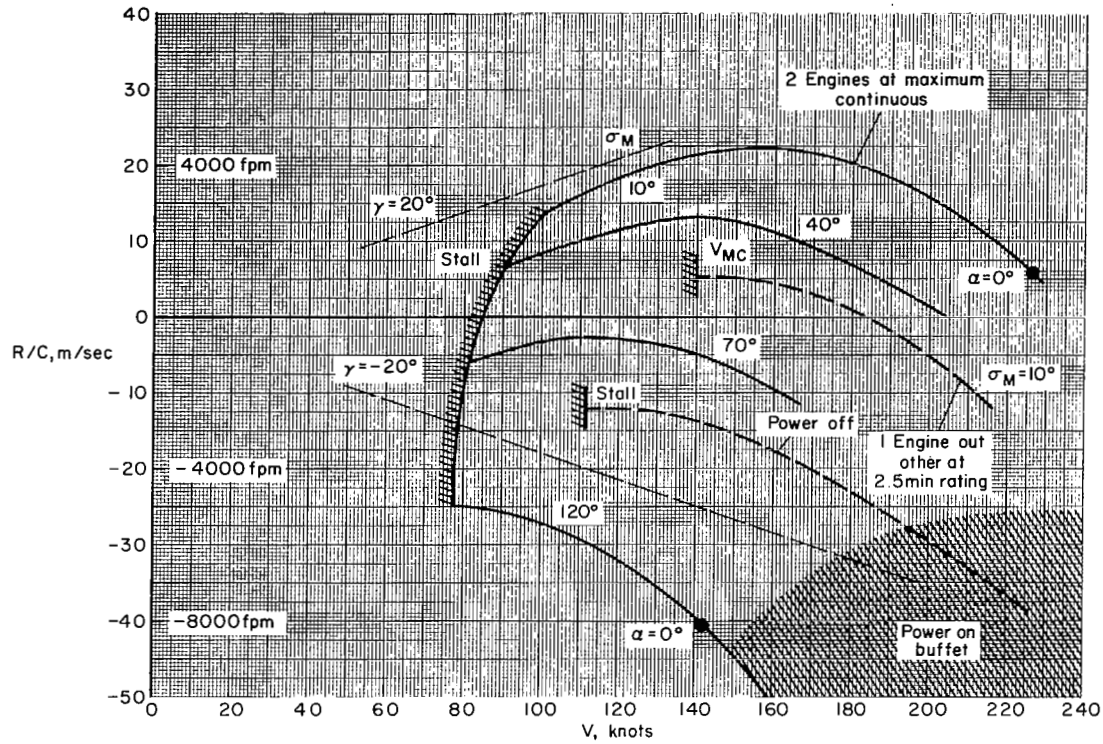

(a) Conventional mode, 2 engines operating, except as noted

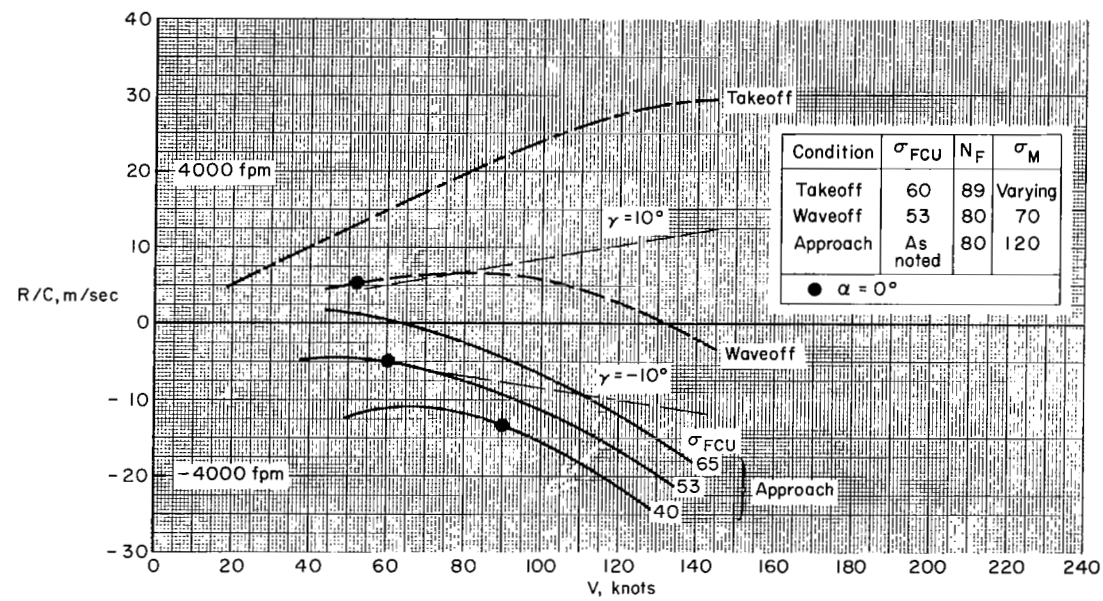

Condition	σ_{FCU}	N_F	σ_M
Takeoff	60	89	Varying
Waveoff	53	80	70
Approach	As noted	80	120

● $\alpha = 0°$

(b) VTOL mode, all engines operating

Figure 11.– Low-speed characteristics with 45° flaps and gear down; dV/dt = 0, m = 19,500 kg, h = 1,000 m, 8° C.

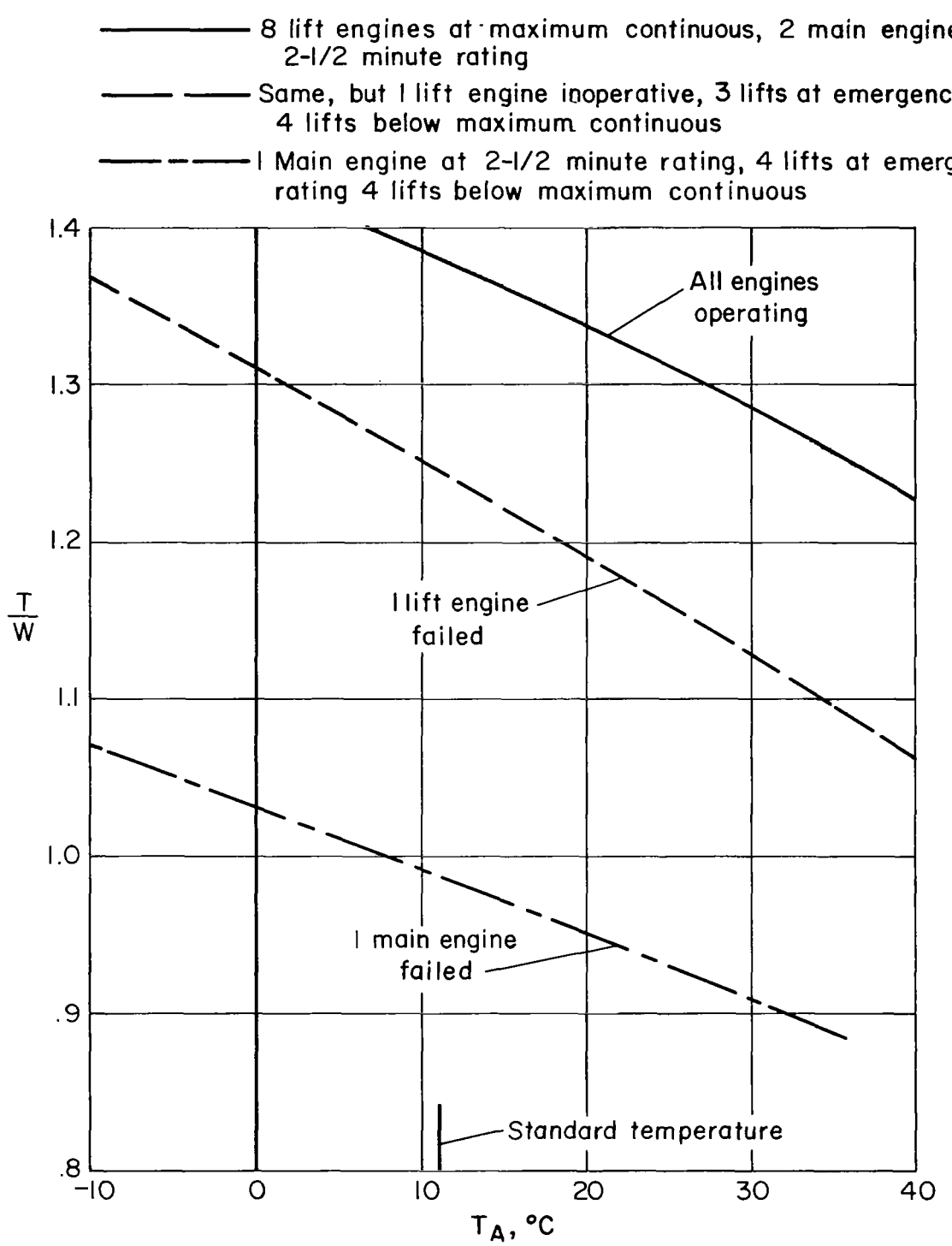

Figure 12.– Thrust-weight ratio in hover out-of-ground effect and in lateral balance; m = 18,500 kg, h = 600 m, $\sigma_M = 95°$, $\theta = 5°$.

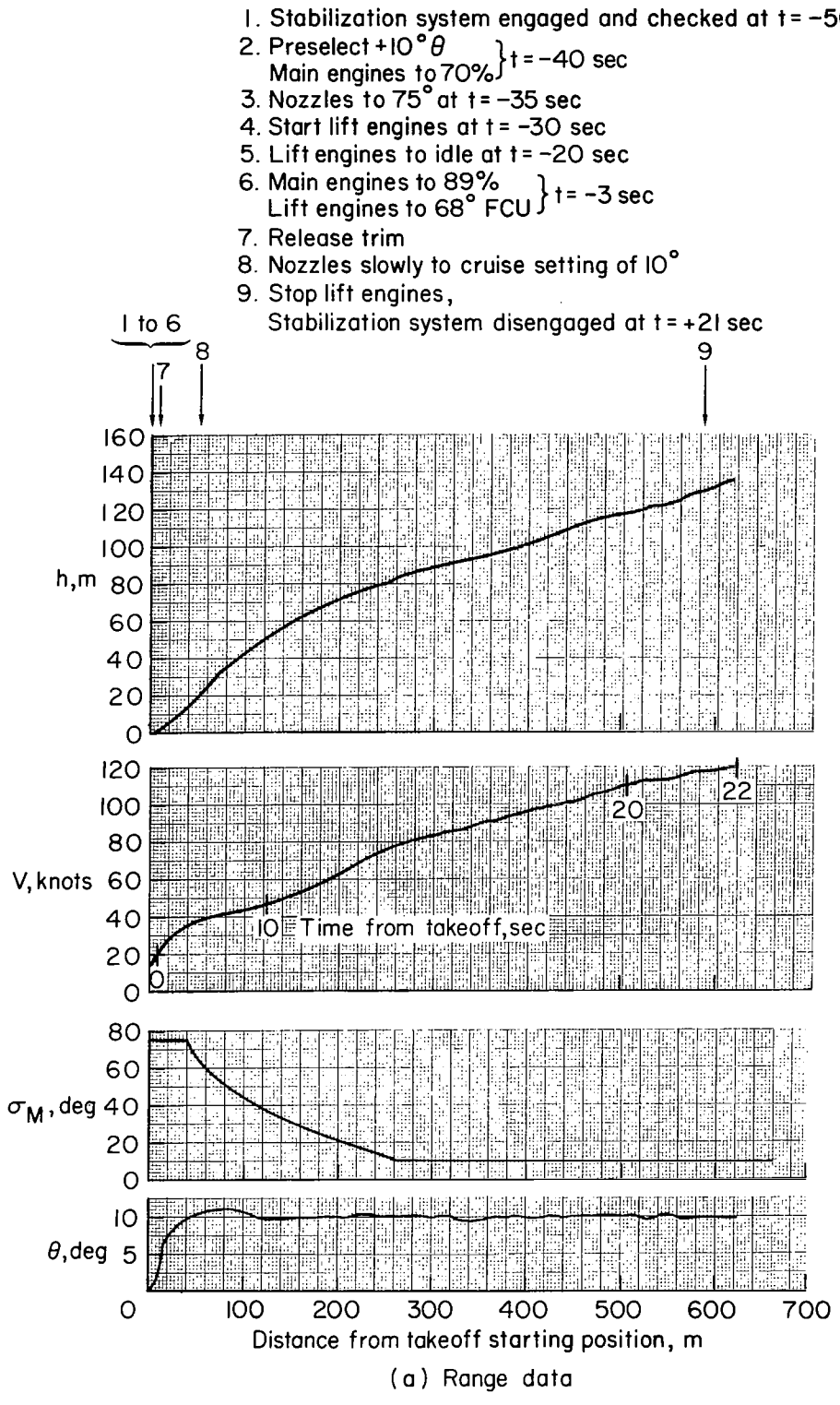

Figure 13.– Vertical takeoff; m = 21,000 kg, 6–12 knot direct headwind.

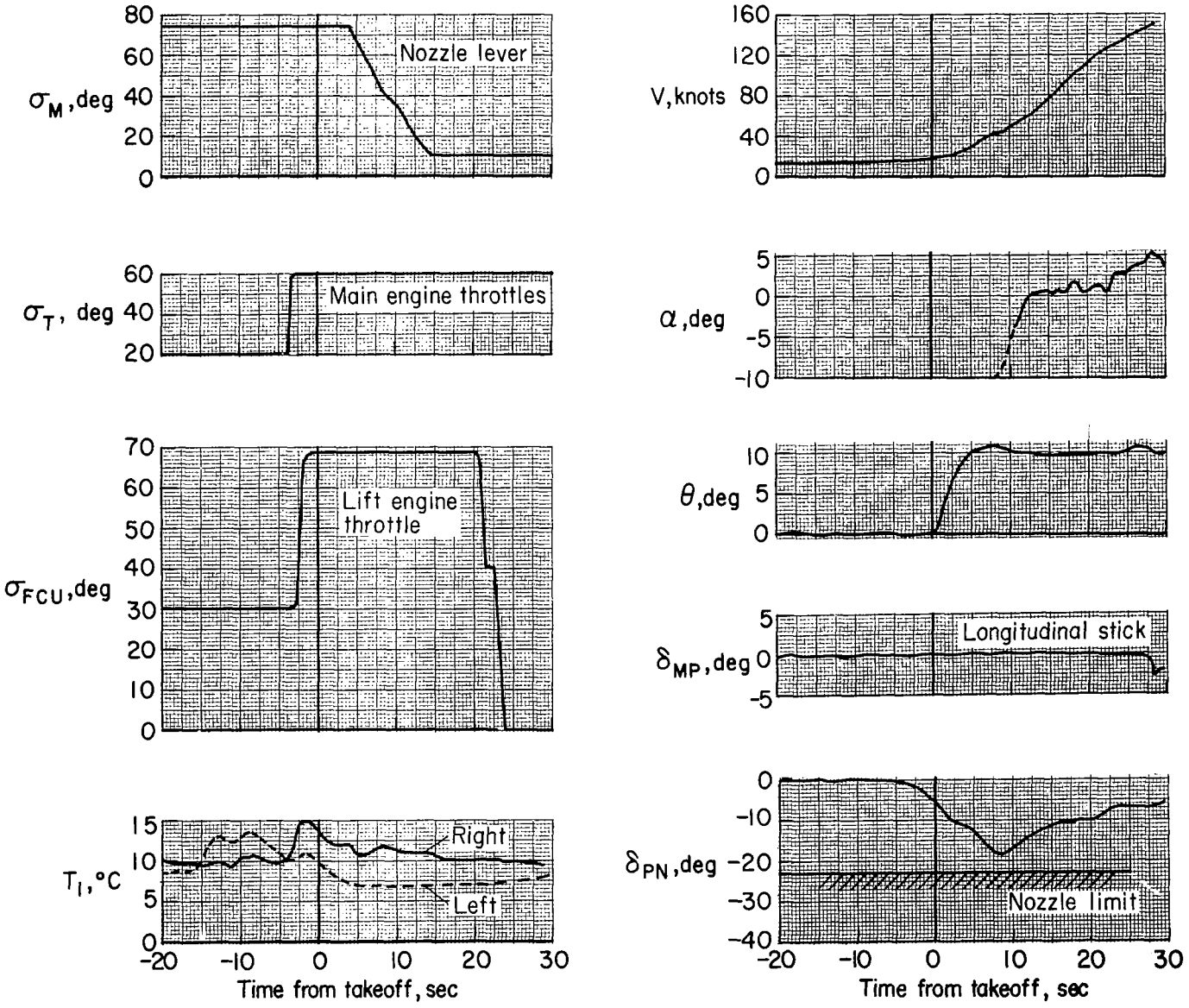

(b) Time history

Figure 13.– Concluded.

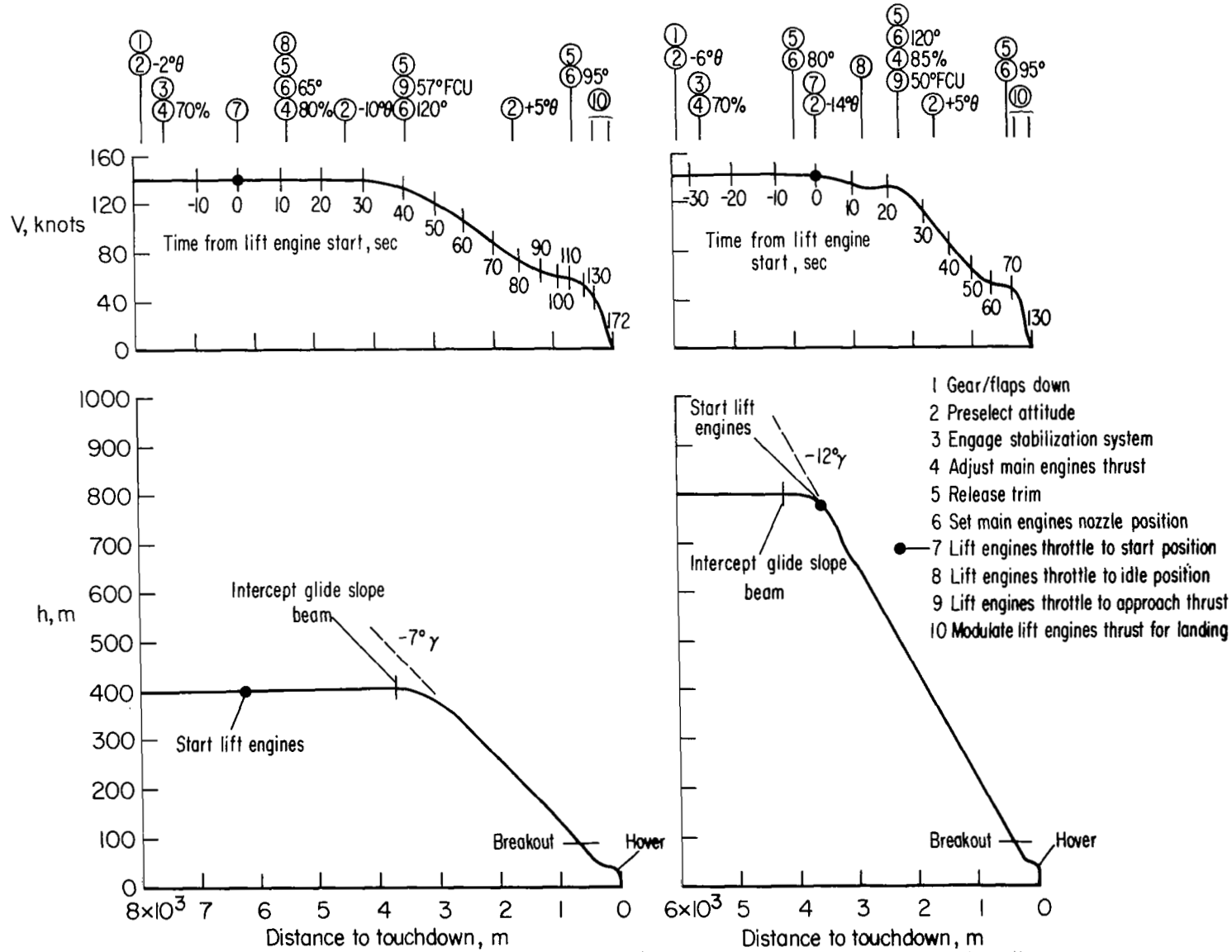

(a) 7° glide slope, lift engines started in level flight (b) 12° glide slope, lift engines started on glide slope

Figure 14.– Schematic of simulated IFR approaches.

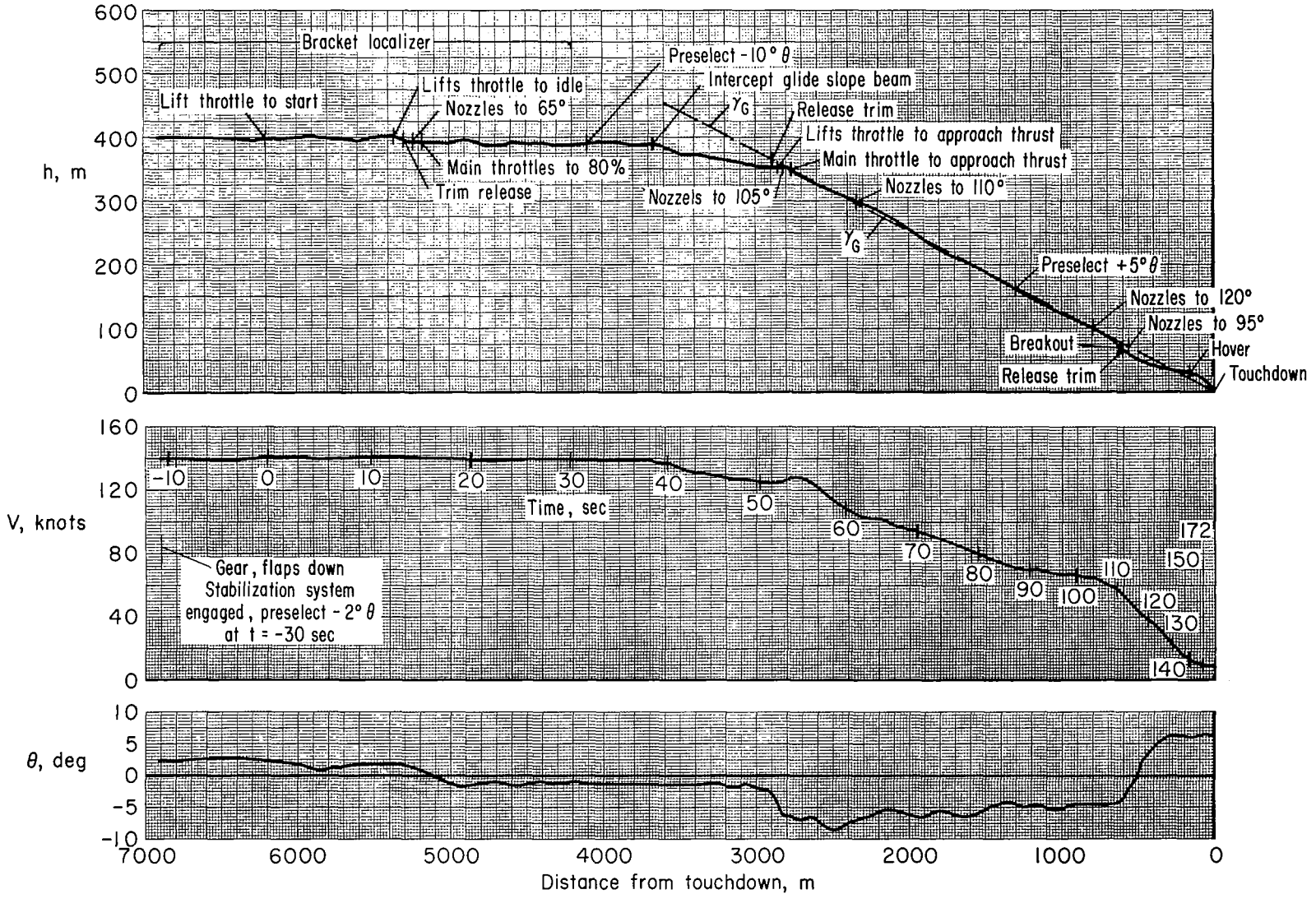

(a) Range data

Figure 15.– 7° simulated IFR approach starting lift engines in level flight; m = 18,750 kg, wind 12–16 knots 60° to 90° from right, $\gamma_G = 7° \pm 1°$.

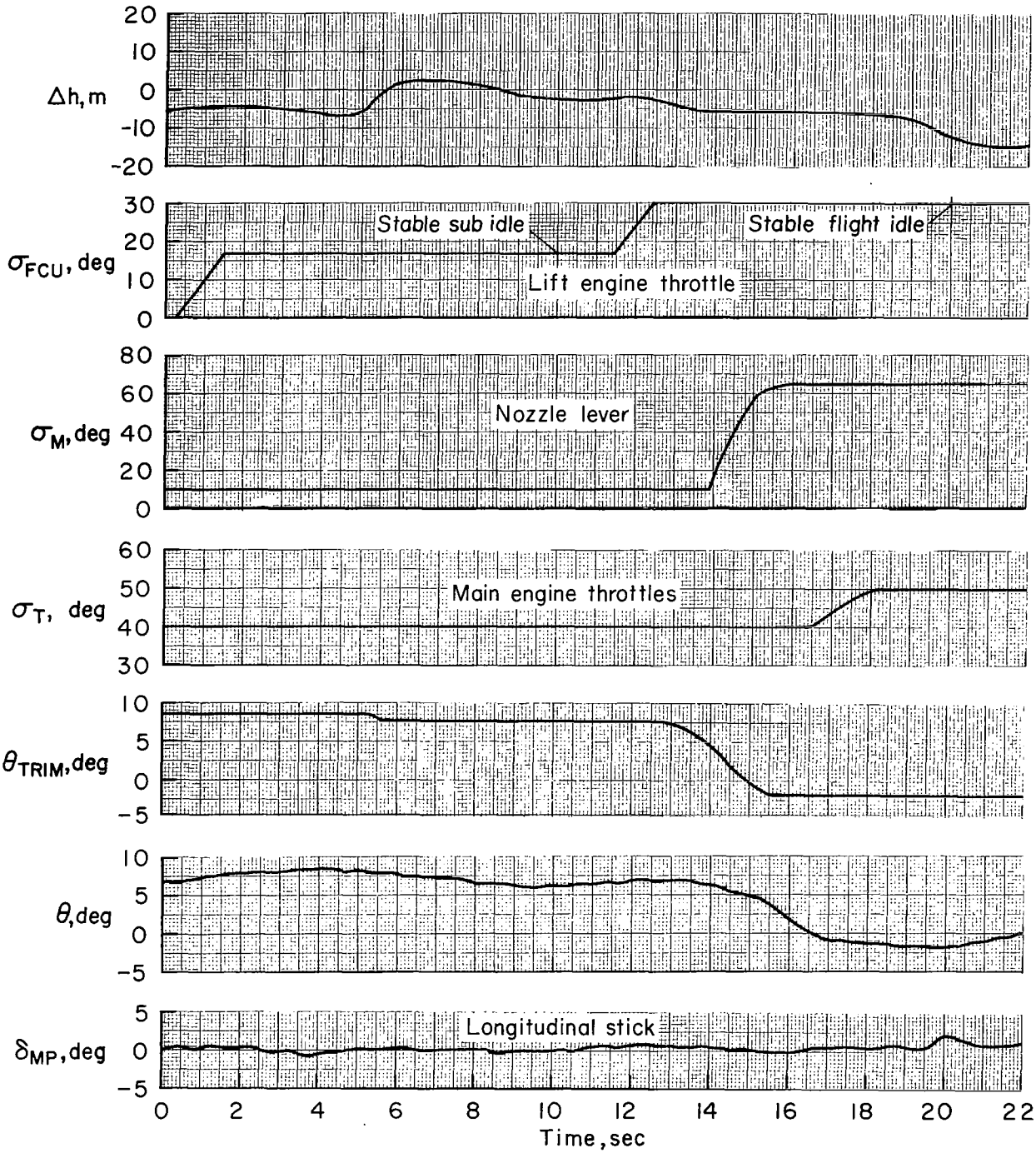

(b) Time history of lift engine start

Figure 15.– Continued.

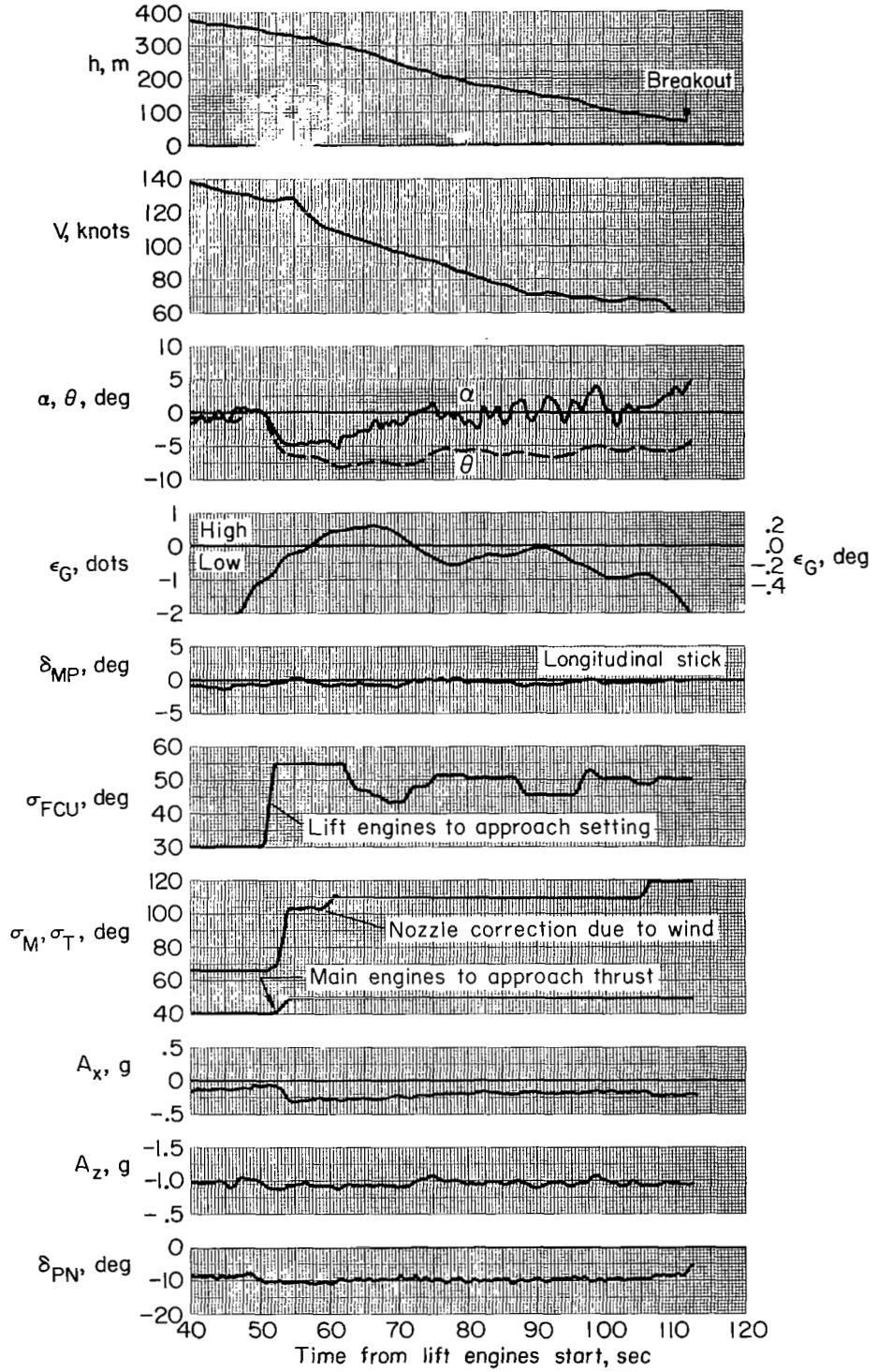

(c) Longitudinal parameters in approach

Figure 15.– Continued.

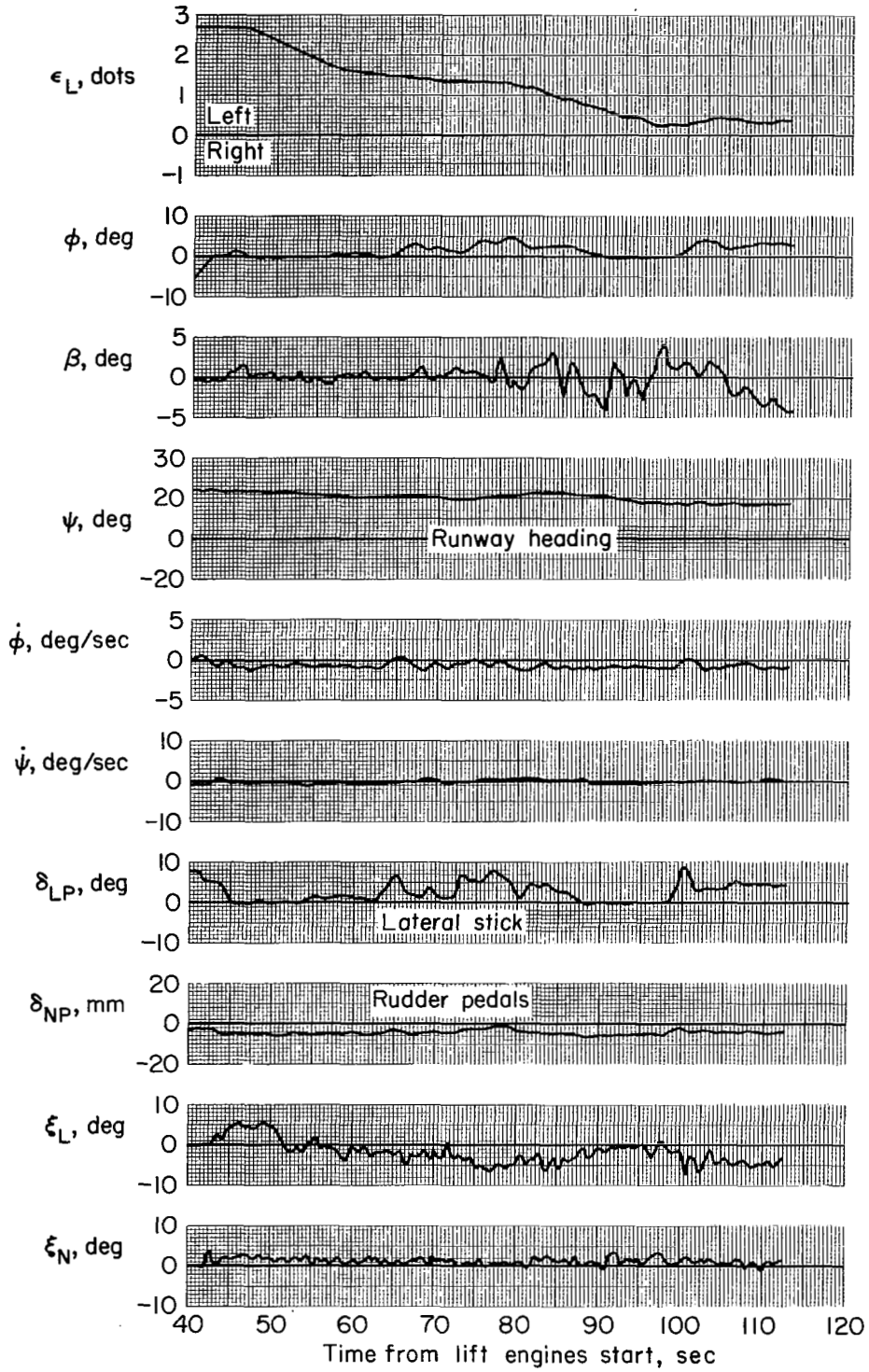

(d) Lateral – directional parameters in approach

Figure 15.– Continued.

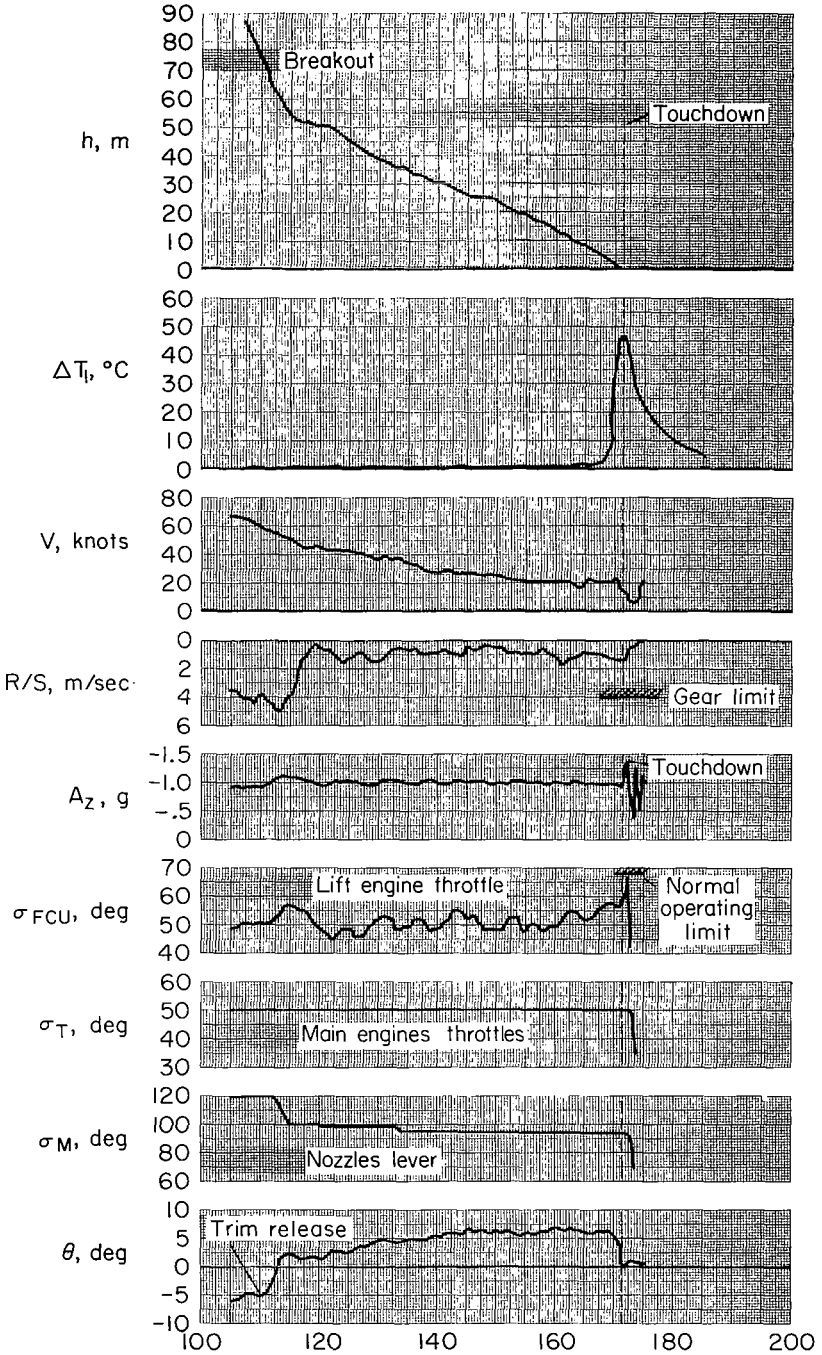

(e) Flare and vertical landing

Figure 15.– Concluded.

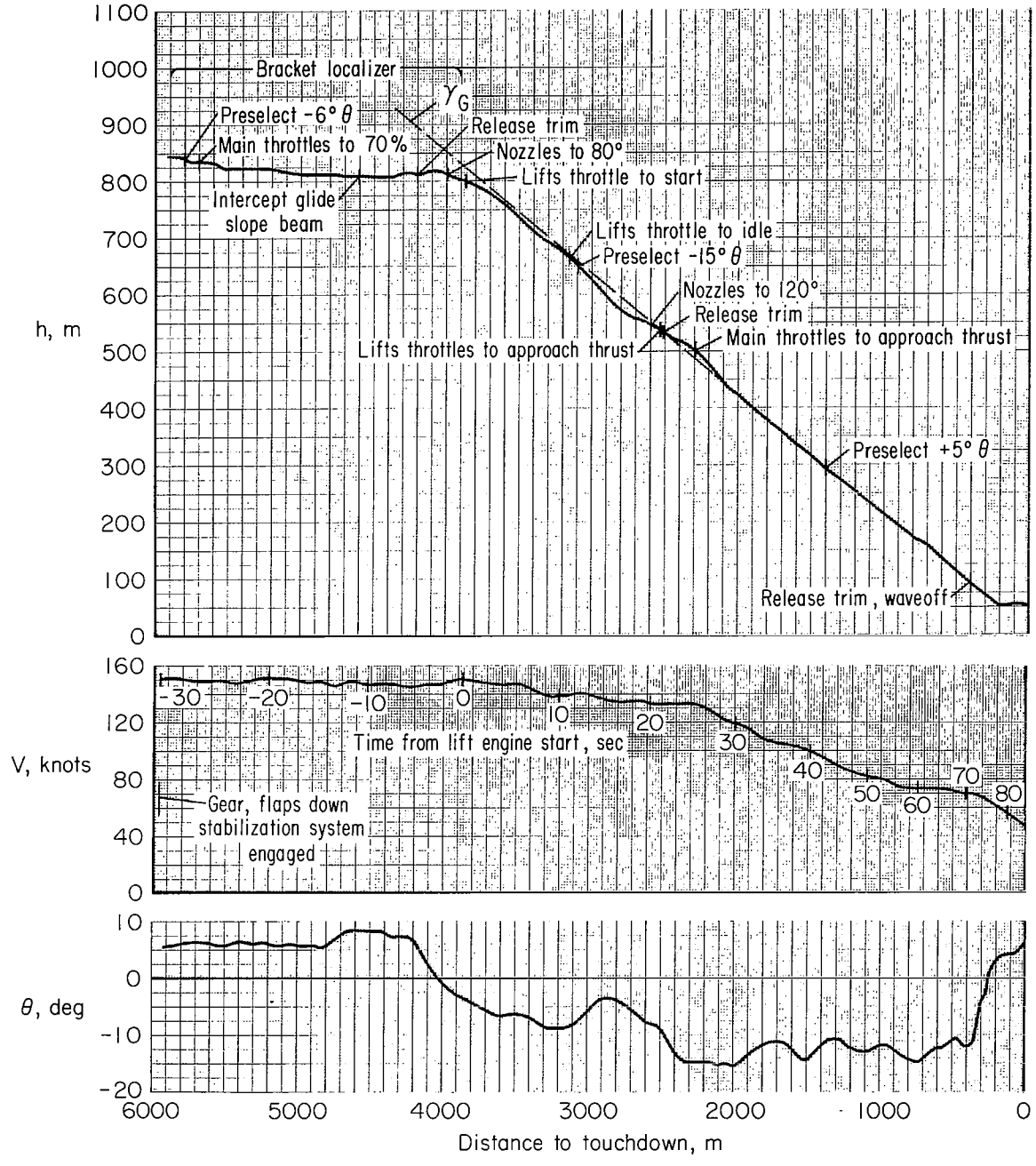

(a) Range data

Figure 16.– 12° simulated IFR approach starting lift engines on glide slope; m = 19,500 kg, wind 15 knots from right, $\gamma_G = 12° \pm 2°$.

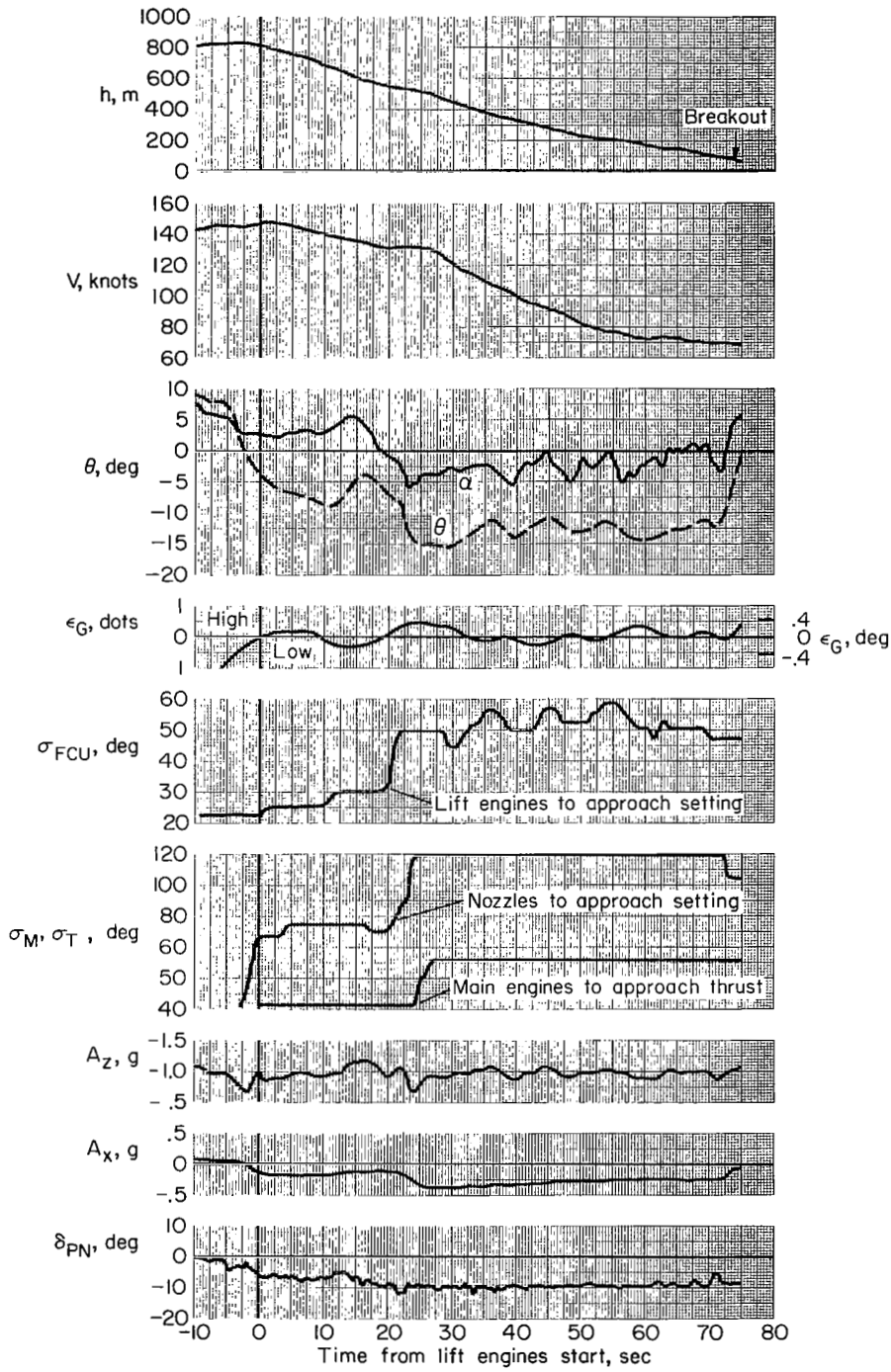

(b) Longitudinal parameters in approach

Figure 16.– Continued.

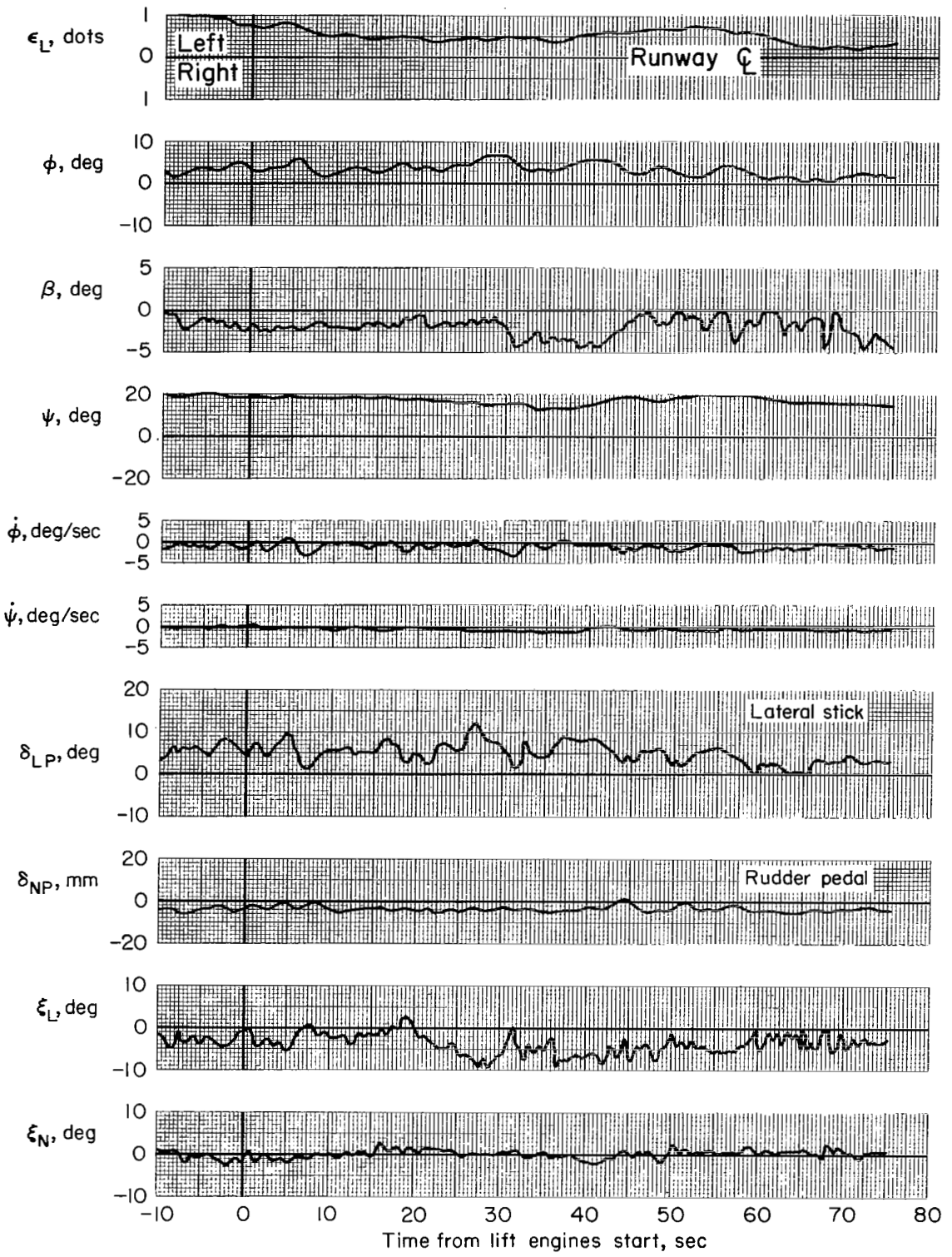

(c) Lateral-directional parameters in approach

Figure 16.– Concluded.

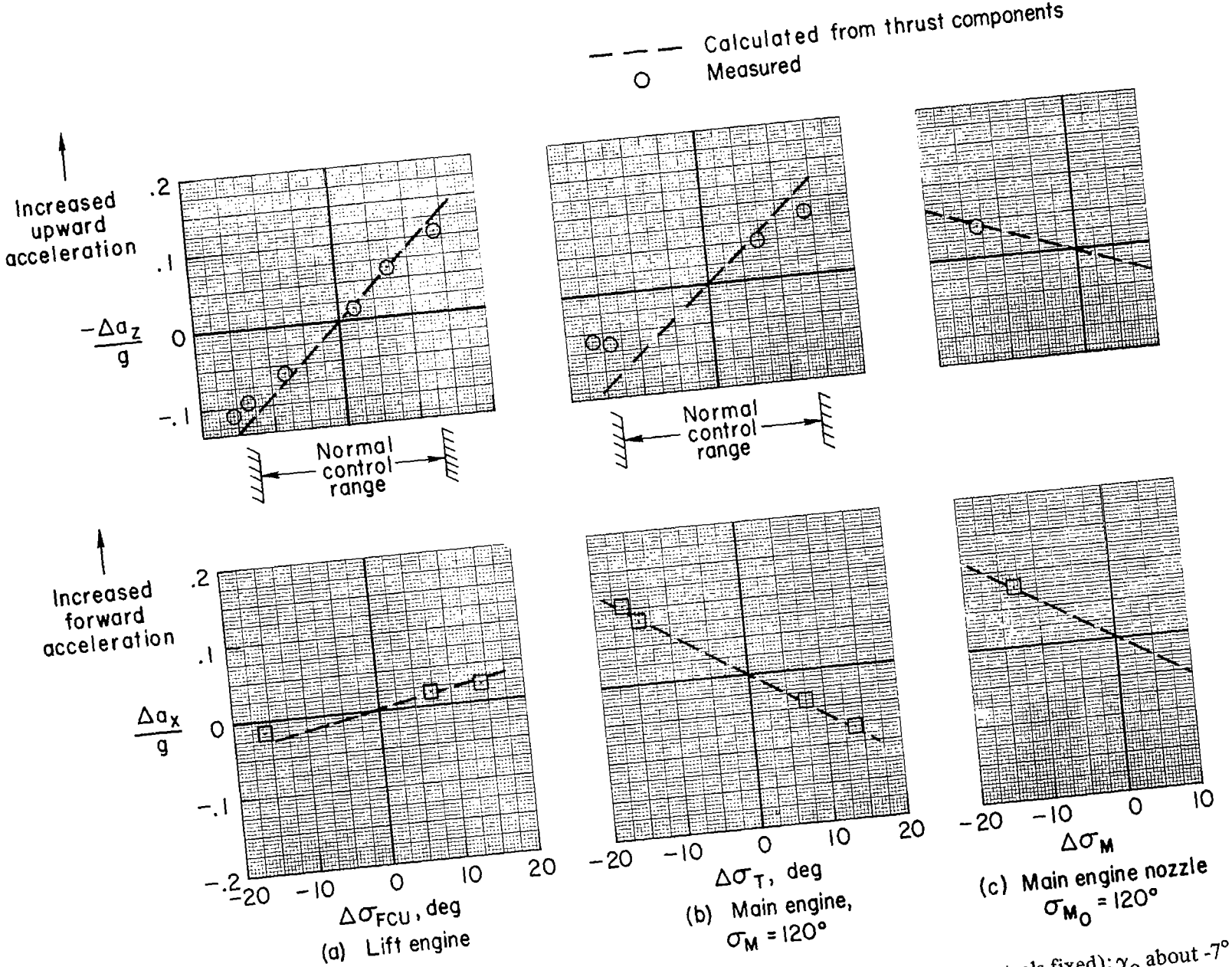

17. Incremental accelerations produced by each longitudinal control (with remaining controls fixed); γ_O about -7°, about -0.05 g, V = 50 to 80 knots, m = 19,500 kg.

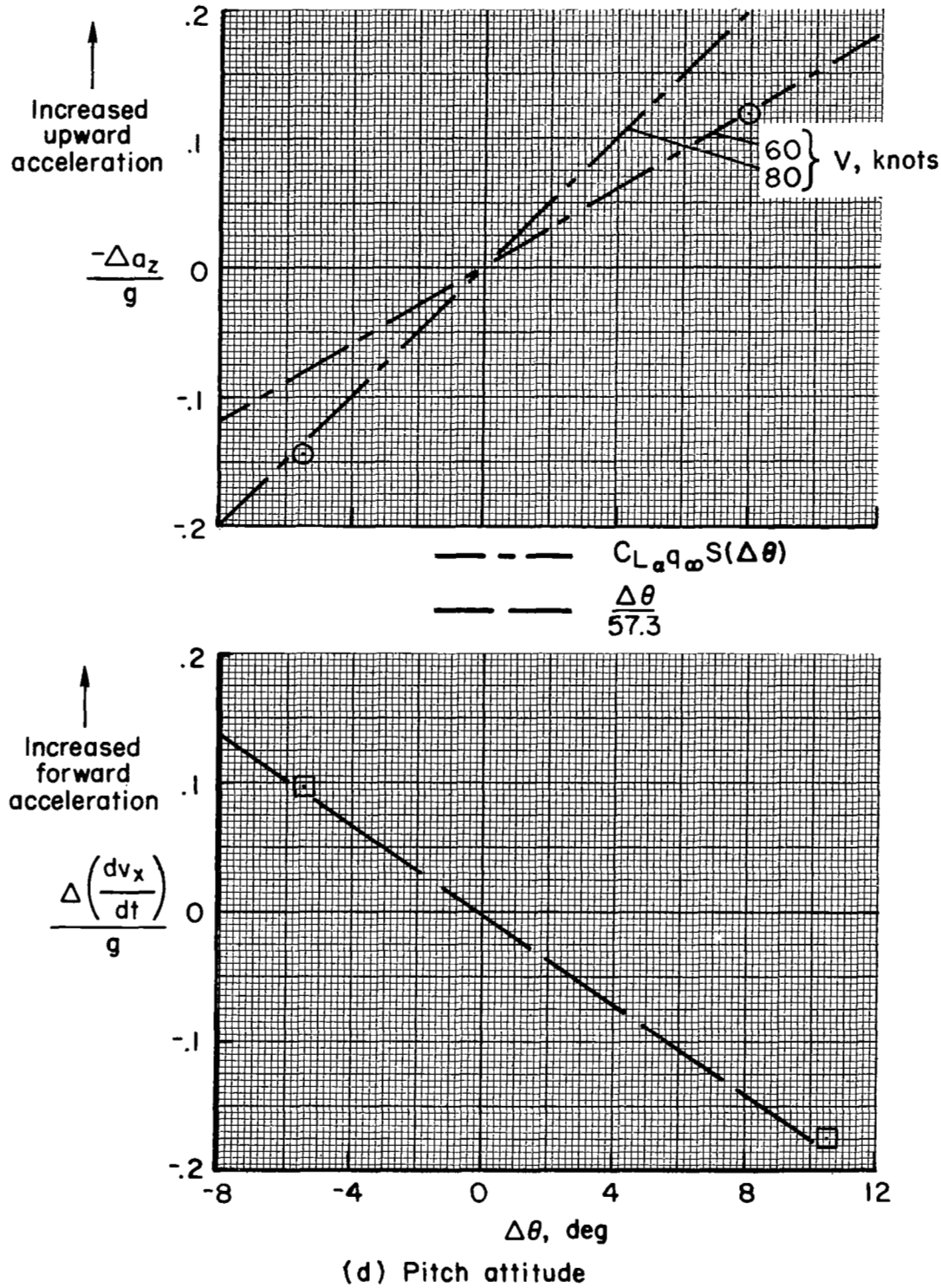

Figure 17.– Concluded.

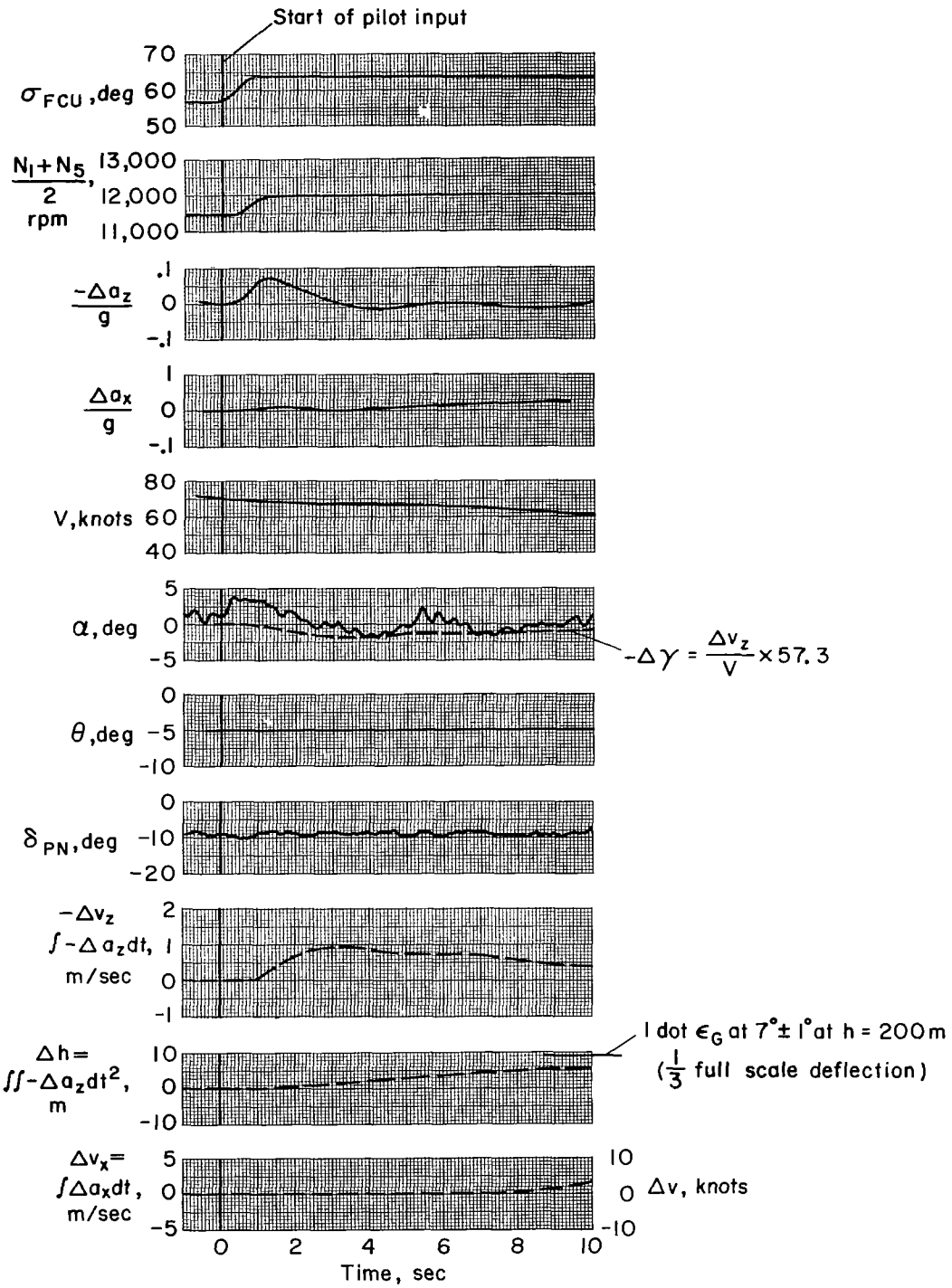

(a) Lift engine step with fixed attitude

Figure 18.– Longitudinal response produced by each control (with remaining fixed); γ_o about -7°, a_{x_o} about -0.05, V = 50 to 80 knots, m = 19,500 kg.

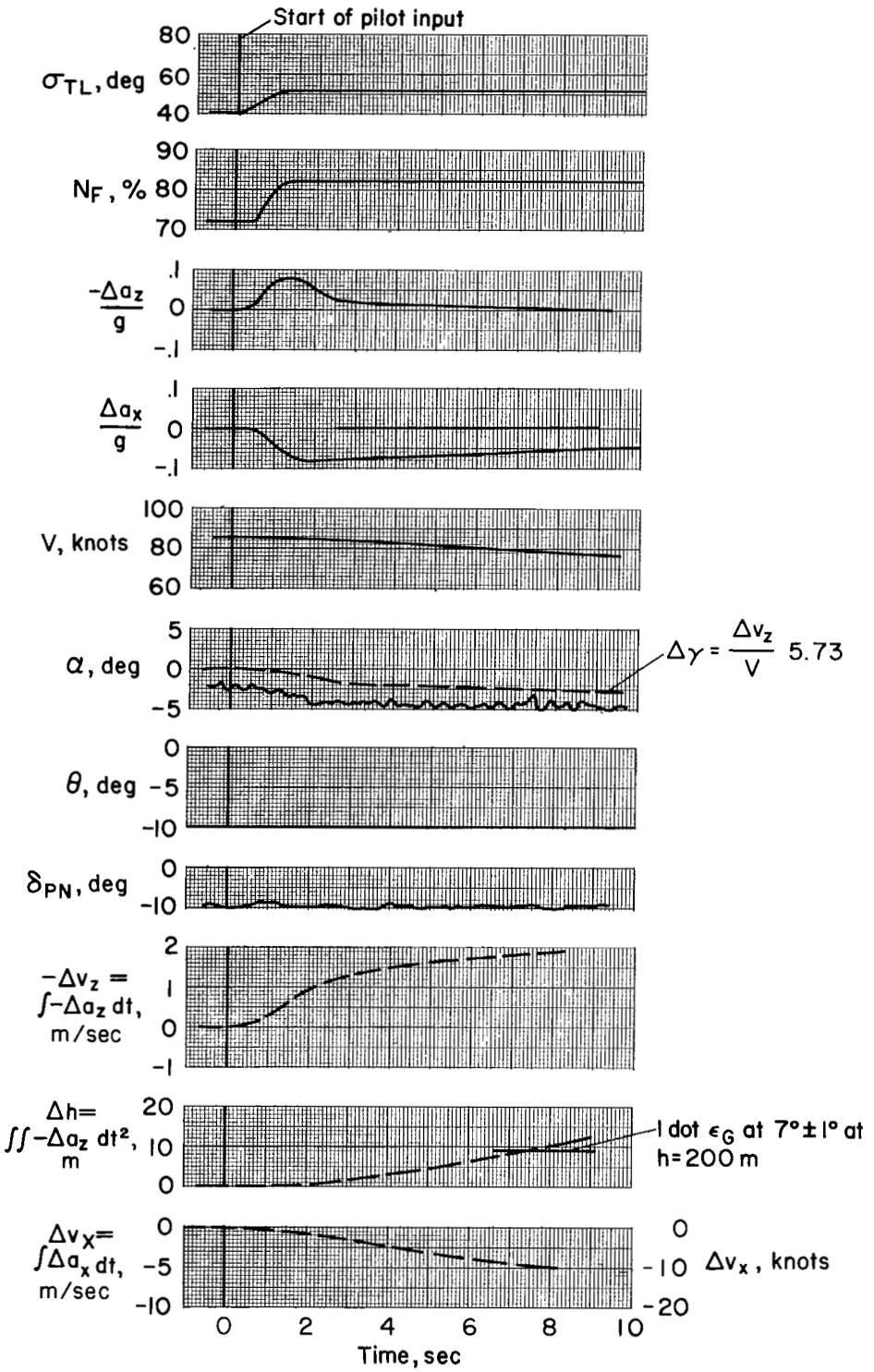

(b) Main engine step with fixed attitude

Figure 18.– Continued.

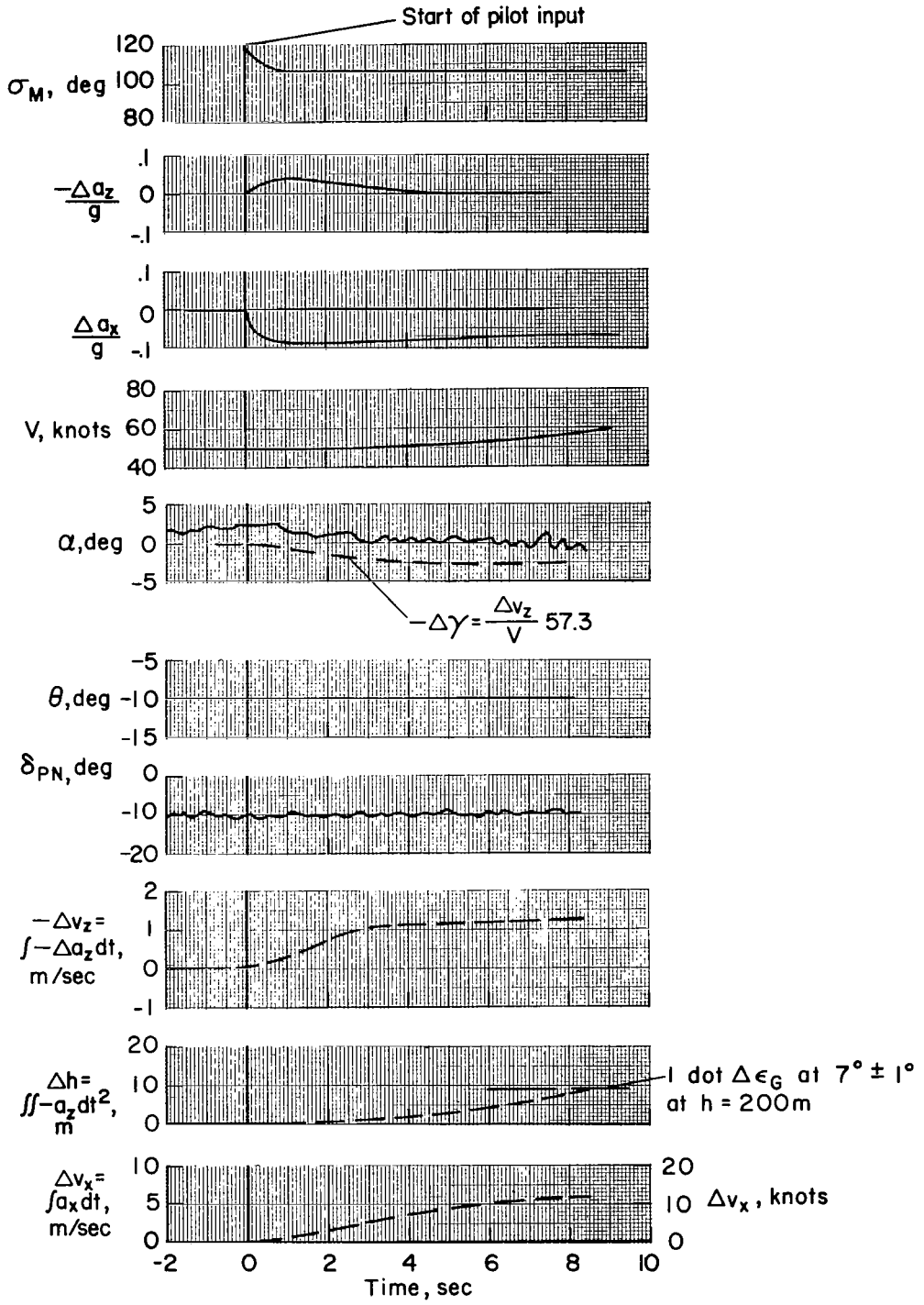

(c) Main engine nozzle step

Figure 18.– Continued.

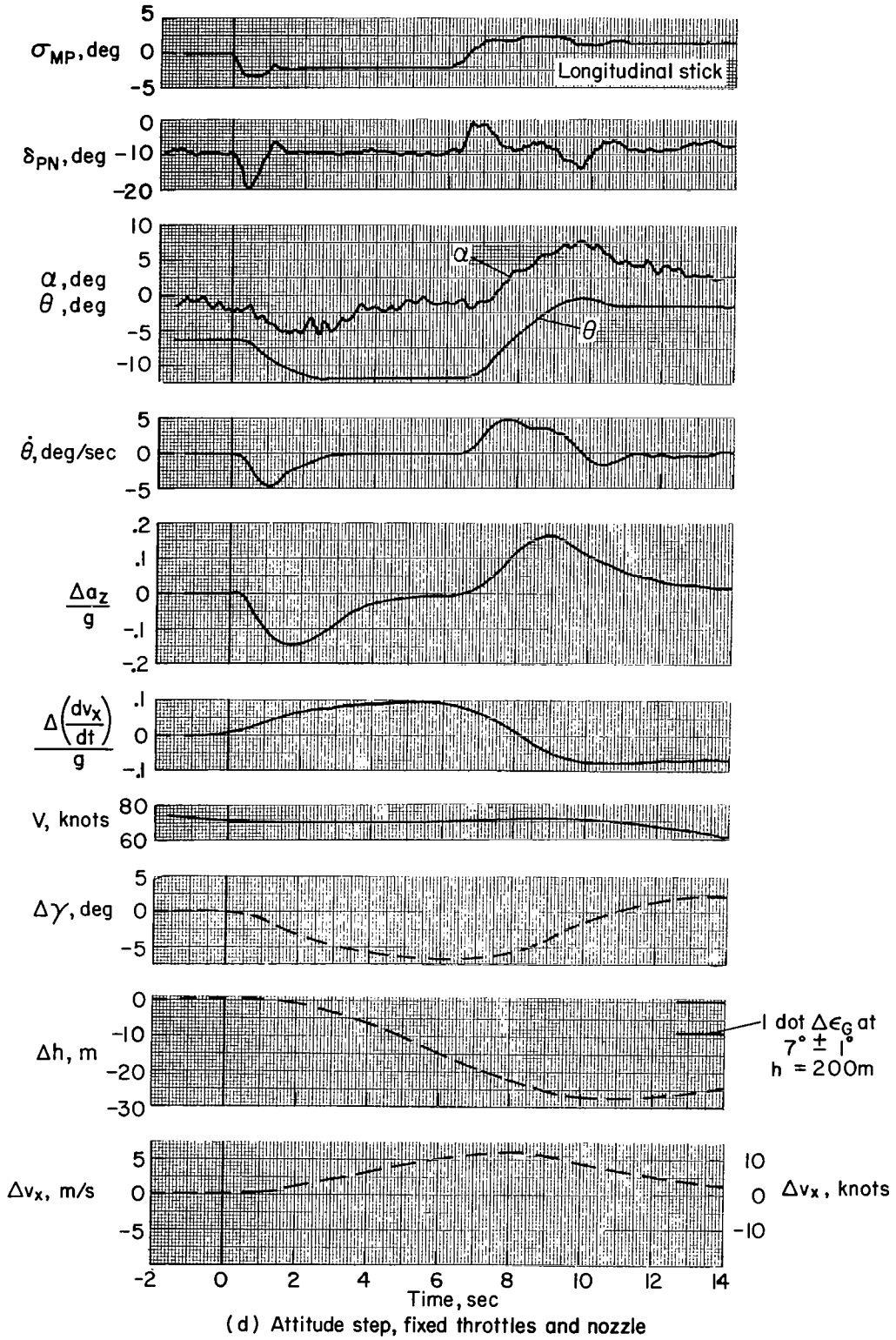

(d) Attitude step, fixed throttles and nozzle

Figure 18.– Concluded.

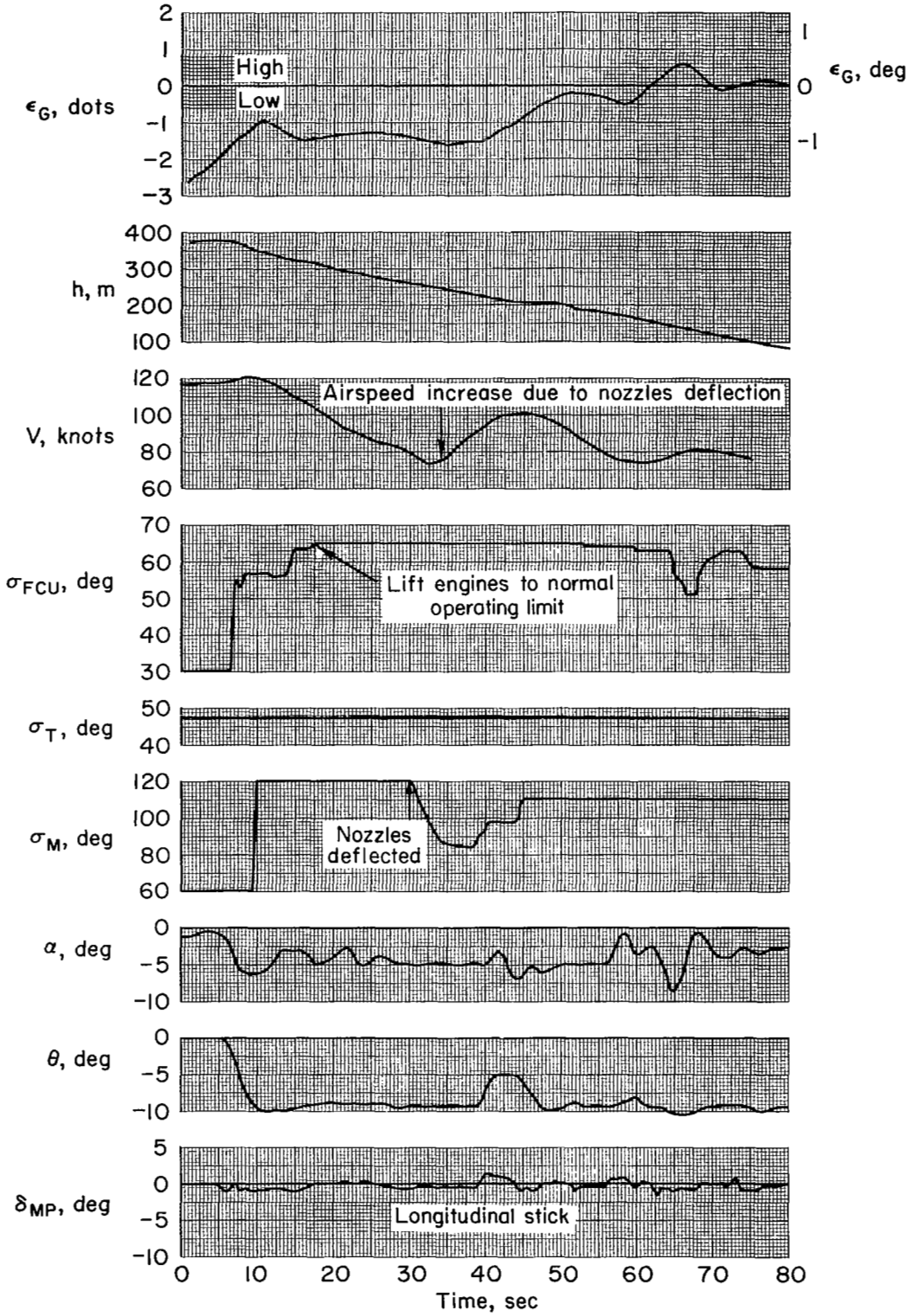

Figure 19.— Correction for 1-1/2 dot low error attempted by lift engines; $\gamma_G = 7° \pm 2°$.

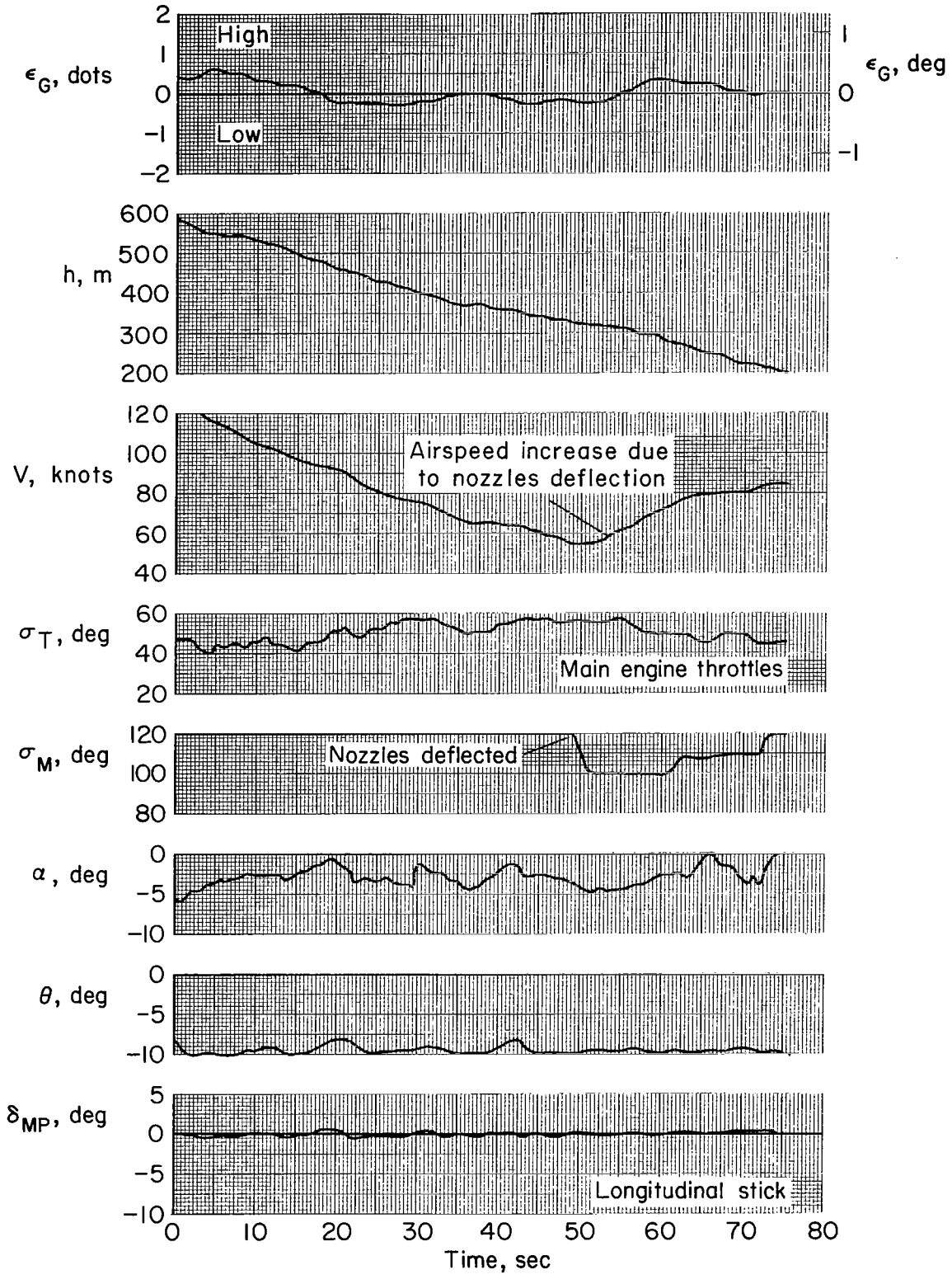

Figure 20.– Effect of main engine thrust modulation on glide-slope tracking; $\gamma_G = 7° \pm 2°$.

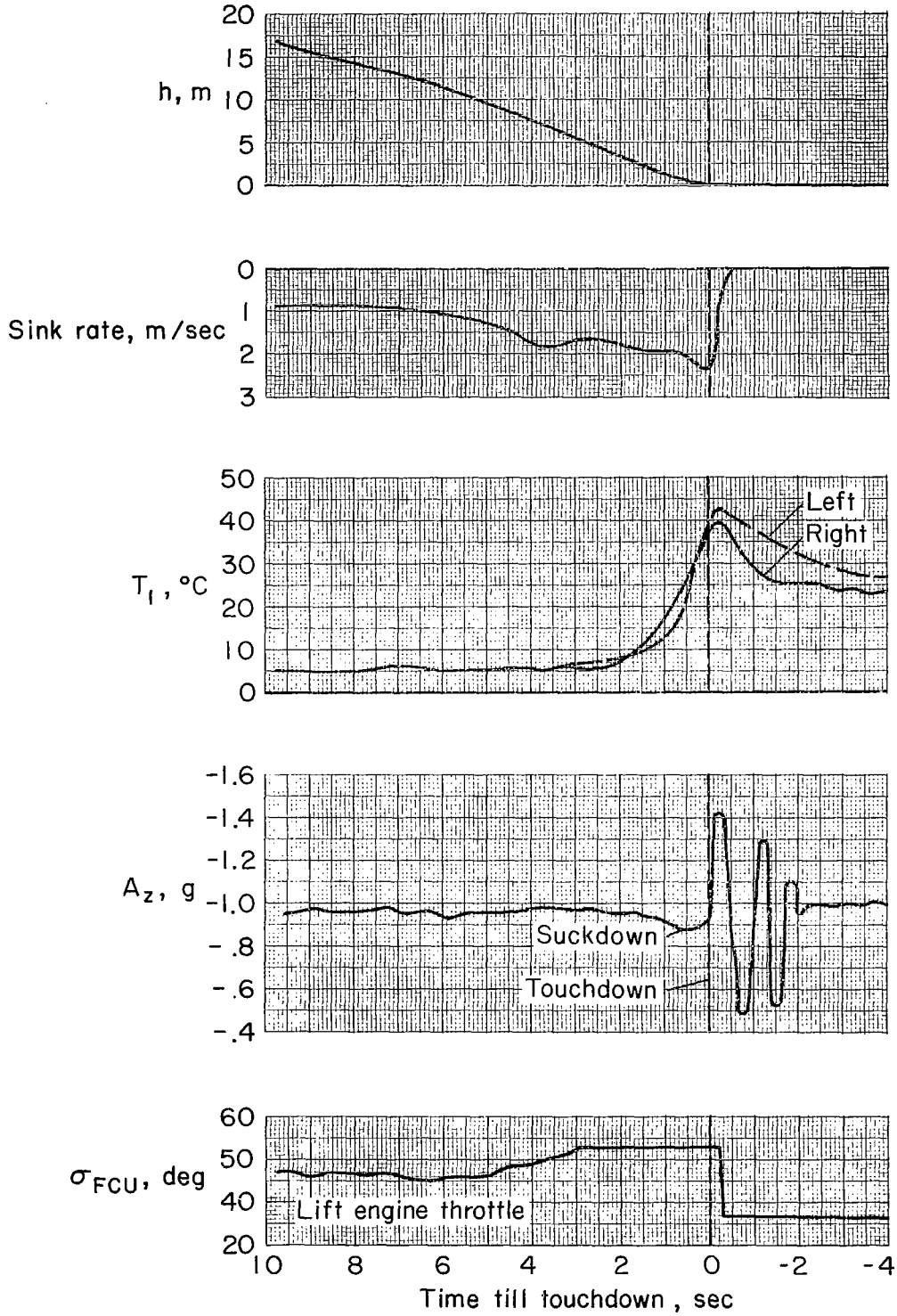

Figure 21.– Lift loss in vertical landing.

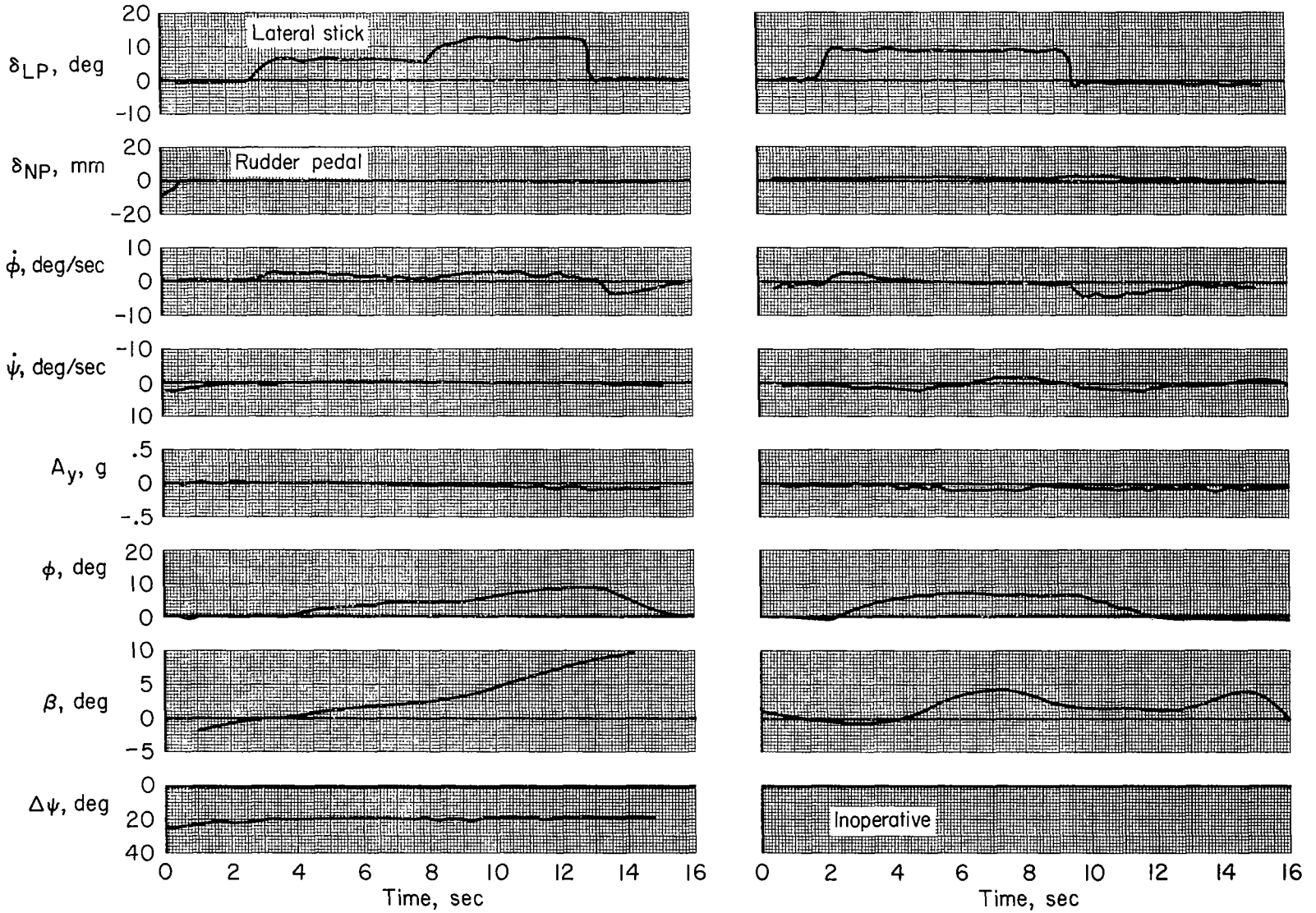

(a) Yaw stabilization on

(b) Yaw stabilization off

Figure 22.– Lateral attitude steps without directional control inputs; V = 70 to 90 knots, m = 19,500 kg.

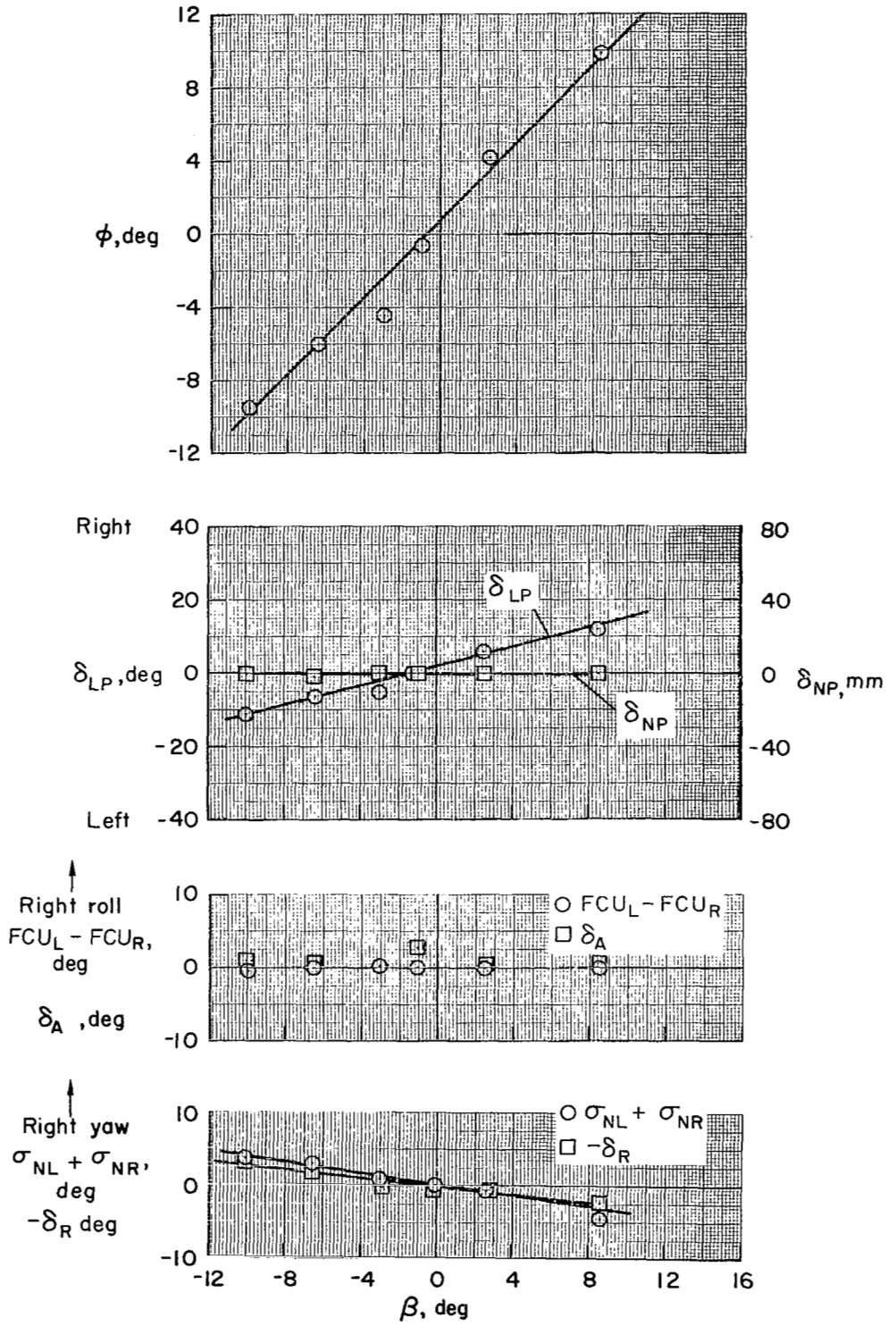

Figure 23.– Static lateral-directional characteristics with stabilization engaged; V = 70 to 90 knots, $\gamma_o = -7°$, $\sigma_{FCU} = 57°$, $N_F = 80$ percent, $\sigma_M = 120°$, m = 19,500 kg.

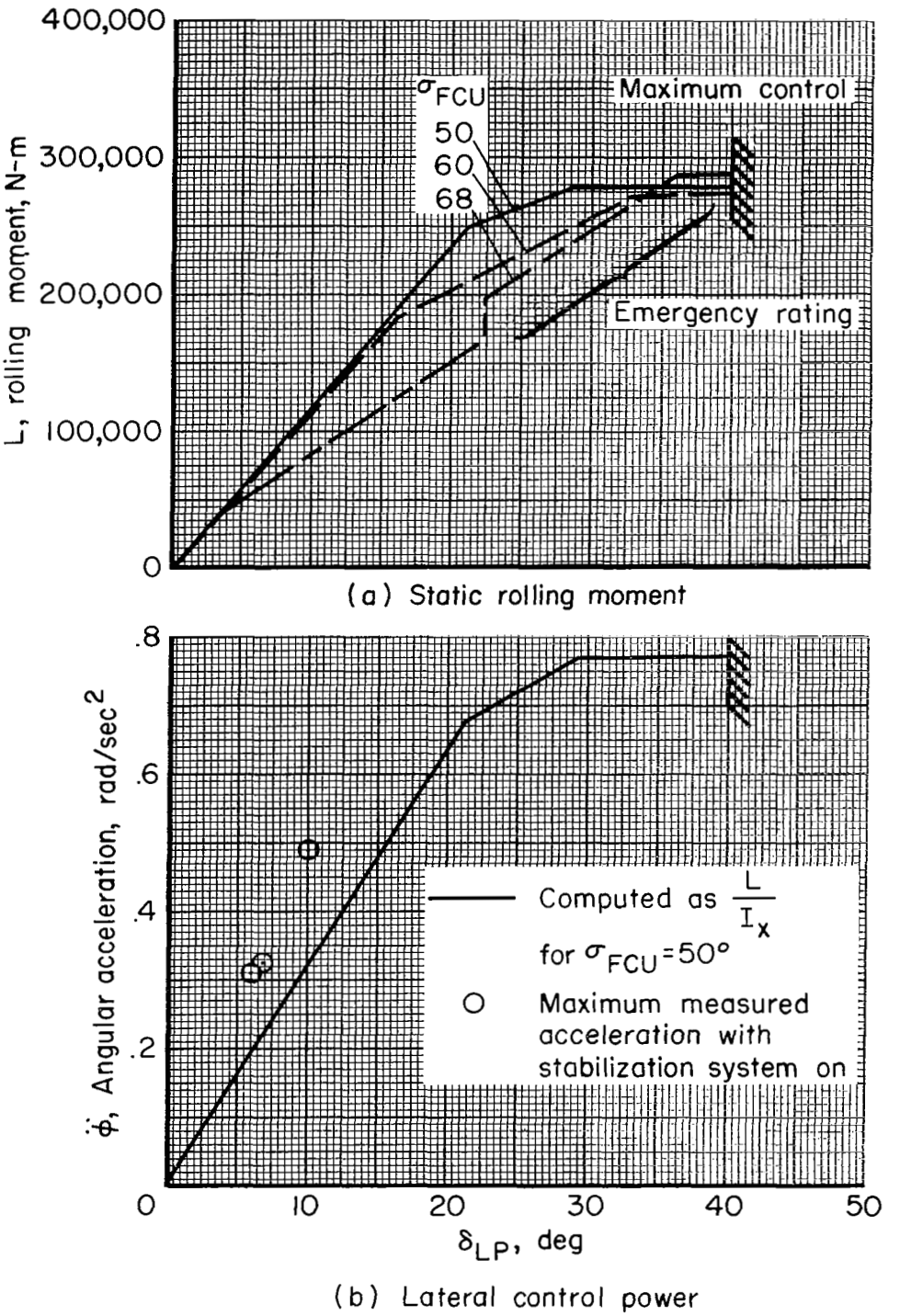

Figure 24.– Lateral control capability in hover; m = 19,000 kg, I_x = 385,000 kg-m^2.

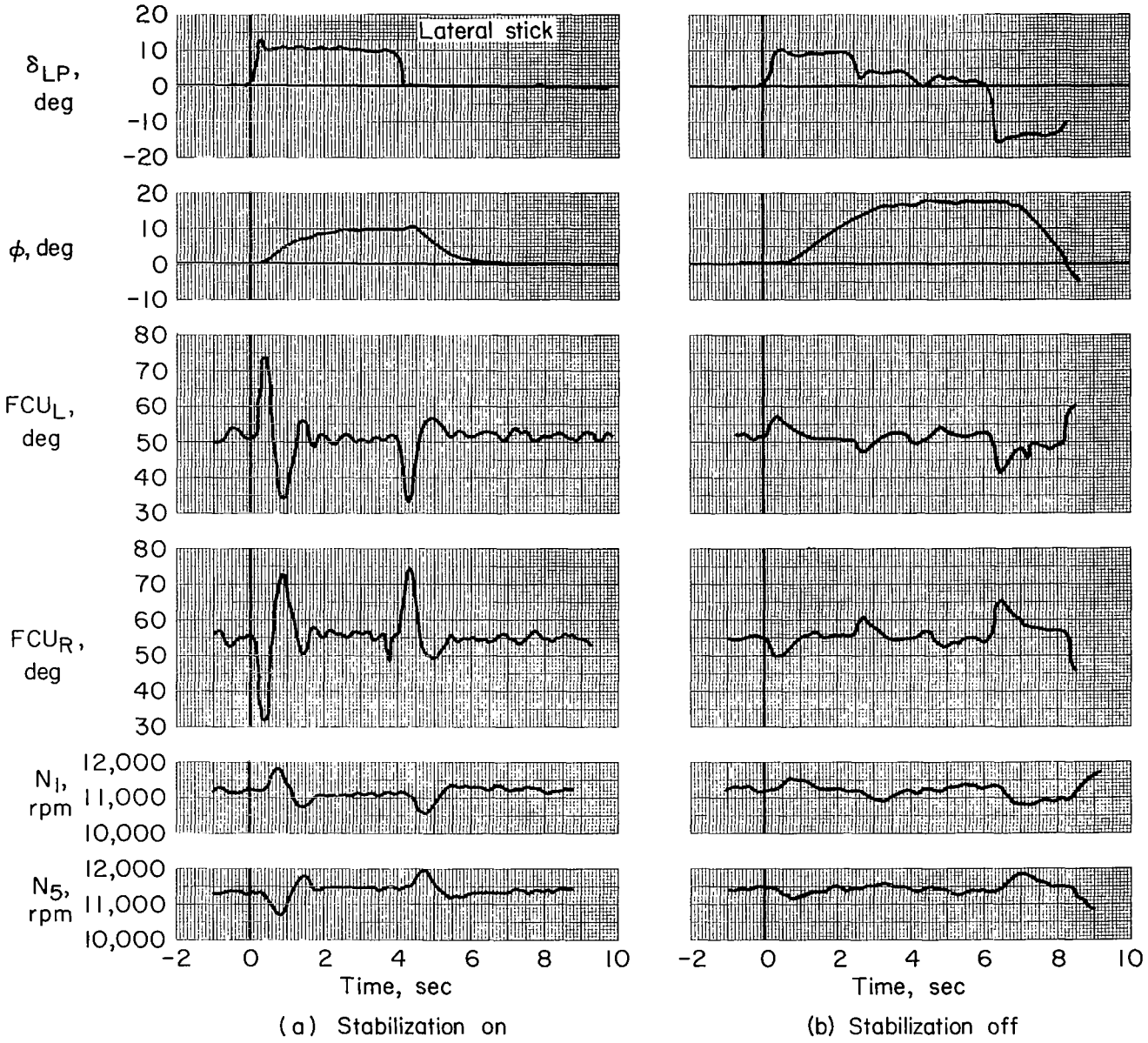

Figure 25.– Response to lateral control input; hover rig on pedestal.

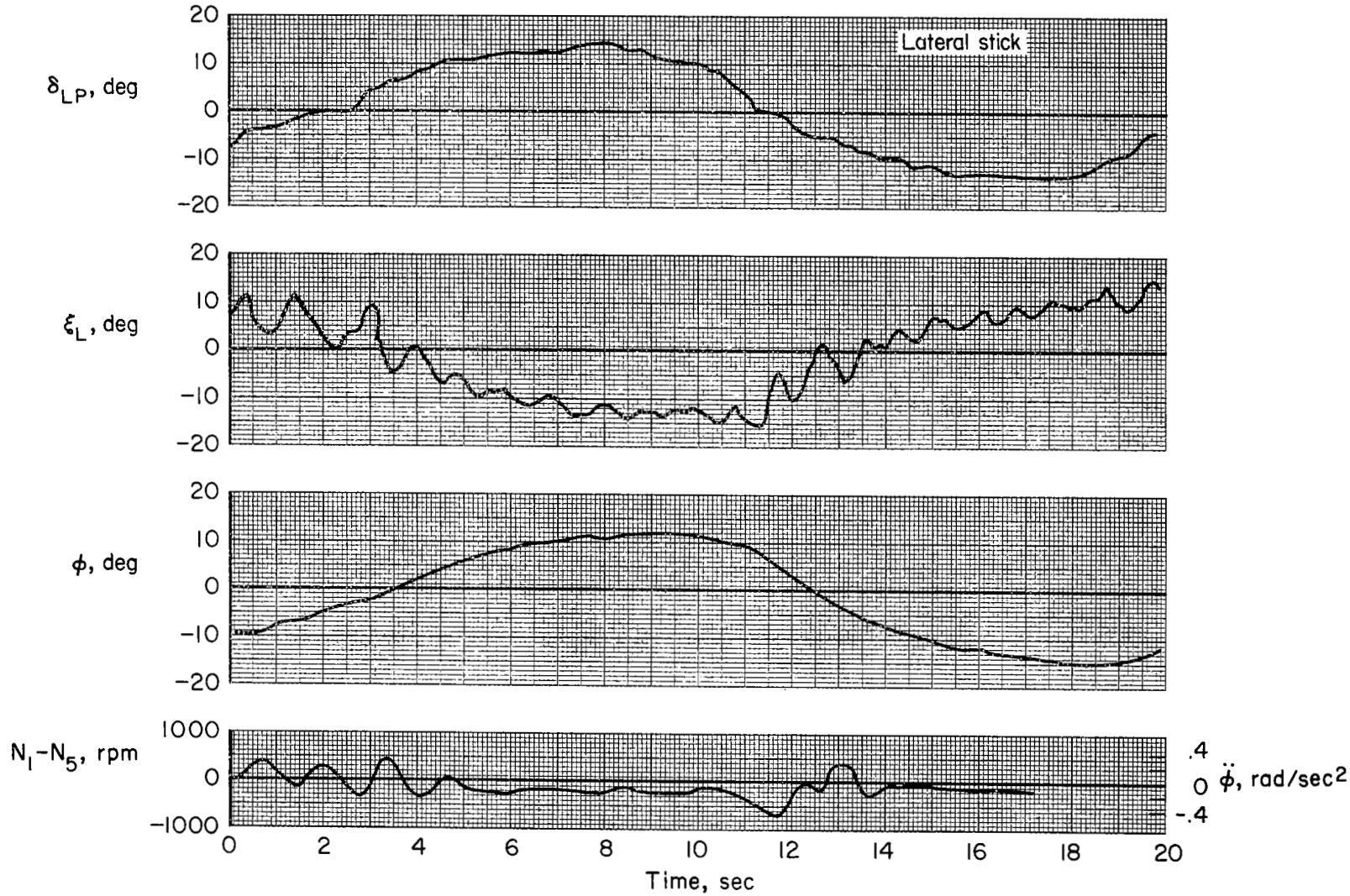

Figure 26.– Lateral maneuvering in hover.

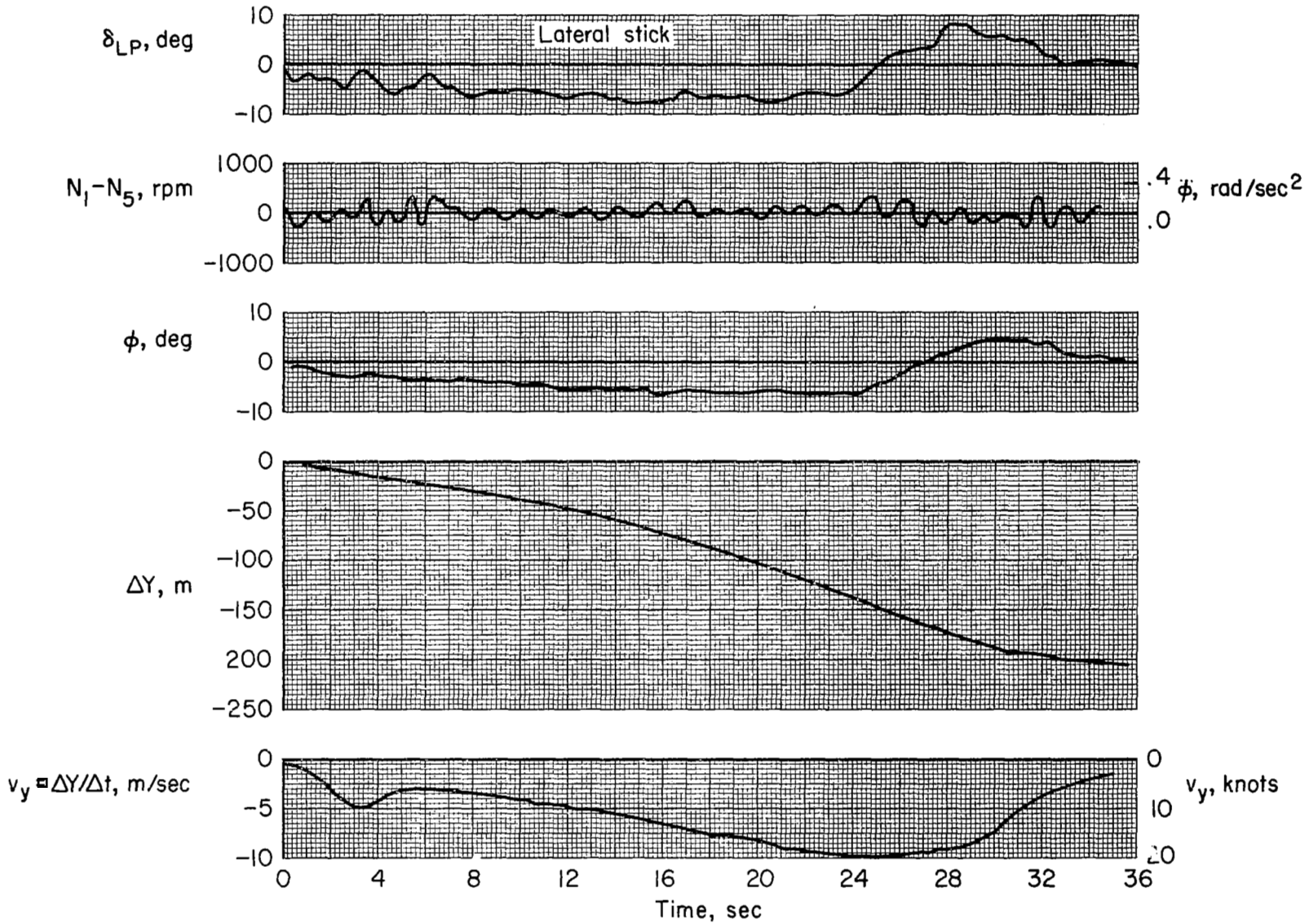

Figure 27.– Slow buildup to maximum desired lateral translational velocity in hover.

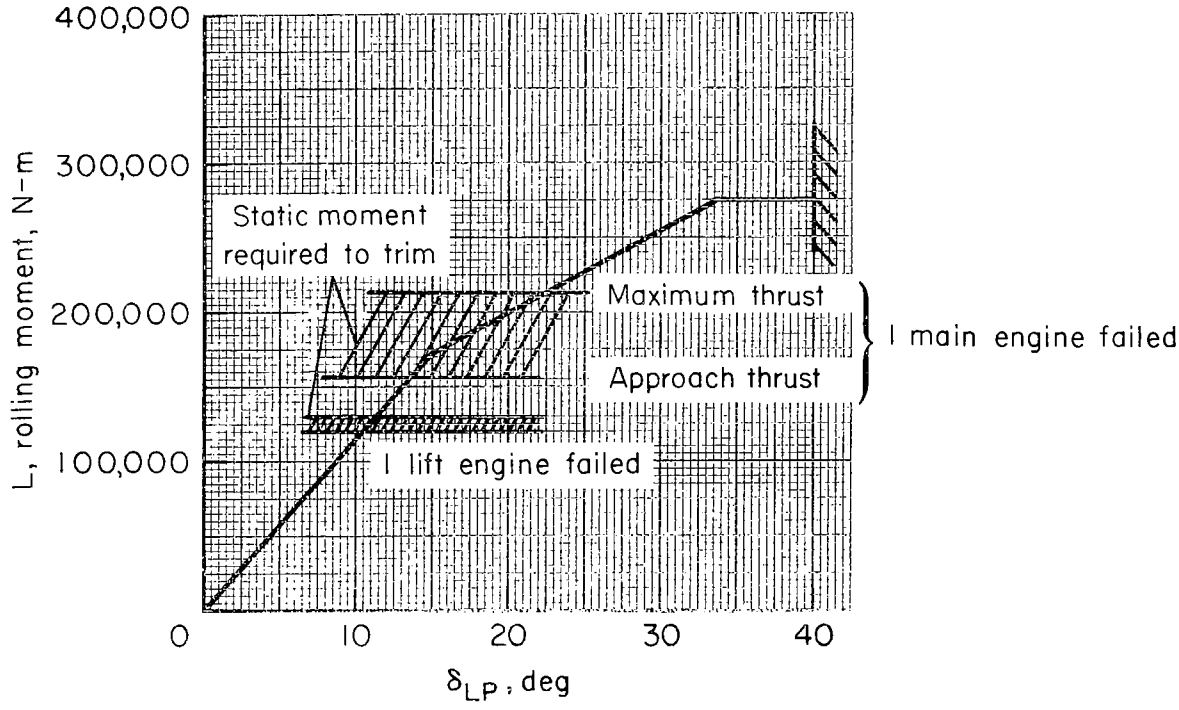

Figure 28.– Lateral control to balance an engine failure; $\sigma_{FCU} = 60°$.

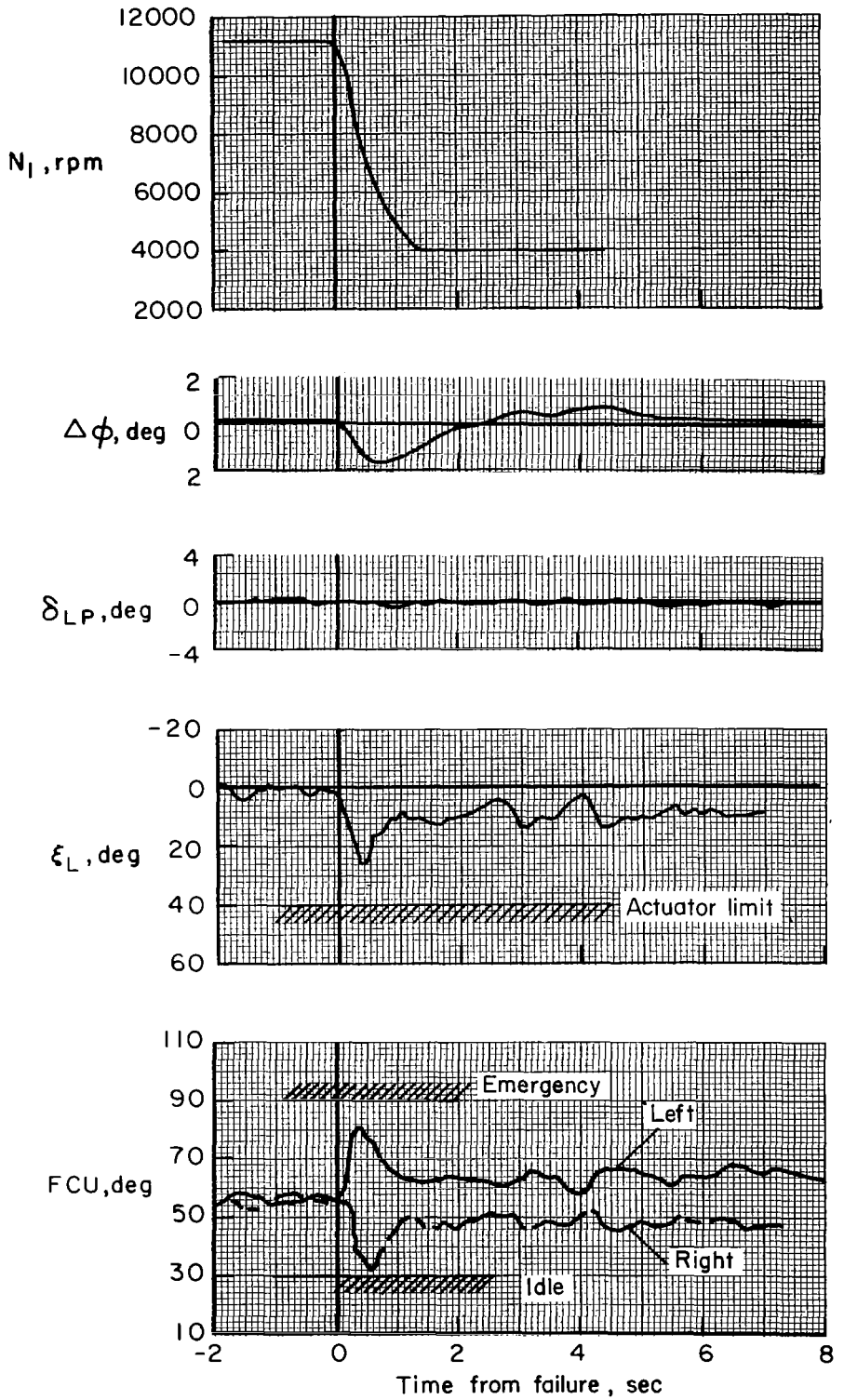

Figure 29.– Lateral response to lift engine failure without pilot correction; hover rig on pedestal.

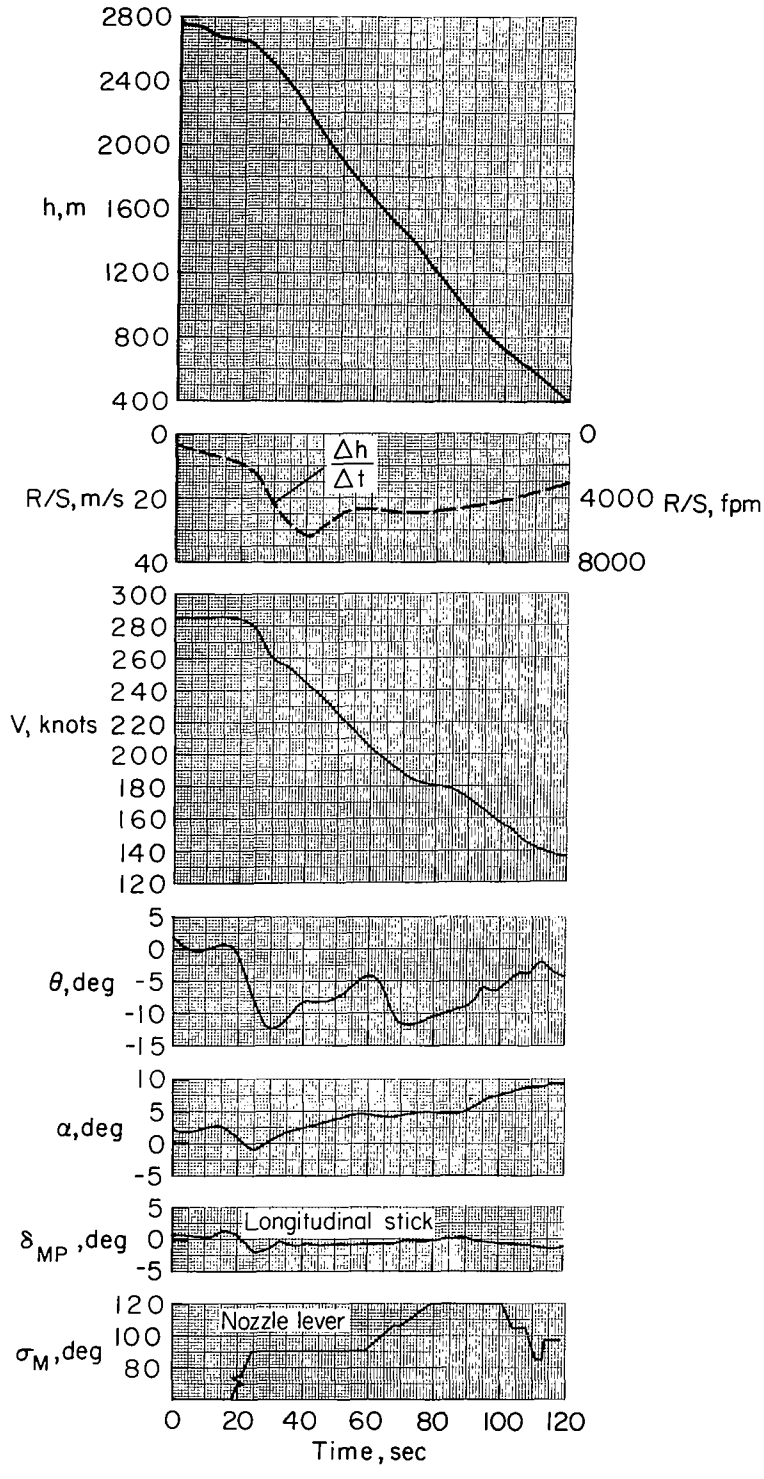

Figure 30.– Letdown from cruise to preapproach using main engine nozzle deflection; N_F = 72 percent.

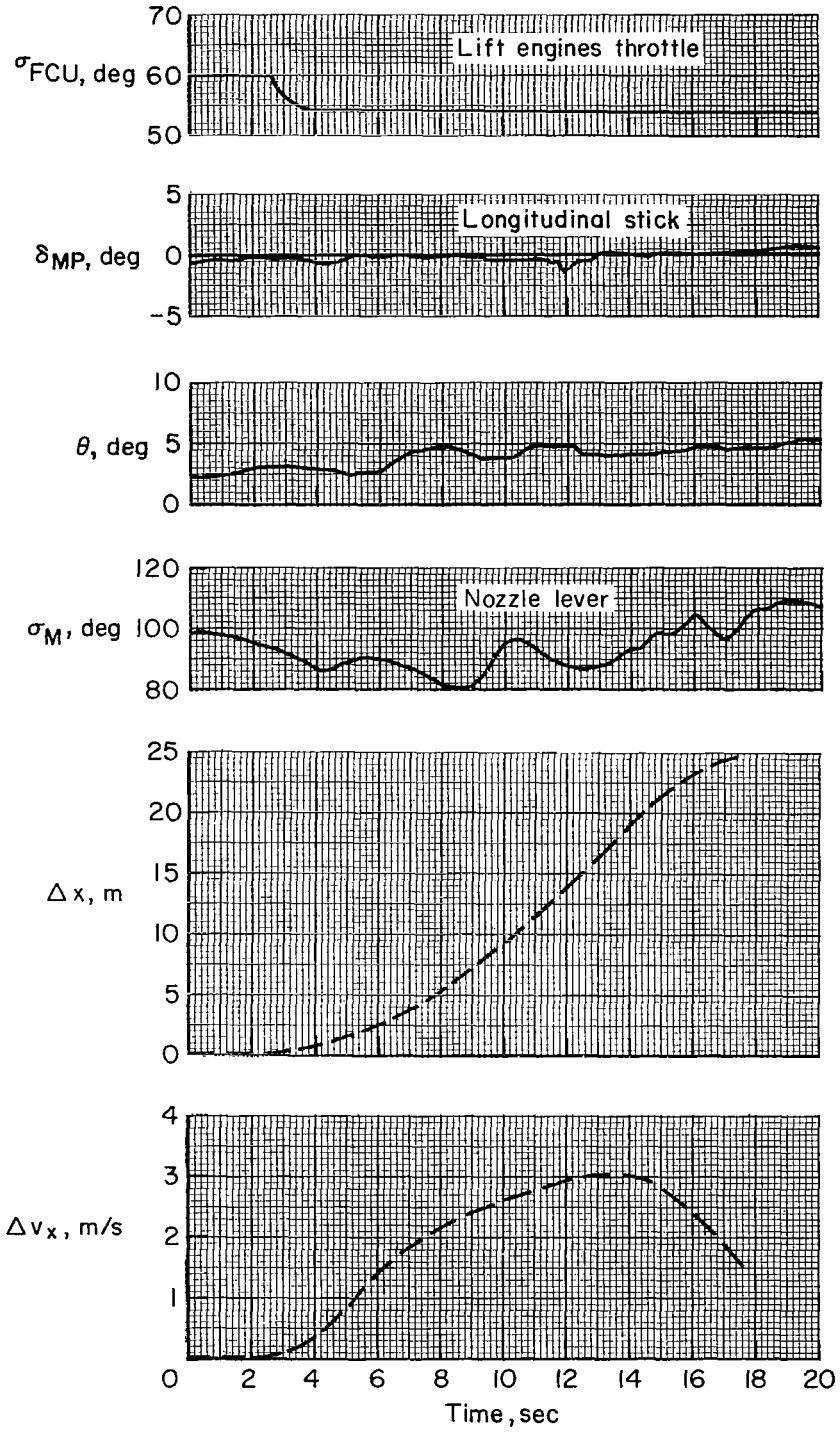

(a) By main engine nozzle deflection

Figure 31.– Longitudinal translation in hover.

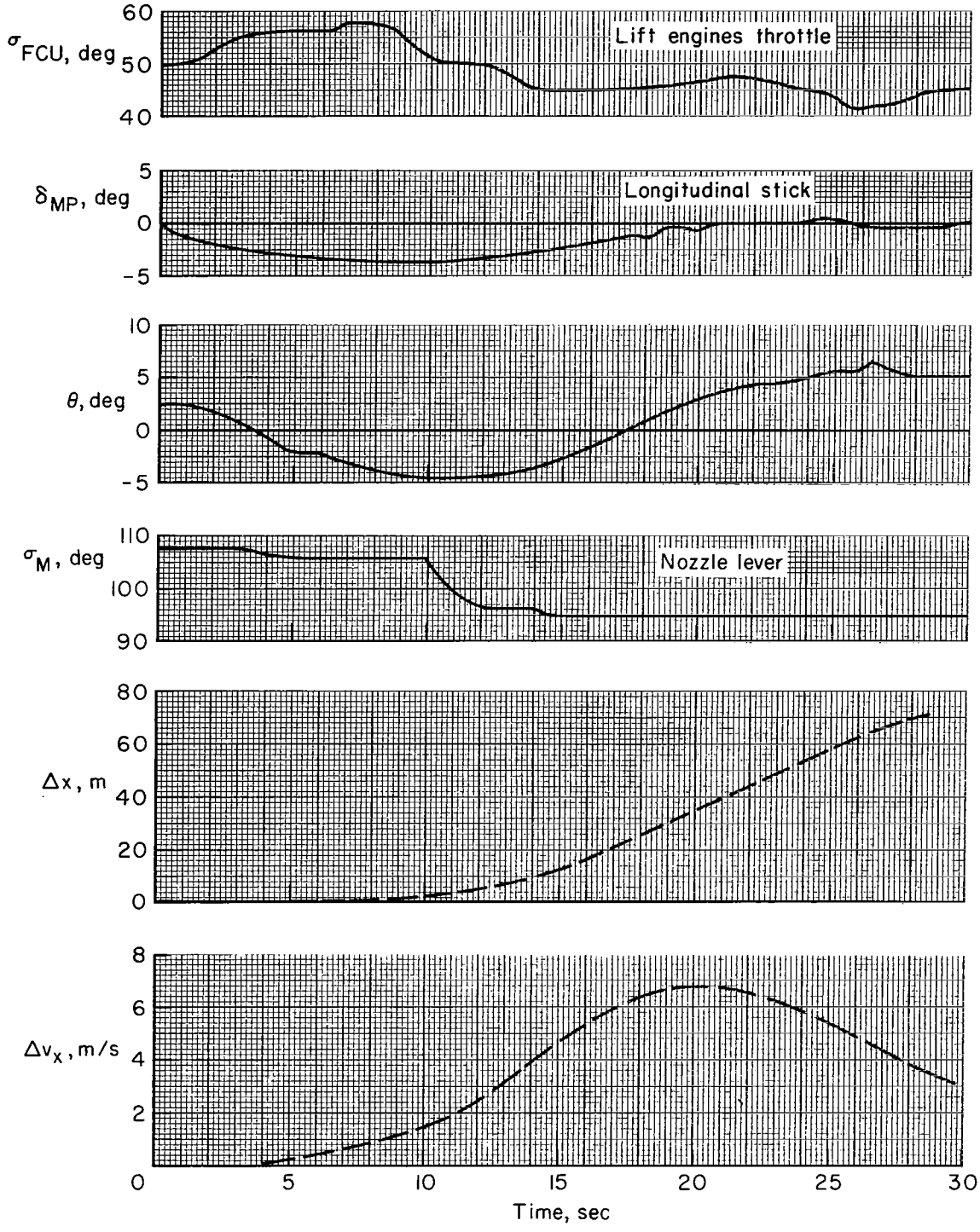

(b) By attitude and nozzle

Figure 31.– Concluded.

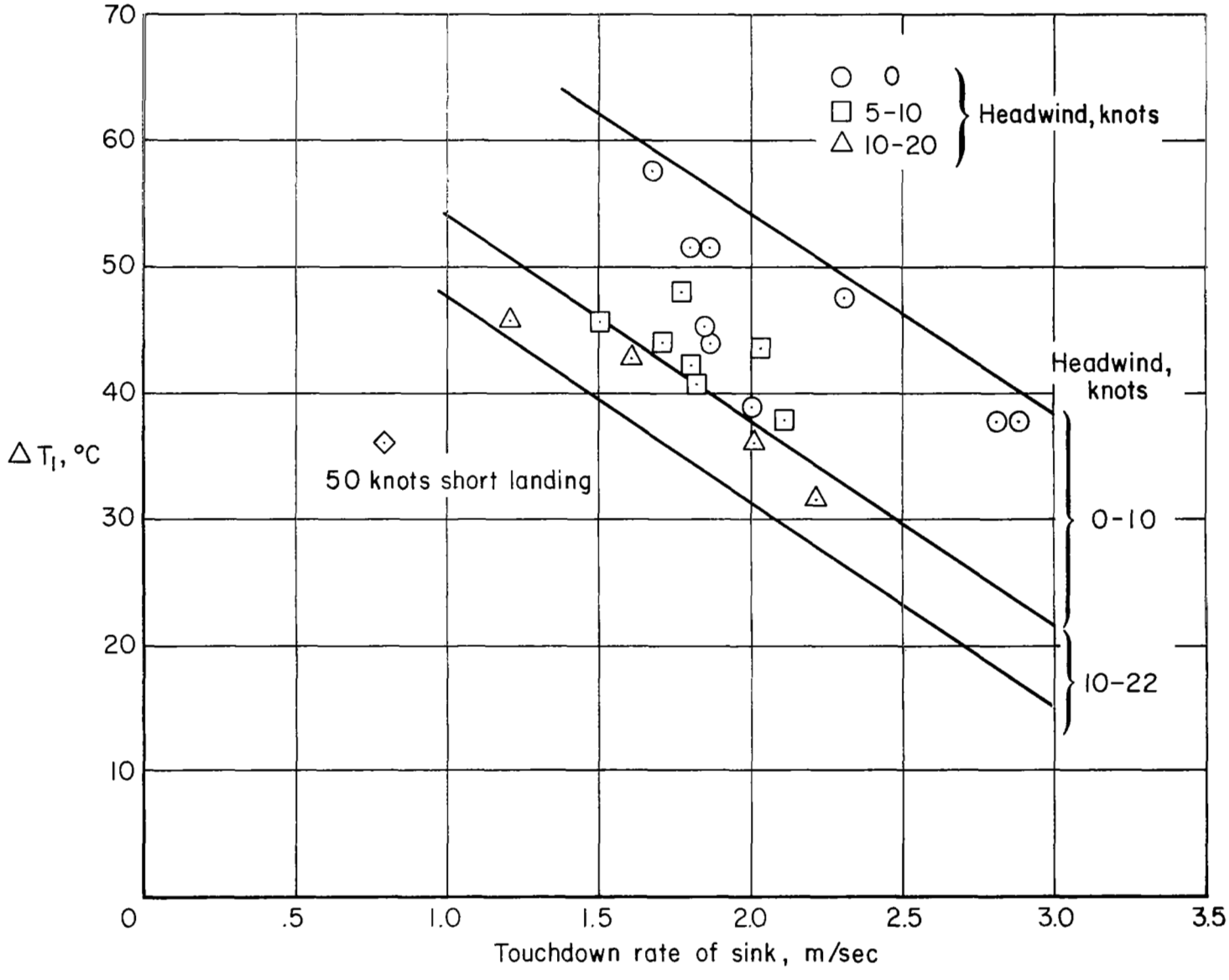

Figure 32.– Effect of sink rate and wind on reingestion during vertical landing.

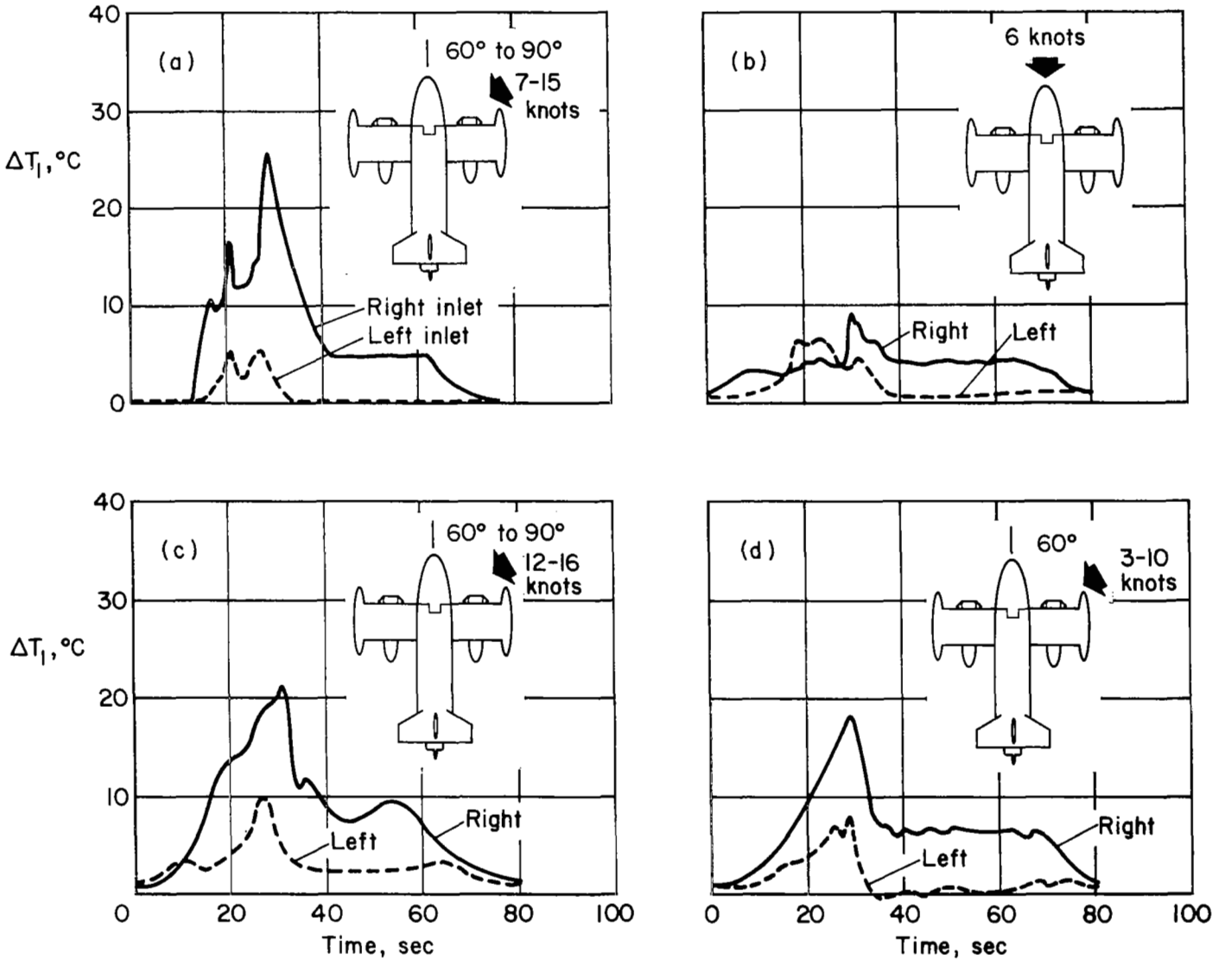

Figure 33.– Vertical takeoff reingestion with different wind conditions.

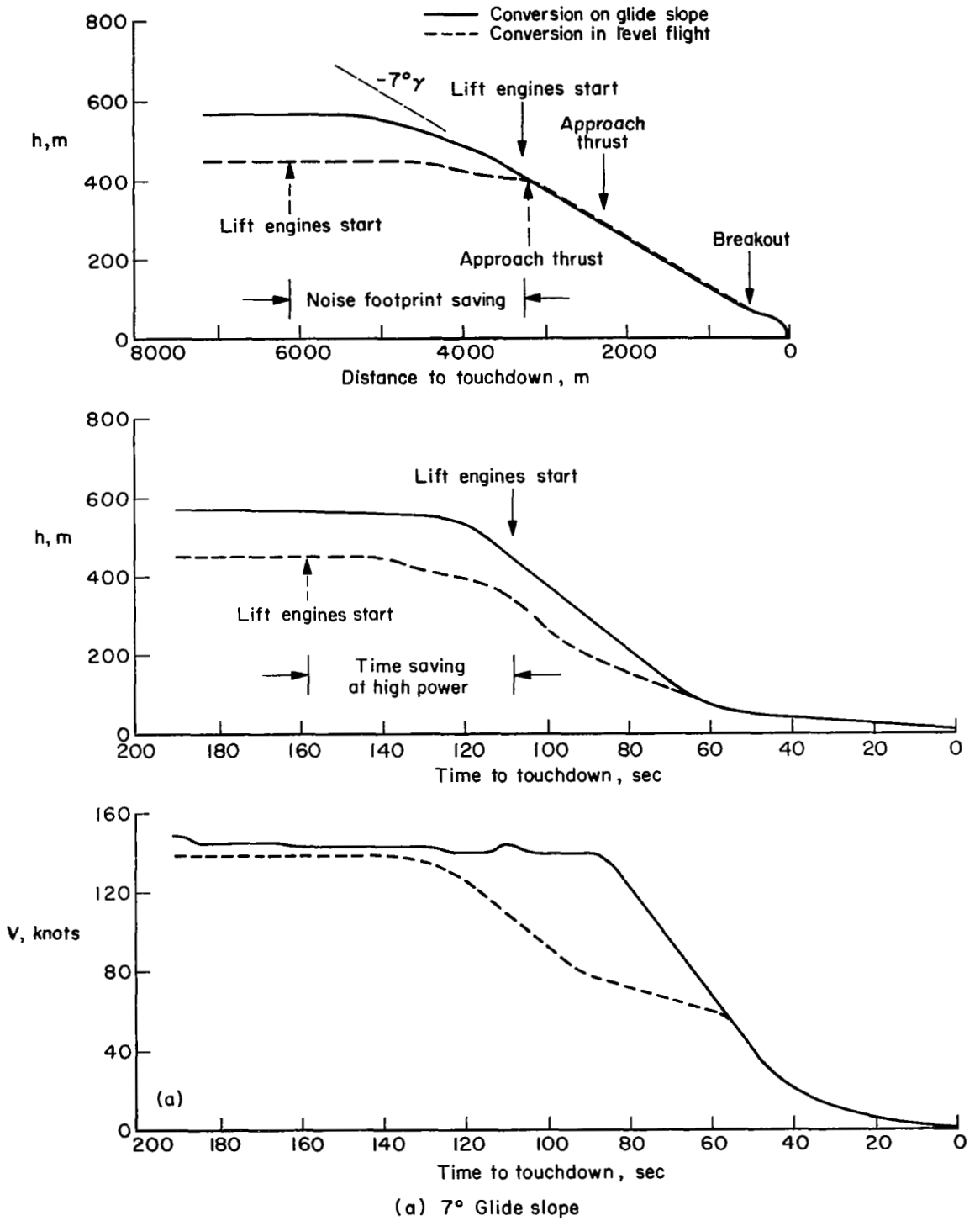

(a) 7° Glide slope

Figure 34.– Comparison of time and distance for different approaches.

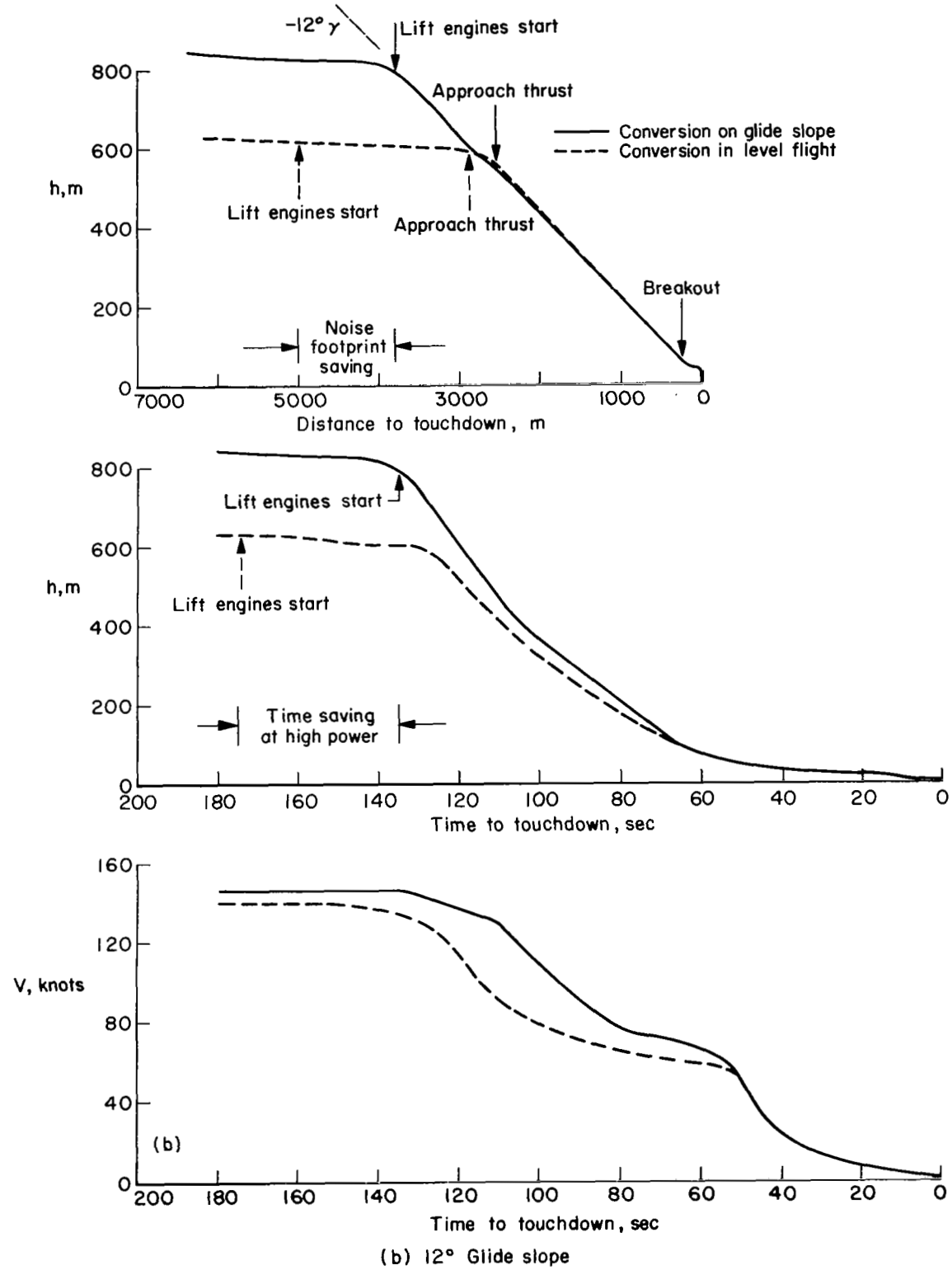

(b) 12° Glide slope

Figure 34.– Concluded.

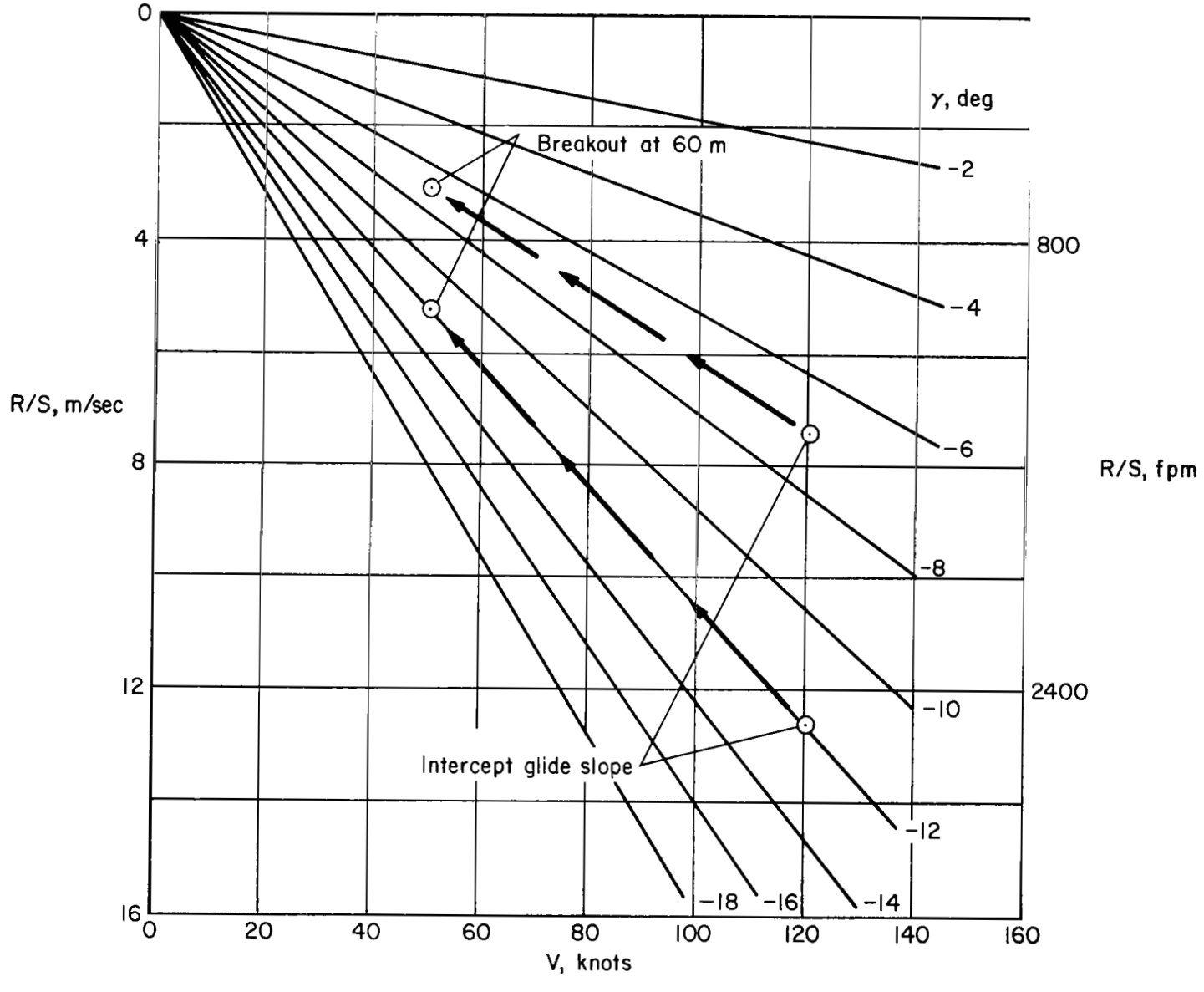

Figure 35.– Variation of rate of sink with airspeed and flight-path angle, zero wind.

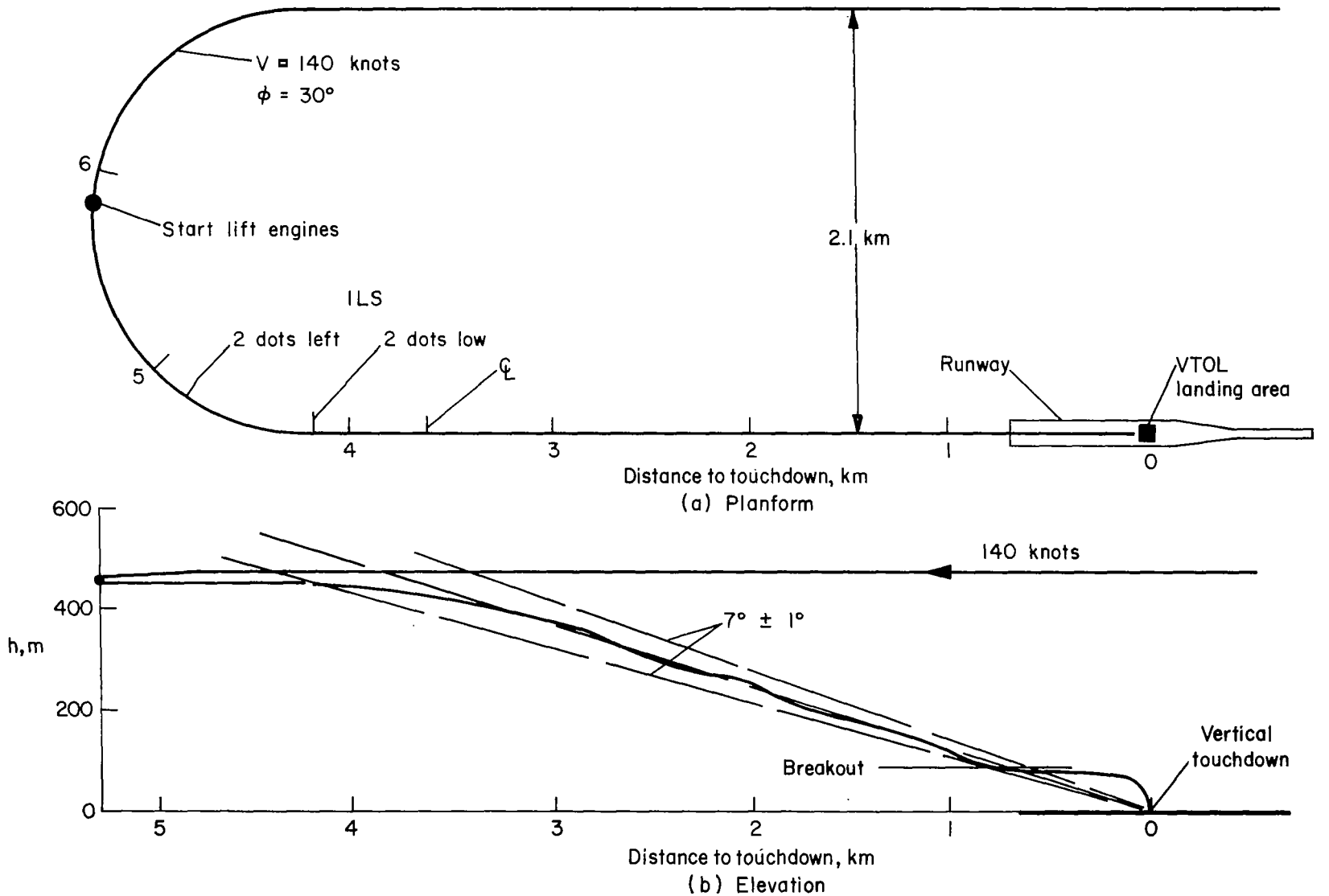

Figure 36.– Close in pattern, starting lift engines during turn.

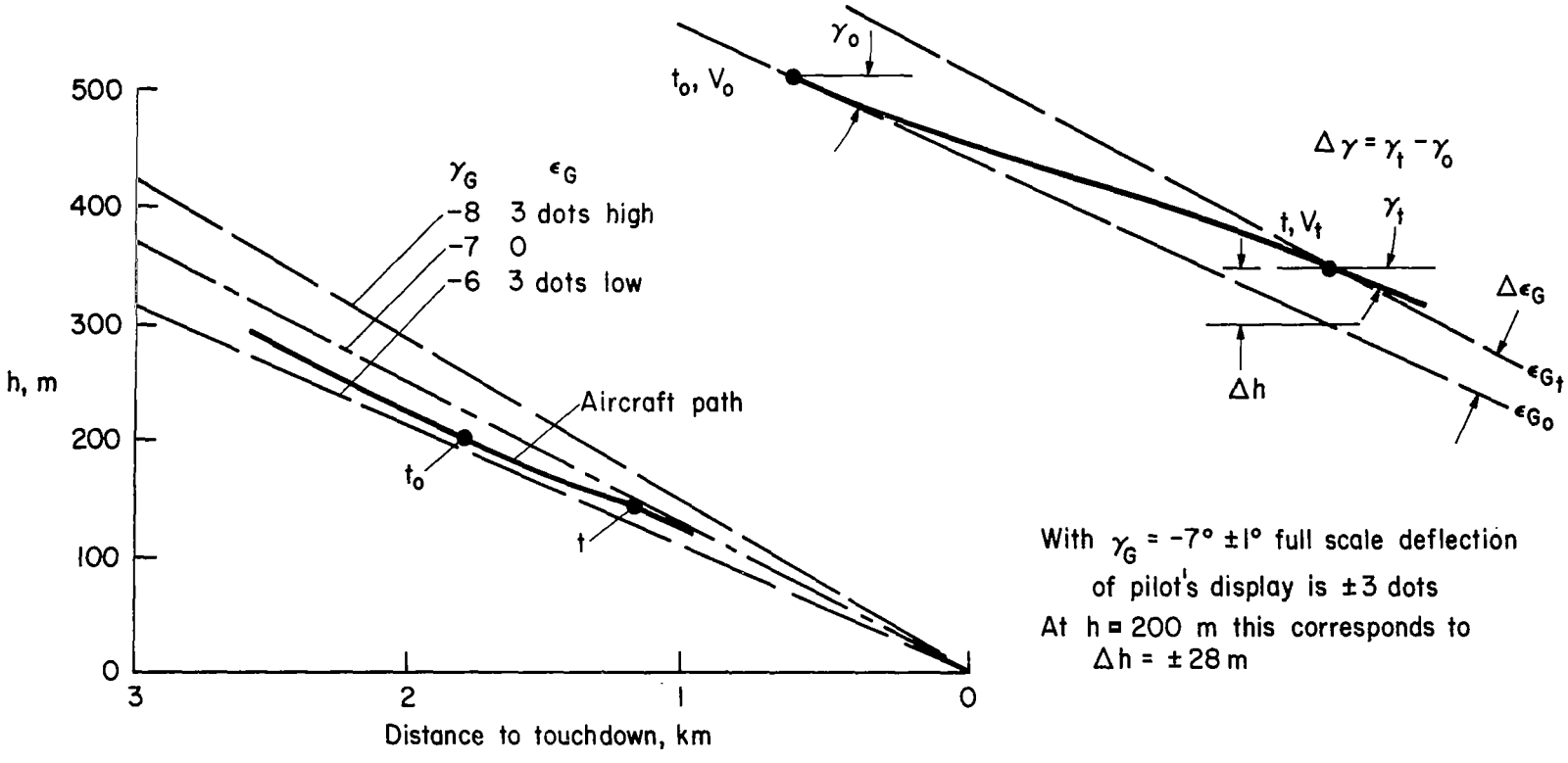

Figure 37.— Flight-path relations.

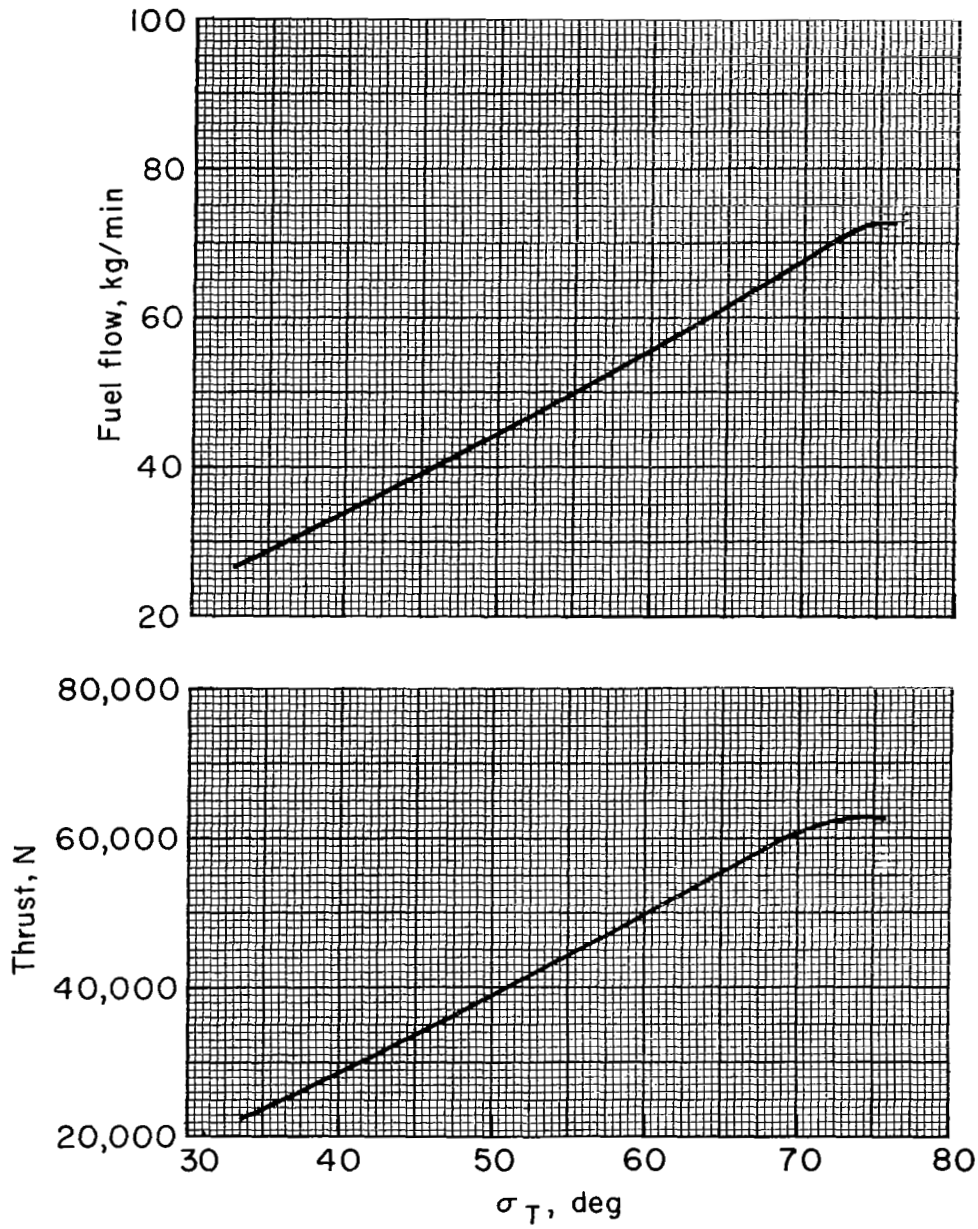

(a) One main engine

Figure 38.– Thrust and fuel flow characteristics at V = 0, h = 600 m, T = 11° C.

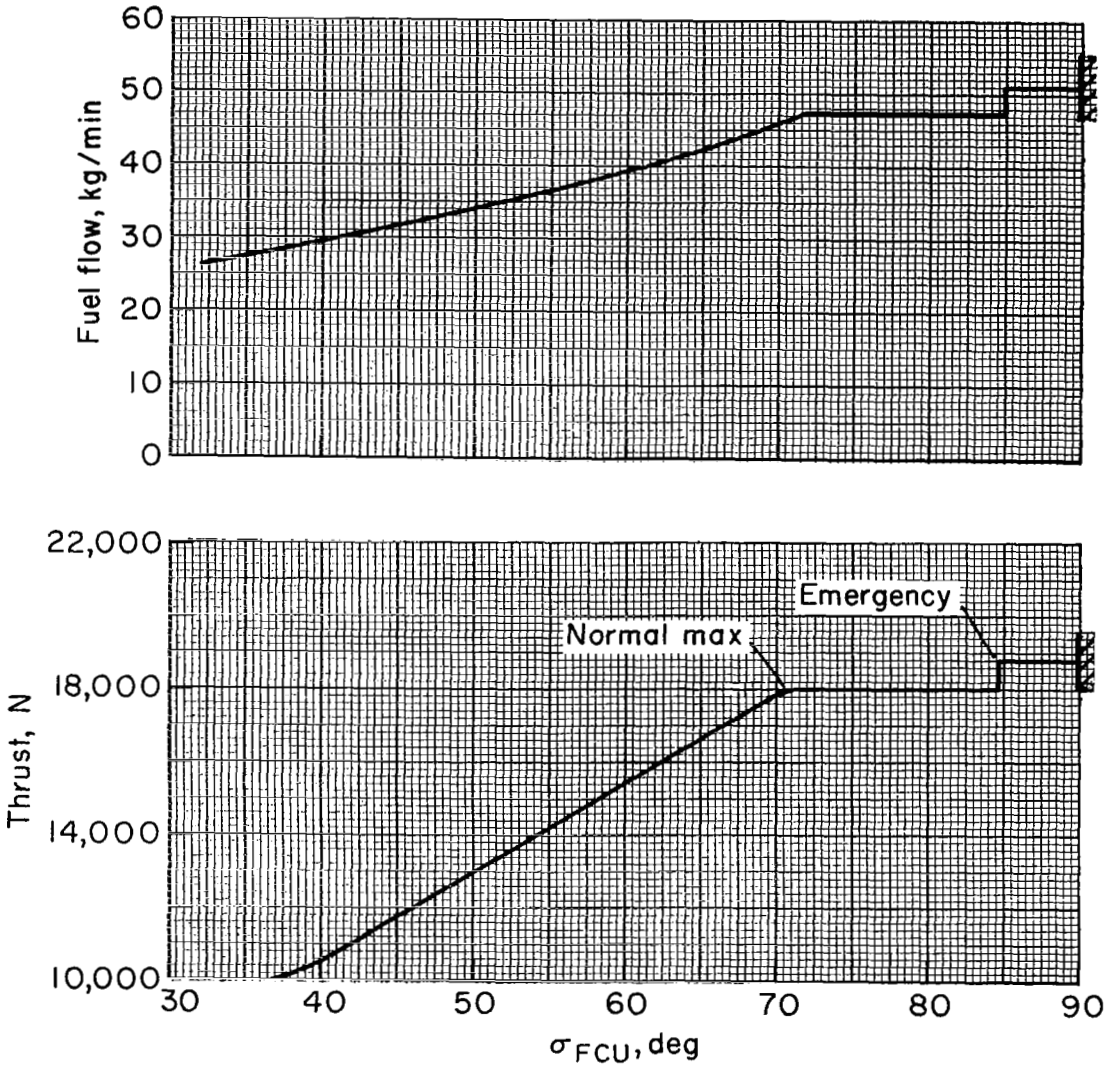

(b) One lift engine

Figure 38.– Concluded.

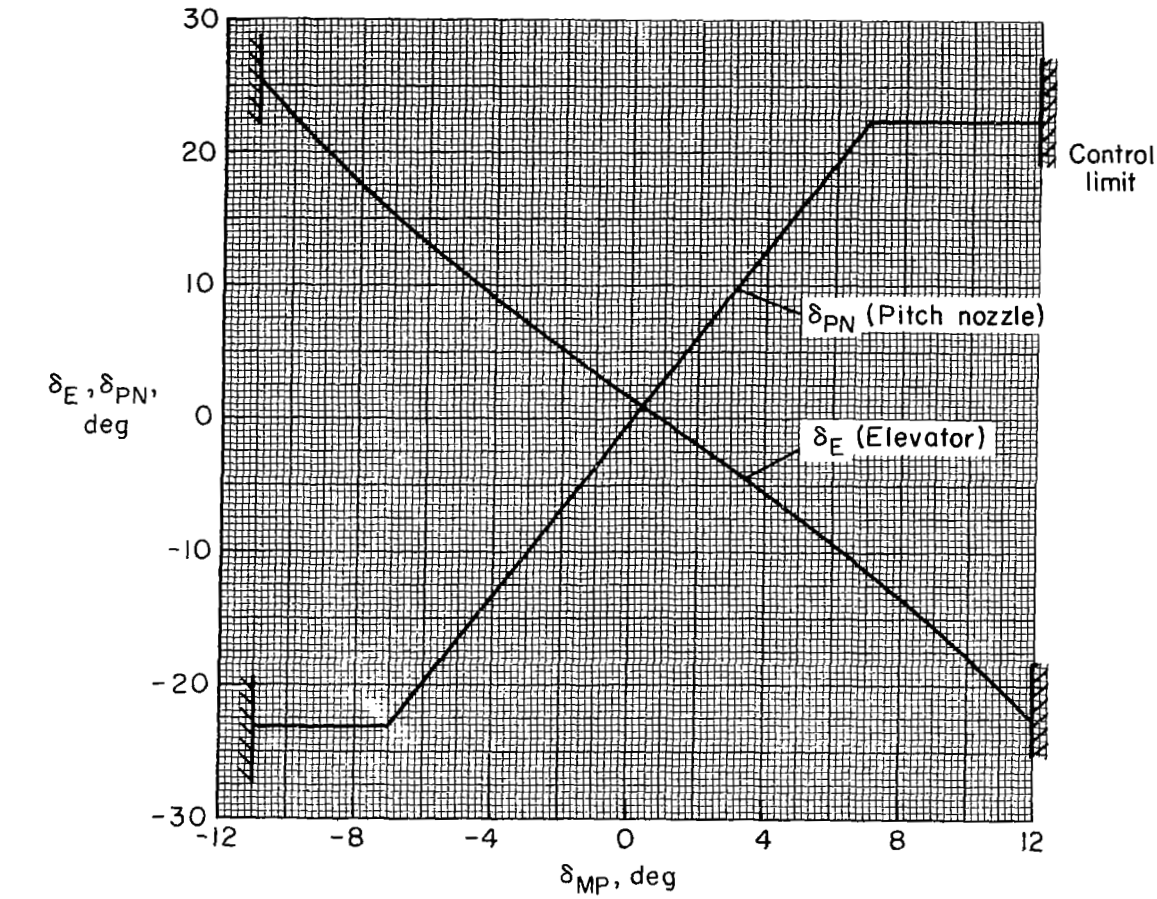

(a) In hover maximum angular acceleration is ±0.22 rad/sec^2 at N_F = 80%, m = 20,000 kg

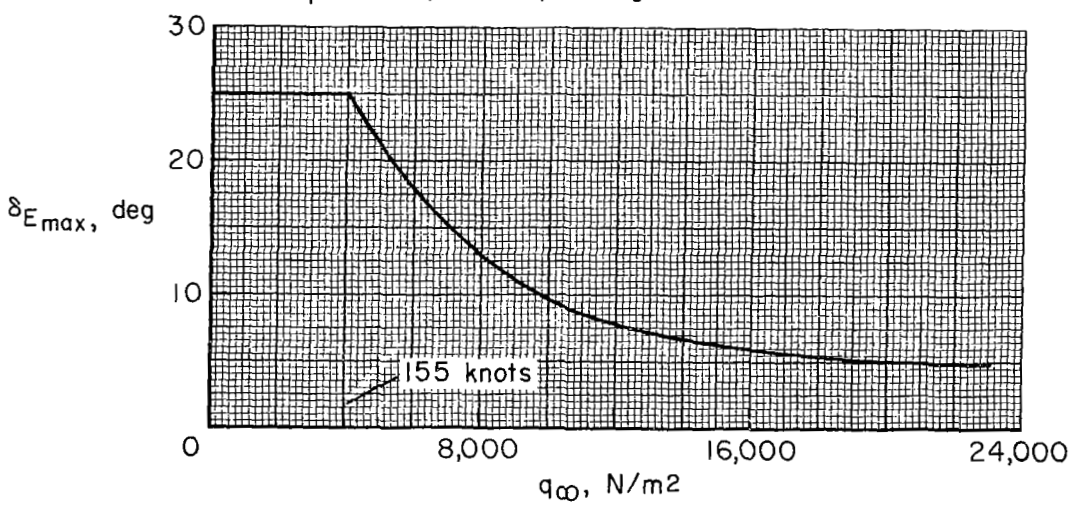

(b) Gear changer relations

Figure 39.– Longitudinal-control relations.

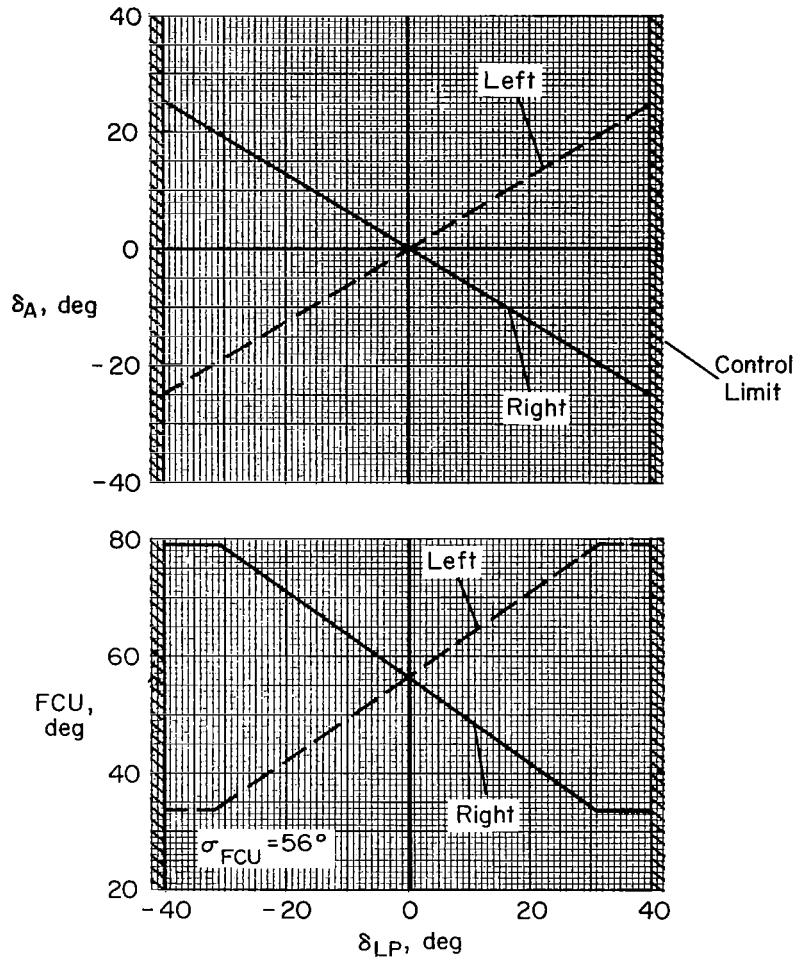

(a) In hover maximum angular acceleration is ±0.78 rad/sec^2 at m=20,000 kg

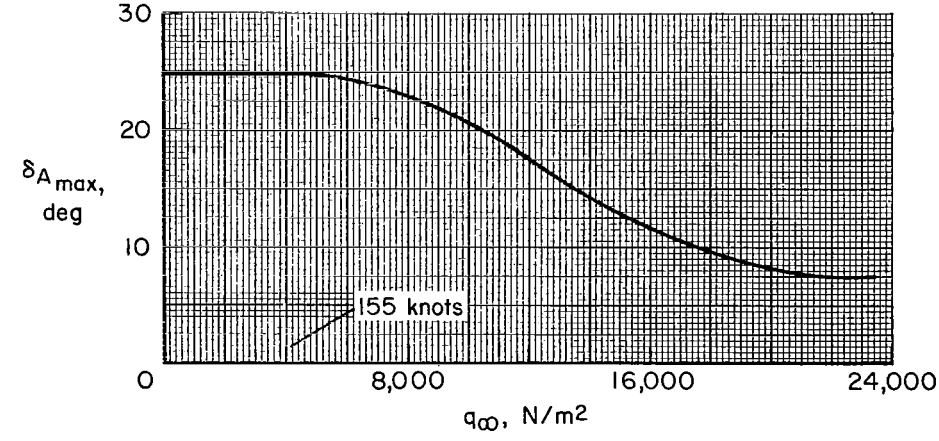

(b) Gear changer relations

Figure 40.– Lateral-control relations.

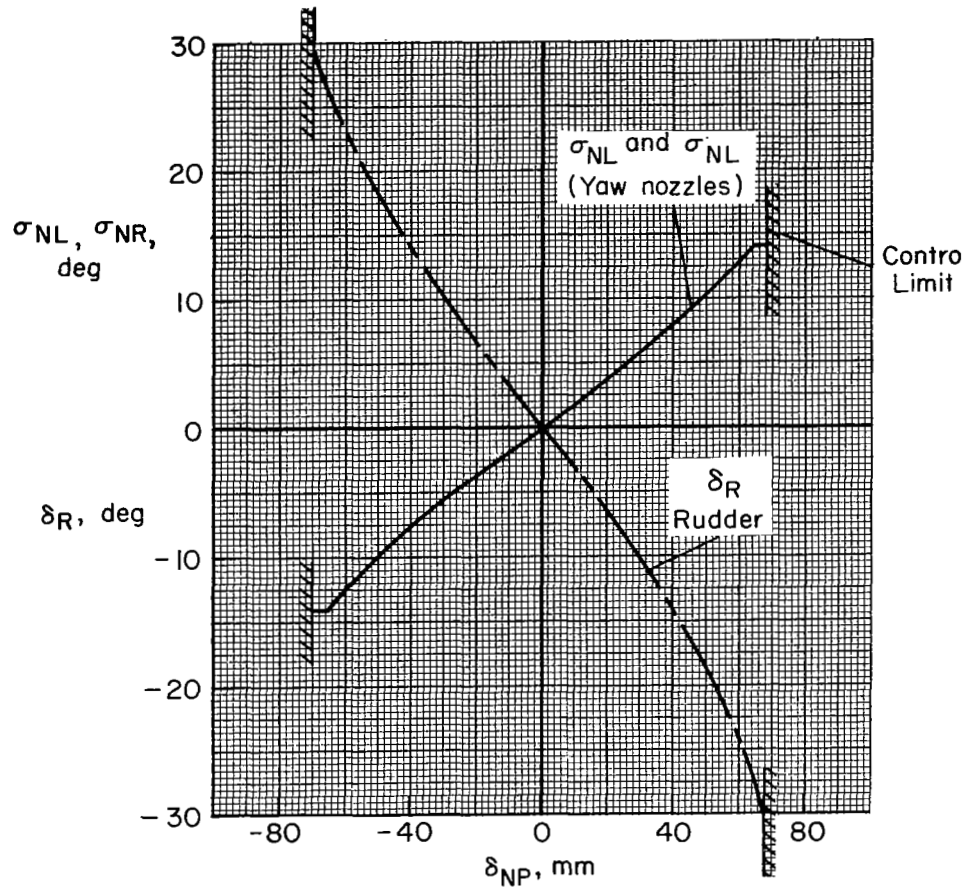

(a) In hover maximum angular acceleration is ±0.38 rad/sec^2 at m = 20,000 kg

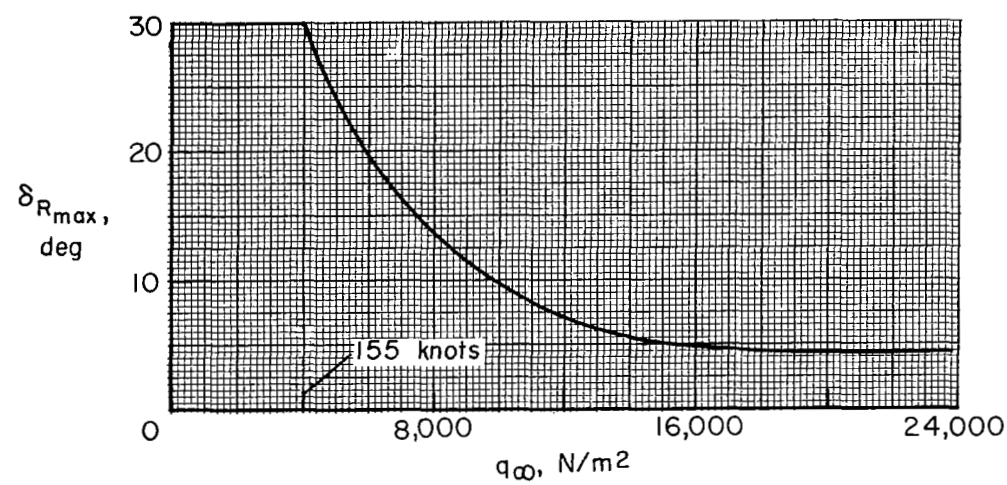

(b) Gear changer relations

Figure 41.– Directional-control relations.

NASA-Langley, 1972 —— 2 A-4023